

STRUCTURAL ANALYSES OF EXPOSED PRE-CRETACEOUS
BEDROCK GEOLOGY IN THE NEW JERSEY REGION

BY GREGORY C. HERMAN

A dissertation submitted to the

Graduate School-New Brunswick

Rutgers, The State University of New Jersey

in partial fulfillment of the requirements

for the degree of

Doctor of Philosophy

Graduate Program in Geological Sciences

Written under the direction of

Professor Roy Schliche

and approved by

Roy Schliche

Michael J. Carr

Robert E. Sheridan

Richard D. Webb

New Brunswick, New Jersey

January, 1997

ABSTRACT OF THE DISSERTATION

Structural Analyses of Exposed Pre-Cretaceous Bedrock Geology in the New Jersey Region

by GREGORY C. HERMAN

Dissertation Director:
Professor Roy W. Schlische

This work presents a set of structural geology studies conducted in and around New Jersey that focus on the geometry of bedrock geology. The work stems from a cooperative effort by the N. J. Geological Survey (NJGS) with the U. S. Geological Survey (USGS) to revise the geologic map of New Jersey and from research on the geometric framework of fractured bedrock aquifers. Chapter 1 presents a new tectonic interpretation for the central part of the New York Recess. In this interpretation the region contains a multiply-deformed, parautochthonous fold-and-thrust system of Paleozoic age. It differs from previous models in which the entire region north of the Newark basin was considered to be allochthonous. Chapter 2 presents a data model developed with the NJGS for managing, analyzing, and displaying geologic data using personal computers (PC) and the ARC/INFO (UNIX v. 7.0) geographic information system (GIS). Chapter 3 presents the results of an outcrop-based fracture study within a six-quadrangle area of the central New Jersey region. The origin, spatial variability, and orientations of fractures mapped within parts of three major fault blocks of the Mesozoic Newark basin are shown to be primarily influenced by tectonic faults. Unmineralized fractures are grouped into bed-parallel and other (non-bedding) fracture sets for analyzing their distribution, orientation, spacing, and spatial variability relative to mapped faults and folds. Bed-parallel fractures are most frequently aligned subparallel to the faults bordering the basin on its northwestern margin. Non-bedding fractures display more variability as they

frequently are aligned subparallel to intrabasin faults. The strike of non-bedding fractures systematically varies across the region to reflect the strike of a nearby faults and are less commonly oriented across bedding strike or at moderate angles to fault strike.

Non-bedding fractures display the most variability in strike where bedding is gently warped and folded. Fold traces are frequently aligned approximately normal to fault strike. The most frequently mapped non-bedding fracture sets in the central part of the Newark basin have inter-fracture spacing from 4 to 20 cm. The distance between non-bedding fractures oriented subparallel to a major fault decreases towards the fault to less than 50 fractures per meter starting at about 2 km away from a fault.

ACKNOWLEDGEMENT

This work represents my contribution to a group effort in updating the geologic interpretations for the New Jersey region. Most of the data are compiled from 1:24,000 and 1:100,000 scale maps by the NJGS. Other data were compiled from research on the structure of fractured bedrock aquifers. Many workers from the NJGS and the USGS influenced this dissertation, especially those involved with the COGEOMAP program (1985-1990).

I thank the staff of the NJGS for providing data and technical support for this research. Haig Kasabach, Dick Dalton, and Bob Canace gave me the opportunity to participate in the COGEOMAP program and conduct structural geologic studies in northern New Jersey. I especially benefited from working closely with Don Monteverde who mapped the lion's share of the Valley and Ridge Province. Don also contributed field data and helped build the Field data Management System. His constructive reviews of structural interpretations and database methods are very much appreciated. I also enjoyed field mapping with Don, Bob, Dick, Hugh Houghton, Rich Volkert, Jim Mitchell, and Maggie Kaeding. Maggie also made a significant contribution by helping start the Field data Management System. I thank Hugh Houghton for introducing me to the geology of the Newark basin, for helping me map the Flemington fault zone, and for the use of his field data. I thank Butch Grossman for his editing expertise, helping me hone my technical writing skills, and for the many discussions surrounding this work. Mark Fiorentino worked closely with me producing the map of the Green Pond Mt. Region and sparked a fascination with digital cartography. Mark French contributed analytical and computer skills by constructing the GIS tool that automatically plots structural symbols on ARC/INFO map compositions. This tool incorporated an original plotting algorithm written by Mark Fiorentino. I thank Dr. Karl Muessig, Leslie McGeorge, Alena Baldwin-Brown, and Gail Carter of the N.J. Department of Environmental Protection

(NJDEP) Division of Science & Research for their funding support for research into the structural analyses of fractured bedrock aquifers. I thank Suhas Ghatge, Don Jagel, Dave Pasicznyk, and David Hall for geophysical support. ShayMaria Silvestri, Mary Santesiero, and Samantha Manburg provided technical support.

Dave Pitcher of Exxon Exploration Co. deserves special acknowledgment and thanks for his efforts in obtaining the seismic-reflection profile and deep-well data presented in Chapter 1. Texaco, Inc. contributed deep-well geophysical data.

I thank Dr. Roy Schliche, Dr. Robert Sheridan, and chairmen Dr. Michael Carr and Dr. Richard Olsson of Rutgers University Geology Department for their critical reviews of manuscripts and providing a positive atmosphere to pursue scientific research. The stipends provided for classes and research were very much appreciated. I thank Dr. Joseph Hull and Dr. Alexander Gates for the stimulating discussions and field excursions focusing on tectonic structures in the New Jersey Highlands and for their reviews of my work. I also benefited greatly by field investigations and exchanges of ideas on central Appalachian tectonics with Dr. Peter Geiser, Dr. Thomas Anderson, Dr. Mark Evans, Dr. MaryBeth Gray, Dr. Michael Hozik, Dr. Jonathan Husch, Dr. Walter Spink, Dr. Roger Faill, Robert Metsger, Dr. Philip LaPorte, Dr. George Stevens, and Dr. Anita Harris. It was also a pleasure associating with Dr. Jack Epstein, Dr. Nick Ratcliffe, Dr. Peter Lyttle, Ronald Parker, and Avery Drake of the U.S. Geological Survey.

Finally, I thank my family for their patience and support in accomplishing this degree. Special thanks to Heidi Sue for bearing the extra work load at home.

TABLE OF CONTENTS

	page
Abstract.....	ii
Acknowledgments.....	iv
List of Tables.....	ix
List of Illustrations.....	x
Introduction.....	1
 Chapter 1. Foreland Crustal Structure of the New York Recess, Northeastern U.S.A.....	 3
Introduction.....	3
Geologic Setting.....	4
Paleozoic Cleavage in Cover Rocks.....	8
Seismic Reflection and Drilling Data.....	10
Bedrock Lithic Groups and Seismic Stratigraphy.....	11
Structural Interpretation of Exxon Seismic profiles.....	13
Paleozoic Fold-and-Thrust belt in New Jersey.....	17
Cross Section Interpretations.....	20
Discussion.....	27
Conclusions.....	31
 Chapter 2. NJGS Bedrock Geology Digital Data Model; Field Data Management, ARC/INFO GIS, Digital Cartography, and Electronic Data Publishing.....	 73
Introduction.....	73
Document Notation and Software Trademarks.....	73

	page
Background.....	74
Overview of the NJGS FMS.....	76
FMS-DOS Data Files.....	77
FMS-DOS Analysis Programs.....	78
FMS-UNIX.....	81
NJGS Digital Cartography using FMS-UNIX (Arcplot).....	82
Bedrock Geology GIS Coverages.....	86
Digital Processing of Bedrock Geologic Coverages.....	86
Bedrock Coverages and Coverage Attributes.....	89
N.J. Geological Survey Metadata.....	90
Discussion.....	92
Chapter 3. Digital Mapping of Fractures in the Mesozoic Newark basin:	
Developing a Geological Framework for Interpreting Movement of	
Ground-water Contaminants.....	124
Introduction.....	124
Geologic Setting.....	124
Methods.....	126
Results.....	131
Azimuth Histogram Analysis of Faults, Folds, and Fractures.....	131
Map Analysis of Non-bedding Fracture Densities.....	133
Domain overlap analysis.....	134
Conclusions and Discussion.....	136

	page
Appendix A. Geologic-Unit Variables Used by the NJGS for Developing GIS Geologic Themes.....	157
Appendix B. NJGS Metadata-File Format.....	164.
References.....	166
Vita.....	179

LIST OF TABLES

	page
Table 1.1 Regional cross-section tectonic dimensions.....	32
Table 2.1 FMS-DOS Data-Input Files.....	97
Table 2.2 FMS-DOS Data-Output Files.....	98
Table 2.3. FMS Primary and Secondary Structural Variables Used in the FIELDATA File.....	99
Table 2.4. Attributes of ASCII Files Generated Using the INFO <LIST PRINT> Command for GIS Point Coverages of Outcrop Locations and Edited for Use as FMS-DOS Input Files.....	100
Table 2.5. Reference Lists for ARC/INFO GIS Line Attributes Used by The NJGS for Bedrock-Geology Coverages.....	101
Table 2.6. A Comparison of Data Attributes from Three Different GIS-Based Geologic Data Models for a Line Representing an Approximately-Located , Moderately-Inclined, Normal Fault.....	102
Table 3.1. Bedrock Field Stations Recorded by NJGS Geologists for Six Quadrangles in the Mesozoic Newark Basin.....	138

LIST OF ILLUSTRATIONS

	page
Figure 1.1. Generalized bedrock geology of the New York Recess showing the location of the study area, regional cross sections, and nearby seismic reflection data.....	33
Figure 1.2. Generalized bedrock geology of northern New Jersey and adjacent areas showing location of cross sections, Exxon seismic reflection lines with shot points, and two deep petroleum exploration wells.....	35
Figure 1.3. Fence-panel diagram summarizing the distribution and thicknesses of the Paleozoic rocks in the study area.....	37
Figure 1.4. Exxon seismic reflection profiles SD-11, SD-12, SD-13, and SD-14.....	39
Figure 1.5. A summary of the ages, compositions, and thicknesses of the rock units in the study area, the corresponding seismic units, key reflection horizons, and characteristic seismic-reflection configurations used for interpretation of the seismic-reflection data.....	41
Figure 1.6. Borehole data for Texaco well C-1 showing stratigraphic correlation to northwest end of Exxon profile SD-11.....	43
Figure 1.7. Exxon seismic reflection profile SD10.....	45
Figure 1.8. Exxon seismic reflection profiles SD-11 and SD-12.....	47
Figure 1.9. Exxon seismic reflection profile SD13.....	49
Figure 1.10. Geologic interpretations of the Exxon seismic reflection profiles shown in serial arrangement.....	51
Figure 1.11a. Tectonic Map of the Kittatinny Valley, N. J.	53

	page
Figure 2.2. A captured VGA display of the opening menu for the FMS-DOS showing the program options and brief explanations.....	105
Figure 2.3. Illustration of the link between structural-geology symbols in an ARCPlot map composition and structural-geology data contained in a FMS-DOS mesostructure (*.MES) plot file.....	107
Figure 2.4. Modified VGA graphic displays from FRACGEN.PBC	109
Figure 2.5. FMS-DOS VGA screen graphics from ROSESTAT.PBC.....	111
Figure 2.6. FMS-DOS VGA screen graphics from ARCAZMTH.PBC.....	113
Figure 2.7. The directory paths and contents for the set of files that comprise the NJGS FMS-UNIX meso.aml	115
Figure 2.8. The set of ARCPlot form menus accessed through the FMS-UNIX macro meso.aml	117
Figure 2.9. Screen capture of a UNIX file manager showing the directory path to the ARCPlot map composition plate1.map and the graphic files contained in the plate1.map directory.....	119
Figure 2.10. A 3-D exploded-block diagram illustrating the components of a NJGS bedrock geology coverage.....	121
Figure 3.1. Index map showing the location of the study area in the New Jersey part of the Newark basin, major geologic faults, 7.5 minute quadrangles, and Counties.....	139
Figure 3.2. Generalized geologic map of a six-quadrangle area in the New Jersey part of the Mesozoic Newark basin.....	141

Figure 3.3. Map showing the distribution of outcrops in the study area where structural data were measured, the set of structural domains used for examining structural trends, and circular histograms summaries of the structural orientations for bedding and other fracture sets for each domain.....	143
Figure 3.4. Diagram illustrating the system used for separating subparallel fractures into classes of fractures based on inter-fracture spacing	145
Figure 3.5. Maps showing the distribution of bedding-plane fracture sets based on the ARC/INFO GIS coverages.....	147
Figure 3.6. Maps showing the distribution of unmineralized non-bedding fracture sets based on the ARC/INFO GIS coverage.....	149
Figure 3.7. Relative frequency histogram plots showing the comparison of structural bearing for fault traces, unmineralized fractures, and fold traces in the study area.....	151
Figure 3.8. Maps showing the distribution of fracture sets in part of the Newark basin based on their recorded fracture densities.....	153
Figure 3.9. Maps showing domain overlap analysis of five fracture sets.....	155

INTRODUCTION

The potable water supply in New Jersey region became stressed during the late 1970' and early 1980's because of increased consumption through periods of below-average rainfall and short-term drought. This spurred the public to pass a bond in 1981 to fund studies to assess the State's water resources with respect to consumptive supplies and demands. Part of these funds were appropriated to revise the Geologic Map of New Jersey with an emphasis on delineating and characterizing the State's aquifers. In 1985 the NJGS and the USGS began a cooperative mapping program (COGEOMAP) to revise the State geologic map of New Jersey at a scale of 1:100,000. COGEOMAP field work ended in 1982.

Many interim products were published during COGEOMAP that illustrated various geological structures and explained some of the geological methods used for deriving new regional interpretations. However, many other data, interpretive methods, and research results remain to be explained and documented. A primary objective of this dissertation is to record the details surrounding my contribution to the Statewide mapping initiative. Another primary objective is to show how the geological details collected during the regional initiative can also be used for addressing site-specific issues related to ground-water availability and ground-water pollution.

This work is divided into three chapters. Most of the interpretive methods and geological details that were used for preparing the regional cross sections for the revised Geological Map of New Jersey are included in the first chapter. Chapter 1 focuses on the geometry and kinematics of the foreland fold-and-thrust belt in the central New York recess. Special emphasis is given to regions where Paleozoic bedrock crops out, thereby allowing application of balanced geometric analysis for deriving current and palinspastic cross section interpretations. The map areas of focus include the Valley and Ridge province of New Jersey, the southwestern New Jersey Highlands, and bordering areas of

the Pocono Plateau of Pennsylvania and New York State. A regional tectonic synthesis for the Paleozoic rocks is presented with generalized maps and balanced cross sections. A regional geologic profile is also schematically derived from composited seismic-reflection profile data.

Chapter 2 describes the computer-based (digital) methods that were codeveloped with other staff of the NJGS for managing and analyzing bedrock geological structures useful to hydrogeologic studies. These methods are also currently being used by the NJGS for development of GIS themes and publishing digital cartographic maps (Herman and others, 1994; Pristas and Herman, 1995). The methods summarized in Chapter 2 are applied in Chapter 3 for a mesostructural study conducted in Mesozoic bedrock of the Newark rift basin. These types of regional tectonic analyses help to constrain the geologic framework for more site-specific remedial investigations conducted in fractured-bedrock aquifers.

CHAPTER 1. FORELAND CRUSTAL STRUCTURE OF THE NEW YORK RECESS, NORTHEASTERN U.S.A.

Introduction

The objective of this chapter is to elucidate the foreland tectonics of the central part of the New York Recess using data from seismic-reflection profiling and geological mapping to construct balanced cross sections. This study focuses on data obtained during a cooperative study with the U. S. Geological Survey to revise the state geological map of New Jersey (Drake and others, 1994). Structural interpretations based on seismic profiles are included for bordering parts of the Pocono Plateau in Pennsylvania and New York. About 120 km of Exxon Co., U.S.A. seismic-reflection data that extend to mid-crustal depths are shown along three parallel profiles. Paleozoic stratigraphic data in the region are summarized from various structural profiles and a deep hydrocarbon exploration well. A synthetic seismogram and conventional velocity survey for the well provide a stratigraphic tie to the seismic-reflection data for most of the Paleozoic cover. The Paleozoic cover sequence requires a unique set of modeling criteria for balanced cross-section analysis because of multiple deformation. Present thrust faults and related folds have been palinspastically restored for the Alleghany orogeny into a stylized foreland-fold sequence attributed to the Taconic orogeny. Gravity and magnetic data for the Valley and Ridge province were compared and utilized in preparing the structural interpretations. The basement structures that can be related to cover strains are shown, and the strain history for the cover rocks is discussed.

Geologic Setting

The New York Recess spans the junction between the central and northern Appalachian Mountains of eastern North America (Fig. 1.1). The bedrock north of the Mesozoic Newark rift basin includes both Proterozoic basement and Paleozoic cover. The tectonic complexity of this region systematically increases eastward from the Pocono Plateau through the Valley and Ridge and into the Highlands (Fig. 1.2). The Pocono Plateau contains little structural relief and only mildly-deformed Paleozoic rocks that form a gently-dipping, west-facing homocline (Fisher and others, 1970; Wood and Bergin, 1970; Berg and others, 1980). The regional fold-and-thrust belt mapped farther eastward has long been recognized as a complex, polydeformed terrane variously ascribed to the Grenville (1 Ga), Taconic (450-500 Ma) and Alleghany (234-260 Ma) orogenies (Bayley and others, 1914; Lewis and Kummel, 1914; Drake, 1969; Rodgers, 1970). Those parts of the fold-and-thrust belt which include Paleozoic cover rocks contain map structures that reflect Paleozoic tectonism. Fold-and-thrust structures of Alleghanian age deform earlier structures throughout the region and involve rocks through Devonian age.

The basement massifs of the Reading Prong mostly contain Grenville-age gneiss, marble, and granitoid rocks (Drake, 1984). Later diabase dikes probably intruded basement during late Proterozoic rifting along the eastern Laurentian margin (Ratcliffe, 1981; Rankin and others, 1989; Drake and others, 1994). Cambrian-Ordovician cover rocks underlie most intermontane valleys in the New Jersey Highlands and the entire Kittatinny Valley. The Cambrian-Ordovician cover extends northwestward from the Kittatinny Valley beneath Middle Paleozoic rocks of Kittatinny Mountain and the Pocono Plateau (Fig. 1.2). Lower and Middle Paleozoic rocks also crop out in the Green Pond syncline in the New Jersey Highlands and adjacent parts of New York (Fig. 1.2). Some isolated fault slices of Silurian conglomerate also crop out along the trace of the Ramapo fault on the northwest border of the Newark basin (Drake and others, 1994).

The Green Pond syncline is a block-faulted and downwarped basin containing stratigraphic and structural evidence indicating at least three phases of Paleozoic compressive deformation in the region (Herman and Mitchell, 1991). The first phase was a broad uplift during the Taconic Orogeny resulting in widespread removal of Cambrian-Ordovician rocks in the central part of the syncline. The second phase involved regional faulting, kink folding, and cleavage development along a northeast trend in cover rocks through Devonian age. The third phase resulted in north-south shortening strain that correlates with cross-cleavage development and oblique fault-slip along the northwest margin of the syncline (Herman, 1987). The second and third phases are attributed to the Allegheny orogeny because they involve rocks of Middle Devonian age and because the progressive clockwise rotation of the recorded finite-strain azimuths correlates with those reported for the Allegheny Plateau in Pennsylvania and New York (Mitchell and Forsythe, 1988; Geiser and Engelder, 1983). Most of the mapped faults were probably active during the Allegheny orogeny based on their involvement of rocks of Devonian age, but they may have originated in basement earlier and may have been subsequently reactivated later during Mesozoic rifting (Lewis and Kummel, 1940; Ratcliffe, 1980). Mallizi and Gates (1989) suggest that the syncline represents a positive flower structure formed by Late Paleozoic dextral transpression with later sinistral strike-slip reactivation.

From Cambrian through Late Ordovician time, the Appalachian basin gradually deepened as it evolved from a carbonate platform at a passive margin to a foreland basin in a convergent margin. The total thickness of Cambrian and Lower Ordovician carbonate rocks is less here than for adjacent areas in the Appalachians, reflecting a depositional setting of comparatively higher structural relief during the early Paleozoic (Rankin and others, 1989). Tectonic uplift and differential erosion of the carbonate shelf by the end of the early Ordovician produced the Beekmantown unconformity, and were probably related

to westward migration of a peripheral bulge stemming from an east-dipping subduction zone of the Taconic orogeny (Jacobi, 1981; Shanmugam and Lash, 1982; Bradley and Kidd, 1991). Resubmergence of the shelf during the Middle Ordovician marked the onset of rapid basin subsidence and deeper neritic-flysch sedimentation followed by progradational influx of terrigenous clastics that extended into late Ordovician time (Hobson, 1963; Drake, 1969; Epstein and Epstein, 1969).

The amount of pre-Silurian erosion of the Cambrian-Ordovician shelf sequence varies widely. In the Kittatinny Valley of New Jersey, the southwest side of the Hudson Valley of New York, and southwest New Jersey Highlands, as much as 91 m of upper Beekmantown strata were locally removed during development of the Beekmantown unconformity (Lewis and Kummel, 1940; Offield, 1967; Markewicz and Dalton, 1977). However, Middle Ordovician Trenton Limestone and subjacent localized clastics rest atop the Beekmantown unconformity with only slight angular discordance (Lewis and Kummel, 1940; Offield, 1967; Markewicz and Dalton, 1977; Monteverde and Herman, 1989). Beekmantown rocks also show localized paleokarstification (Markewicz and Dalton, 1977; Monteverde and others, 1989). Silurian conglomerate locally rests directly on top basement in the central part of the Green Pond syncline (Figs. 1.2 and 1.3) where Cambrian-Ordovician carbonate rocks were completely removed in parts of the Highlands (Finks, 1968). Basal Silurian conglomerate mostly overlies Lower Cambrian dolomite elsewhere in the syncline. However, tectonized shales mapped as Martinsburg Formation locally occur along a major fault along the syncline's western boundary (Kummel and Weller, 1902; Barnett, 1976) which may indicate localized deposition of middle Ordovician flysch directly on basement rocks (Herman and Mitchell, 1991). Erosion of the Cambrian-Ordovician carbonates in parts of the central New Jersey Highlands therefore continued during deposition of Trenton rocks elsewhere, and erosion of the carbonate shelf extended from pre-Trenton emergence to at least the time of deposition of

the Martinsburg Formation.

A regional uplift during the Late Ordovician resulted in the Taconic unconformity that separates underlying flysch from superjacent Silurian molasse in the Valley and Ridge (Rodgers, 1970). The map trace of this unconformity across the New York Recess is shown in figure 1.2. The angular discordance along the Taconic unconformity in New Jersey is at most a few degrees, but is generally at a much larger angle in Pennsylvania and New York (Epstein and Epstein, 1969; Epstein and Lyttle, 1987).

As summarized by Epstein and Epstein (1969), the foreland region began receiving abundant clastics during the lower Silurian in a marginal marine environment from rising Taconic sourcelands to the southeast. A gradual return to prolonged, shallow-marine conditions by lowermost Devonian time is marked by marine shelf-orthoquartzite deposits. Approximately midway into the Lower Devonian, a major regressive event culminated with post-Oriskany emergence, followed by a return to deep neritic conditions, and eventual geosynclinal flysch sedimentation during the Middle Devonian. Subsequent deposits of Middle and Upper Devonian molasse resemble the Middle Ordovician through Upper Silurian flysch-to-molasse sequence.

Compelling evidence points to an early phase of cover folding and faulting throughout the New Jersey Valley and Ridge and Highlands during the Taconic orogeny. This includes the aforementioned pre-Silurian erosion of the Lower Paleozoic shelf sequence, stratigraphic pinch-outs of Middle Ordovician sediments in the region (Hobson, 1963; Monteverde and Herman, 1989), and reconstruction of pre-Silurian cover folds and related structures in southern New York (Offield, 1967; Epstein and Lyttle, 1987). A sequence of three tectonic zones aligned parallel to regional strike was proposed by Epstein and Lyttle (1987) for the Hudson Valley of New York based on styles of faulting and folding within Ordovician parautochthonous flysch. The southwestern parts of these zones are shown in figure 1.2. The zones are southwestward continuations of similar

zones mapped in the Albany, New York region that show faulting, folding, and cleavage in Ordovician flysch strengthening southeastward toward and parallel to the foreland trace of the regional Taconic allochthon (Bosworth and Vollmer, 1981). The line between broad open folding (zone 1) and tight folding and thrust faulting to the southeast (zone 2) extends southwestward from the Shawangunk Mt. region to Middletown, N.Y. (Fig. 1.2). Zone 3 contains overturned folds, thrust faults, and melanges. It parallels the previous line starting about 6 km to the southeast of zone 1.

Paleozoic Cleavage in Cover Rocks

Abundant information about the kinematics and penetrative strains in the regional fold and thrust system is gained from studies of rock cleavage within Paleozoic cover, especially in the Martinsburg Formation (Broughton, 1946; Maxwell, 1962; Drake, 1967a; 1967b; Drake and others 1969; 1985; Groshong, 1976; Epstein and Epstein, 1969; Epstein, 1973; Beutner, 1978; Beutner and Diegel, 1985; Drake and Lyttle, 1985; Herman and Monteverde, 1989; Herman and others, 1994). All varieties of cleavage are grouped here for display purposes into an early regional set (S1) and later localized sets (S2) which overprints bedding (S0) and S1 with structural discordance. S1 includes spaced solution cleavage in Cambrian-Ordovician carbonate rocks, slaty cleavage in the Martinsburg Formation (Broughton, 1946; Drake, 1967a; 1967b; Drake, 1969; Drake and others, 1969; Drake and others, 1985; Drake and Lyttle, 1985), and any spaced cleavage in Middle Paleozoic rocks of the Valley and Ridge Province. S1 is best developed (spacing of a few mm or less) in slates, shales, and argillaceous limestone in the Kittatinny Valley where it commonly obscures bedding and is the dominant parting surface in outcrop. Cleavage is also well developed in siltstone, sandstone, conglomerate, and crystalline limestone in the Kittatinny Valley and Highlands region, but is more widely spaced (less than 1 cm to a few cm). Dolomite is more sparsely cleaved, but generally shows

well-developed solution cleavage with spacing of less than 1 cm to a few cm near reverse faults, within fault horses, and in the hinge areas of tight bedding folds. S1 is poorly developed in some Middle Paleozoic clastic rocks and in hornfels of the Martinsburg Formation near the Beemerville Intrusive Complex (Drake and Monteverde, 1992). S1 spaced cleavage is also diffuse and gently-dipping in the Martinsburg Formation along the base of Kittatinny Mountain from the development of cleavage pressure shadows in interbedded and folded rocks of different competencies (Epstein and Epstein, 1969).

S2 includes all mapped secondary spaced cleavages. S2 displays variable spacing; it locally crenulates S1, or forms more widely-spaced subparallel planes that may offset S1 surfaces with visible shear slip and associated drag folds (figure 8 of Broughton, 1946; figure 25 of Drake, 1969). S2 commonly occurs in the footwall region of large overthrust sheets (Fig. 1.13) and shows both normal slip on northwest-dipping S2 and reverse slip on southeast-dipping S2 (Broughton, 1946; Herman and Monteverde, 1989). Only one slip lineation is recorded for these types of S2. In some locations, particularly near faults with complex movements, multiple sets of systematic cleavage planes reflect complex fault movements and reactivation histories. S3 cleavage is not regional in extent and is beyond the scope of this study.

The age of penetrative cleavage within the Paleozoic cover sequence has been the subject of considerable debate. Field evidence indicates that most cleavages in the foreland stem from the Alleghany orogeny (Epstein and Epstein, 1969; Ratcliffe, 1981; Herman and Monteverde, 1989; Wintsch and Kunk, 1992). However, Ratcliffe (1981) found evidence for pre-Alleghanian tectonic foliation in Martinsburg Formation xenoliths from a Late Ordovician diatreme (Zartman and others, 1967; Ratcliffe, 1981) of the Beemerville carbonatite-alkalic rock complex in the western Kittatinny Valley (Fig. 1.2). Epstein and Lytle (1987) also noted that cleavage in Ordovician rocks in parts of the Shawangunk Mt. region of N.Y. (Fig. 1.1) is locally truncated by overlying Silurian

rocks. Drake and Lyttle (1980) proposed that spaced cleavage in Paleozoic cover may migrate in time progressively toward the foreland and thereby stem from both Taconic and Alleghany orogenies.

Seismic-Reflection and Drilling Data

Four seismic-reflection profiles were collected by Exxon Co. U.S.A. in and near northern New Jersey in 1987 (Figs. 1.1 and 1.2). The profiles extend southeastward from the Pocono Plateau across Kittatinny Mountain into the Appalachian Great Valley. The Exxon data are introduced below as 5-second two-way traveltime (TWT) profile records with full-display, migrated data (Fig. 1.4). Exxon profiles SD-11 and SD-12 were shot separately with about 3 km of overlapping coverage and 2 km strike separation (Fig. 1.2). They are shown together here by edge matching SP 2620 for SD-11 with SP 2001 for SD-12 (Fig. 1.4). The profiles were shot with a Vibroseis source using a 4-second, 4-vibration sweep of 12-72 Hz and a 9-second record length. A split-spread field layout was used with 120 recording channels, resulting in a maximum of 60-fold, common-depth-point data records. Geophone spacing was 24.4 meters with a recording configuration of 1609.8 - 170.7 - Shot Point - 170.7 - 1609.8 meters. Other field parameters include a recording filter of 8 - 90 Hz with the compressional wave recorded as negative values. The profile data were processed by Exxon to a regional reference frame utilizing modern techniques of migration and coherency filtering. The processing sequence included use of refraction statics to reduce long-period statics problems, pre-stack deconvolution, surface-consistent reflection statics to eliminate short-period (<1 spread length) statics problems, and application of a time-variant filter to reduce coherent noise outside the signal bandwidth. The seismic profiles are shown here with approximately equal horizontal and vertical scales using an average velocity of about 4.6 km/s. The line drawings were hand traced from 1 to 24,000 horizontal-scale unmigrated

records. All profile records were digitally scanned and recompiled at a reduced scale.

Proterozoic basement rocks are grouped into a single unit for interpretation of seismic profiles. However, the Paleozoic cover is subdivided into five lithologic groups based on lithologic contrasts reported at the Texaco State Forest Lands C-1 (SFL C-1) deep well in Pike County, Pennsylvania (Figs. 1.2, 1.5, and 1.6), and reflection configurations observed in the seismic profiles. The lithologic groups and seismic reflectors used here (Fig. 1.5) are similar to those used in other seismic reflection studies in the central and southern Appalachians (Beardsley and Cable, 1983; Christensen and Szymanski, 1991; Wilson and Shumacher, 1994).

SFL C-1 was drilled by Texaco, Inc. in 1971 to a total depth of 4240 m. It is located about 25 km southwest along strike from the northwest end of Exxon profile SD11 (Fig. 1.2). A stratigraphic log and borehole geophysical data for SFL C-1 provide a subsurface stratigraphic tie to Exxon profile SD-11 to about 1.7 seconds TWT in the western part of the study area (Fig. 1.6). Sevon and others (1989) noted that the names of all units below the Oriskany Group stem from a drilling log and may not be correctly applied. A synthetic seismogram based on the borehole geophysics shows good correlation with both the geologic log and reflection events from the western end of profile SD-11 (Fig. 1.6). The synthetic seismogram was generated by Exxon from a borehole-compensated sonic log for an areal datum elevation of 487.68 m, and was adjusted for depths below the first check shot at a depth of 152.2 m below the local datum. The synthetic seismogram shows the response from a rarefaction-unit impulse of 20 Hz and a cycle breadth of 31.83 ms. A constant lithologic density of 2.0 g/cm³ was used for modeling the signal responses.

Bedrock Lithic Groups and Seismic Stratigraphy

Figure 1.5 summarizes the lithologic and seismic-reflection characteristics for the

foreland interval of the New York Recess. A pair of seismic reflections directly beneath the base of stratigraphic unit **D** are the strongest and most continuous ones beneath the Pocono Plateau (Figs. 1.6 through 1.9). The lithic group boundary is placed at the top of the upper reflection **H** in the seismic profiles. This horizon has a reflection coefficient of about 0.17, stemming from the lithologic boundary between the Devonian Buttermilk Falls Limestone (about 98 m thick) with the superjacent Marcellus Formation (about 366 m of shale). Although other coherent signals occur above this reference horizon, all subsequent formations are combined for regional structural analysis. The base of stratigraphic unit **SD** correlates to a semi-continuous reflection horizon (**SB** in Figs. 1.7, 1.8, and 1.9) approximately ten reflection cycles below reflection **H** in profile SD-11 (Fig. 1.6). However, a single reflection cannot be traced confidently eastward beyond SP 2500 in profile SD-11. Therefore, the lower boundary was extrapolated into profile SD-12 by using the same number of reflectors below reflector **H**. Further eastward in SD-12 this boundary interval separates parallel-layered reflectors overlying sets of complex-layered reflectors (**cl** in Fig. 1.8) below SP 2200. Stratigraphic unit **S** contains simple-layered reflections in parallel alignment beneath the Pocono Plateau in New York (Figs. 1.7, 1.8, and 1.9). The unit's lower boundary (**OS** in Figs. 1.5, 1.6, and 1.8) is placed among four coherent reflections at the west end of SD-11 based on data for SFL C-1 (Fig. 1.6). This boundary coincides with the regional Taconic unconformity. Its reflection configuration varies elsewhere and displays oblique layering, truncated reflectors, and stratigraphic pinch-outs (**tr** in Figs. 1.8 and 1.9). The position of this boundary in profile SD-10 and the southeast parts of all profiles is uncertain, especially where the reflection configuration is chaotic above 0.8 sec TWT. The lower group boundary is generally diffuse due to the apparent thickening of the underlying lithologic group and local structural complications. Its placement is primarily based on selection of a time interval comparable to other parts of the seismic profiles. Stratigraphic unit **O** shows considerable variations in thickness in

the study area. The unit's lower boundary is reflection horizon **T** (Figs. 1.5, 1.7, 1.8, and 1.9). This horizon is also unclear but generally separates an upper time interval displaying complex- to simple-layered reflections from the lower, simple-layered reflections. The location of **T** is aided by using a constant time interval above the better-defined **B** reflector (Fig. 1.5). A pronounced thickening of this group is seen towards the southeast and southwest in the composite set of geologic profiles (Fig. 1.10). Stratigraphic unit **CO** is mostly dolomite, but is regionally capped by Middle Ordovician limestone that typically grades upward from crystalline wackestone into superjacent black shale of the overlying flysch sequence. This gradation probably accounts for the diffuse reflection horizon **T**. Thick-bedded chert sequences commonly occur directly below the Middle Ordovician Jacksonburg Limestone in the Kittatinny Valley of New Jersey, and thick-bedded sequences of dolomitic shale are common in lower parts of the unit. The group is floored by Hardyston Quartzite of minor thickness, and generally displays a simple-layered reflection configuration. The lower part of the group commonly displays coherent, continuous reflections whereas the upper part commonly displays discontinuous reflections with localized complexities. The unit apparently thins towards the northeast (Fig. 1.10) but is generally interpreted to be of constant thickness (about 350 ms TWT) within a single profile except where disrupted by faulting.

Structural Interpretation of Exxon Seismic Profiles

Each seismic-reflection profile shown here displays both the migrated, full-display records, and conventional line drawings of the unmigrated data. The migrated data preferentially elucidate cover structures, whereas the line drawings clarify basement structures. The line drawings of profiles SD-10, SD-11, and SD-12 were previously published as part of a regional synthesis of deep crustal structures based on seismic-reflection data (Herman, 1992). Some aspects of these earlier interpretations are

revised here.

The regional sole fault is reinterpreted to be entirely confined within Proterozoic basement rather than piercing the Lower Paleozoic sequence beneath the Valley and Ridge province (Figs. 1.7 through 1.10). Also, many northwest-dipping (antithetic) blind faults beneath the Pocono Plateau are reinterpreted to extend upward from the basement into Lower Paleozoic cover rocks (Figs. 1.7 through 1.10). These faults locally offset reflection signals at the base of the cover and form gentle- to moderately-dipping boundaries between acoustic domains in basement. The profile trace of these interpreted faults normally intersect localized diffraction events. The acoustic domains in basement contain arched reflectors with broad and open reflection configurations (Figs. 1.7, 1.8, 1.9) resembling 'roll-over' or 'reverse drag' along normal faults (Gibbs, 1984; Hamblin, 1965). These faults may be Proterozoic rift structures that were locally reactivated as late Paleozoic contractional faults because in places there is no apparent offset of the cover along their up-dip projection (Figs. 1.8, 1.9, 1.10). Most of these basement structures therefore apparently predate Paleozoic deposition and contraction.

Profile SD-10 extends southeast from the Pocono Plateau into the Valley and Ridge Province of New Jersey (Fig. 1.2). The southeast end of the profile crosses the Paulins Kill thrust belt (Fig. 1.11a), where the last map trace of thrust faulted Lower Paleozoic carbonates occurs in the New Jersey foreland. Profile SD-10 shows that the blind faults cutting Paleozoic cover rocks extend for at least 10 km. farther into the Plateau (Fig. 1.7). Ordovician rocks of the Martinsburg Formation are probably tectonized where splay faults locally thicken the cover and underlie broad and open folds in the Silurian-Devonian sequence (SP 2300 to 2600). The system of blind faults is most complex beneath the northwest part of the Valley and Ridge Province (SP 2600 to 3000), where it defines a structural transition between synthetic basement faults to the southeast and antithetic basement faults to the northwest. The sets of antithetic faults beneath the

Pocono Plateau are interpreted as isolated reverse faults whereas those to the south are interpreted as a linked decollement thrust system (Herman, 1992). The southeast end of SD-10 shows a pair of open folds involving the Cambrian-Ordovician carbonates (Fig. 1.7). Only the southeast limb of the synform and the northwest limb of the antiform are interpreted with certainty. The intervening fold limbs are based on field mapping and geophysical data from the exposed fold-and-thrust belts. A northeast-plunging anticline in cover rocks directly southwest of SP 3300 in line SD-10 (Figs. 1.2, 1.11) is projected into the profile interpretation (Fig. 1.10). Thrust faults are shown directly to the southeast although they are not apparent in the seismic record.

Exxon profiles SD-11, SD-12, and SD-13 span the structural transition from the Pocono Plateau to the Hudson Valley in southeastern New York (Fig. 1.2). A slight mismatch of the seismic stratigraphy is apparent where the profile SD-11 and SD-12 are edge matched and the Paleozoic cover is deeper to the southwest (Fig. 1.8). This trend is consistent throughout the region as shown by comparison of the serial profile interpretations (Fig. 1.10).

Structures in profiles SD-11, SD-12, and SD-13 are similar to those in SD-10, but also differ notably. For example, the structural transition between synthetic and antithetic basement faulting occurs farther northwest in New Jersey than in New York (Fig. 1.10). Similarly, faulting in cover rocks beneath the Pocono Plateau generally extends farther northwest in Pennsylvania than in New York. These trends show that foreland-translation strain related to the Alleghany orogeny decreases northeastward from the Pennsylvania Salient (Wilson and Shumaker, 1988) into the central part of the New York Recess. However, faulting of Silurian rocks (profile SD-13) occurs farther northwest than it does in the other profiles, and the amount of tectonic deformation in the Silurian-Devonian foreland apparently increases northeast of profile SD-13 in the Shawangunk Mountain region of New York (Salkind, 1979; Marshak and Tabor, 1989). Therefore, a cross-strike

tectonic axis within the foreland of the New York Recess seems to coincide with the trace of profiles SD-11 and SD-12. This observation is elaborated on below with respect to other work in the region.

The interpretation of structures in the southeast part of profiles SD-12 and SD-13 is complicated by a seismic-data gap and by probable complex fault and fold structures in the Martinsburg Formation (Epstein and Lyttle, 1987). The southeast end of profile SD-13 is located about 2 km northeast of the Middletown, N.Y. gas well (Crom-Wells 1 Fee in Fig. 1.2). Sanders (1983) interpretation of the Hudson Valley region near the well is based on the lithologic well log and geologic mapping (Offield, 1967). The favored interpretation depicts a regional, subhorizontal detachment fault near the base of the Martinsburg Formation that accommodated northwestward foreland thrust translation and is linked to a southeastern overthrust system rooted in Proterozoic basement (Fig. 8 of Sanders, 1983). This detachment was proposed to separate northwest-inclined hanging-wall rocks from subhorizontal footwall carbonates. The Exxon profiles show considerable structural complexity above the proposed detachment horizon, although resolution of continuous, discrete structures is hampered by poor seismic resolution above 0.8 sec TWT (Figs. 1.7, 1.8, and 1.9). Nevertheless, this stratigraphic horizon commonly shows localized shear strain in the Kittatinny Valley whereas other wedge faults and folds affect the entire Cambrian-Ordovician cover sequence (Herman and Monteverde, 1989).

The seismic-reflection data show that the lower Paleozoic cover dips gently northwest from the Valley and Ridge Province beneath the Pocono Plateau. This foreland interval developed structural relief from contraction and wedging of basement and cover rocks on a complex system of blind faults that form the foreland boundary of the regional fold-and-thrust belt. Estimates of translation displacement related to blind-thrusting beneath the Pocono Plateau ranges upward to 5 km with strain decreasing northeastward along strike.

Paleozoic Fold and Thrust Belt in New Jersey

The Paleozoic fold-and-thrust belt in New Jersey consists of abundant low- to moderate-angle reverse faults in Lower Paleozoic rocks of the Kittatinny Valley and southwest part of the New Jersey Highlands (Drake and Lyttle, 1980; Herman and Monteverde, 1989; Monteverde and others, 1994; Drake and others, 1994). Elsewhere in the Highlands Lower and Middle Paleozoic cover rocks generally contain moderately- to steeply-dipping faults that commonly display complex fault-slip motions resulting from superimposed non-coaxial strain (Ratcliffe, 1980; Hull and others, 1986; Mitchell and Forsythe, 1988; Herman and Monteverde, 1989; Millizzi and Gates, 1989; Herman and Mitchell, 1991). The Paulins Kill and Jenny Jump - Crooked Swamp (JJCS) thrust belts are in the central and southeast parts of the Kittatinny Valley, respectively (Fig. 1.11).

The Paulins Kill thrust belt marks the northwest limit of exposed thrust faulting. It consists chiefly of imbricated Cambrian-Ordovician carbonates underlying the Paulins Kill Valley (Fig. 1.2). Although no basement rocks are mapped at the surface, positive aeromagnetic anomalies directly correlate with the map traces of open and upright cover anticlines indicating regional basement involvement in both cover folding and thrust faulting (Figs. 1.11b and 1.12). Thrust faults mostly dip southeast and are symmetrically arranged behind a central, parautochthonous footwall sequence occupying the northwest part of the valley (Figs. 1.2 and 1.11). Thrust faults terminate laterally into fault-propagation folds in the Martinsburg Formation (Fig. 1.11a). Northwest of the valley, the Martinsburg Formation dips gently to moderately northwestward, locally contains upright- to-steeply-inclined folds, and pervasive S1 cleavage (Drake and others, 1969; 1985, Epstein and Epstein, 1969; Herman and others, 1994). To the northeast, the Martinsburg Formation contains a system of fold culminations and depressions with fold geometry and cleavage relations similar to those in the Paulins Kill foreland (Herman and Monteverde, 1989; Drake and Monteverde, 1992). The Beemerville carbonatite-alkalic

rock complex also underlies parts of this region and locally crops out, most notably near the Taconic unconformity (Maxey, 1976; Ghatge and others, 1992; Drake and Monteverde, 1992; Drake and others, 1994). The Stone Church - Halsey synclinorium borders the Paulins Kill thrust belt to the southeast and the JJCS to the northwest (Fig. 1.11a). This interval is structurally more complex, commonly showing steeply to gently inclined folds and multiple cleavage sets (Broughton, 1946, Maxwell, 1962; Davis and other, 1967; Epstein and Epstein, 1969; Groshong, 1976; Beutner and others, 1977; Beutner, 1978; Drake, 1969; Drake and others, 1985; Beutner and Diegel, 1985; Drake and Lyttle, 1985; Herman and Monteverde, 1989; Herman and others, 1995).

The JJCS thrust belt exposes Proterozoic basement, Lower Paleozoic Cambrian-Ordovician carbonates, and the Ordovician Martinsburg Formation (Fig. 1.11a). Most of the mapped faults dip southeast and comprise arrays of diverging, connecting, and rejoining splay-faults that locally form duplex structures (Herman and Monteverde, 1988, 1989). The imbricate thrust sheets of the JJCS generally plunge northeastward, so that successively higher and presumably older thrust sheets occur in that direction. The relative age of the stacked thrust-fault slices assumes a general break-forward sequence of structural development only for the overthrust phase of deformation. Other wedge faults show apparent 'out-of-sequence' structural developments (Morley, 1989) with subsidiary synthetic splay faults and antithetic, break-back thrusts modifying overthrust fault slices. These wedge faults locally delaminated the cover, resulting in a tectonically shortened and a thickened Lower Paleozoic sequence. They are common in convergent foreland terrain at widely-varying scales (Cloos and Broedel, 1943; Price, 1986). The full range of structures is best represented in the footwall of the Jenny Jump thrust fault where a series of klippen, mostly composed of Lower Paleozoic dolomite, lie within a synformal cleavage fold or 'cleavage trough' in the Martinsburg Formation (Fig. 1.13). The thrust faults that sole the klippe

along the foreland margin of the JJCS originated at lower crustal levels and rose to their current structural position near the base of the Martinsburg Formation. The presence of these structures demonstrate the likelihood of blind detachment faults existing at the base of the Martinsburg Formation in adjacent regions (Sanders, 1983). Another set of map-scale cleavage folds occurs in Martinsburg cover immediately foreland of the northeast part of the Paulins Kill thrust belt (Fig. 1.11a). The structures depicted in the footwall of the Jenny Jump overthrust are probably also developed here.

The boundary interval between the JJCS and the New Jersey Highlands is complex where it involves overthrust faults and other moderate- to high-angle splay faults that locally juxtapose basement and cover (Figs. 1.2, 1.11a, 1.12, and 1.13). The overthrust faults are more common in the southwest whereas the high-angle splay faults are abundant in the northeast. The latter set of faults mostly shows normal dip slip with basement in the footwall and cover in the hanging wall (southeast end of cross sections E and F in Figs. 1.11a and 1.12). Although the thrust faults probably result from Alleghanian tectonism, the more-steeply inclined normal faults probably have a complex history that may involve episodic tectonic movements ranging from the Proterozoic through the Mesozoic (Hague and others, 1956; Ratcliffe, 1981; Gillespie, 1987).

The southwest part of the New Jersey Highlands contains complex, anastomosing shear zones within basement that locally produce open and upright folds in overlying cover (Fig. 1.14). The shear zones are similar in geometry and metamorphic grade to ductile deformation zones in basement rocks of the Appalachian Blue Ridge Province, where they occur at a wide range of tectonic scales away from major fault zones (Mitra, 1979; Boyer and Mitra, 1988). Such shear zones produce bulk, non-coaxial, inhomogeneous shortening (Bell, 1981) which is compatible with the variably plunging nature of the overlying fold axes in the cover (Fig. 1.14). The age of the shear zones and related cover folds is unknown. However, both may stem from early Paleozoic tectonism,

based on the regional observation that an early set of cover folds is cut and translated northwestward by later thrust faults (Merchant and Teet, 1954; Herman and Monteverde, 1989). Faults mapped in basement elsewhere in the New Jersey Highlands are commonly steeply inclined, with cataclasite and mylonite fault fabrics that contain retrograde mineral assemblages of pyroxene, amphibole, mica, chlorite, epidote, and quartz (Hull and others, 1986; Mallizi and Gates, 1989; Gates, 1993). These faults also show complex geometry and movements of speculative ages.

Cross-Section Interpretations

Overthrust faults are most apparent where older rocks overlie younger ones along moderate- to gently-dipping structural discontinuities. Overthrust faults are less apparent where they have cut through previously-folded strata and juxtaposed fold-limb segments, because the resulting map pattern often contains areas showing 'out-of-sequence' geometry when compared to simple break-forward thrust-fault relations in flat-lying strata (Figs. 2 and 3 of Morley, 1989). Thrust faults within the Kittatinny Valley, New Jersey have northwest-verging, gentle- to moderate-dipping tectonites locally preserved in outcrop. Invariably, associated fault traces for 'out-of-sequence' structures strike into areas where they show ordinary older-over-younger structural relations, as for the leading edge and margins of the Crooked Swamp syncline (Figs. 1.11a and 1.12). The tectonites are commonly composed of Middle Ordovician Jacksonburg Limestone with mesostructures showing high shear strain through subparallel alignment of bedding and spaced cleavage, top-to-the-northwest fold drag, down-dip lineations, and strained fossils locally.

Cross-section analysis of these multiply-deformed structures requires at least two stages of palinspastic reconstruction. The first stage removes translation strain and related fold strains (F2) stemming from thrust faulting and requires the construction of blind

structures to restore early (F1) cover folds (Fig. 1.12). Secondary reconstruction models then try to account for other folding strains stemming from F1 sinuosity. Penetrative strains related to intragranular bulk deformation and regional cleavage development need more study before their effects can be integrated into multiple palinspastic reconstructions.

Four regional cross sections are shown for those parts of the fold-and-thrust belt in New Jersey where Lower Paleozoic cover rocks are abundant (A, B, C, D in Fig. 1.2).

The cross sections depict three tectonic stages:

- 1] present-day structures (Fig. 1.15),
- 2] palinspastically reconstructed fault trajectories affecting early (F1) cover folds and subjacent basement (d2 of Fig. 1.16), and
- 3] a broadly-arched Cambrian-Ordovician passive margin showing convex-upward curvature (d1 of Fig. 1.16).

All the interpretations show the current position of the sole thrust detachment fault, the location of which is based on regional seismic reflection data (Herman, 1992). Any vertical strains associated with crustal flexure stemming from thermal effects, exhumation, or sedimentary loading are beyond the scope of this paper and require further study.

Tectonic contraction values for the region stem from palinspastic reconstruction of the Cambrian-Ordovician carbonate part of the cover layer. This part of the cover chiefly consists of dolomite, and is stiff in comparison to the overlying Ordovician flysch. This 'stiff layer' is assumed to have undergone negligible (<10%) amounts of secondary intragranular bulk strain. Mesoscopic cleavage in the stiff layer is commonly restricted to near-fault intervals and to the hinge regions of F2 folds (Herman and others, 1994).

The cross sections are oriented approximately normal to regional strike to minimize inaccuracy in apparent stratigraphic thickness and to permit evaluation of tectonic contraction strain (Geiser, 1988). Interpretations of both current and F1 structures rely upon standard methods of down-plunge projection for planar and

parallel-folded structures (Ragan, 1985; Ramsay and Huber, 1987). The projection of F1 folds is along the bearing and plunge of S0 and S1 intersection lineations based on field measurements. The projection of F2 structures and thrust-fault planes is along the bearing and inclination of S1 and S2 intersection lineations and fault-plane measurements as available. Apparent-dip values for bedding, cleavage, and fault-dip data are based on the apparent dip calculation of De Paor (1988, equation 9). Structures are interpreted for both the current and restored structures at the same time using trial-and-error geometric alignment (Woodward and others, 1985).

Fundamental cross-section-modeling assumptions include plane strain and the conservation of both volume and the length of cover beds between current and restored cross sections. Plane strain restricts bulk deformation to planes parallel to each section. Finite-strain studies of regional cleavage within the Martinsburg Formation support the use of constant volume and plane strain in the cover (Beutner and others, 1977; Beutner, 1978; Beutner and Diegel, 1985). Out-of-plane deflections at oblique thrust ramps only cause small strain deviations when applying a plane strain assumption (Elliott, 1976; Apotria and others, 1994). Constant bed lengths are maintained between current and retrodeformed structures following the methods of Dahlstrohm (1969) and Boyer and Elliott (1982) only for the Cambrian-Ordovician stiff layer. Penetrative layer-parallel-shortening (LPS) strains in the overlying Jacksonburg Limestone and Martinsburg Formation require special attention for palinspastic reconstruction. Cambrian-Ordovician dolomites commonly contain joints and shear fractures whereas Middle Ordovician limestone and clastics are more cleaved (Herman and other, 1994). Pervasive, penetrative rock fabrics in the dolomite stiff layer are usually restricted within the region to occur near faults and fold hinges. A modeling assumption was therefore made to equate S2 penetrative strains and fault-propagation fold strains in the Martinsburg Formation to brittle shear strains and fault-bend-fold strains in the stiff layer when

restoring present structures to a pre-thrust (d2) configuration. This assumption is supported by the lack of regional detachment faulting at the contact of the stiff layer with overlying shales and slates. Localized shear strains mapped at this horizon are spatially linked to underlying wedge faults in the stiff layer (Herman and Monteverde, 1989; Monteverde and others, 1995). The manner in which penetrative strains from S1 cleavage are treated for palinspastic reconstruction are discussed below.

Other modeling assumptions include using a break-forward sequence of structural development for the largest overthrust faults branching from the sole fault. Also, second- and third-order cover folds are mapped as F1 structures if their axial-surface traces are cut by overthrust faults or if Middle Ordovician stratigraphic pinch-outs, facies changes, and extensive paleokarst development mark these structures (Hobson, 1963; Monteverde and Herman, 1989). F1 structures are generally broad and open in the Kittatinny Valley and become more closed and gently inclined southeastward towards and into the Highlands (Herman and Monteverde, 1989). Broad and open F1 cover folds in the Kittatinny Valley show a direct correlation with positive magnetic potential-field anomalies. These trends support the assumption that basement is generally attached to the overlying cover in normal stratigraphic succession, and that cover-layer anticlines are cored by basement rocks with higher magnetic susceptibilities than cover-layer rocks (Telford and others, 1976; Jagel, 1990; Ghatge and others, 1992).

The projection, construction, and restoration of the F1 structures are intricate because of their doubly plunging fold geometry, and because "blind" F1 segments are locally concealed beneath footwall regions of overthrust faults. Complications are few where imbricated thrust sheets compose duplex fault arrays showing hanging-wall and footwall fold segments in adjacent positions (for example, Fig. 1.11a between Jenny Jump Mt. and the Crooked Swamp syncline). However, the interpretation of F1 footwall structures is elusive where faults show few or no lateral variations in dip throughout large

areas and where erosion has removed a substantial part of the F1 hanging-wall. In some cases, the wavelength and extent of the blind F1 footwall sequence are locally constrained with magnetic profiles (Fig. 1.12), or by use of a 'minimum fold solution' for sections lacking useful magnetic data. In this case, restored F1 fold structures are also constrained by the fold geometry of the hanging wall. For example, the duplex thrust structure shown in figure 1.12 (E-E') retrodeforms to a F1 anticlinorium with a southeast-dipping fold limb. Because the aeromagnetic data for this area are ambiguous compared to the southwest, only a single syncline is required for the blind footwall segment to complete a F1 fold structure. More complicated reconstruction can be developed using additional fold pairs, as long as thrust translation strains between adjacent, serial sections demonstrate uniformity (for example Fig. 1.12, sections F-F', G-G', and H-H'). This technique commonly results in a geometric solution resulting in minimal thrust-translation values. The final geometry of 'blind' F1 structures is refined by simultaneous adjustment of bed-lengths, profile areas, and bedding and fault cut-off geometry between current and restored sections (Woodward and others, 1985). The interpretation of 'blind' folds also assumes geometric similarity with exposed structures, because they occur in the same tectonic environment, consist of the same lithic units, and belong to the same structural family (Woodward and others, 1985).

F2 cover folds include fault-bend, fault-propagation, and drag folds. Fault-bend folds are most widespread in the Cambrian-Ordovician stiff layer where they are relatively broad and smooth in contrast to the sharper, kink-style fault bends described for fault trajectories in flat-lying sedimentary wedges (Rich, 1934; Suppe, 1983). The geometry of these folds depends of the trajectory of thrust faults in the cover, which are generally subparallel to inclined limbs and broadly flatten and splay through fold hinges (Figs. 1.12 and 1.13). F2 fault-bend folds originate at thrust-fault inflection points and affect all earlier structures in overlying rocks, following the assumption of the break-forward

tectonic sequence. Palinspastic F1 structures for the Cambrian-Ordovician stiff layer are restored first and serve as a guide for helping constrain the reconstruction of the overlying Martinsburg Formation. F1 folds are restored by unfolding their limbs by the amount of F2 interlimb angles along the trace of the F2 axial surfaces during simultaneous line-length and area-balancing iterations.

F2 fault-propagation folds are frequently mapped as third- and fourth-order structures in blind-thrust Martinsburg rocks of the Kittatinny Valley. Palinspastic reconstruction of these structures relies on trial-and-error alignment of unit contacts while preserving sinuous bed-lengths and profile areas between current and restored sections. F2 drag folds are minor structures that primarily occur near the footwall of exposed thrust faults or with swarms of strain-slip cleavage (Herman and Monteverde, 1989). Penetrative strains from drag folding are restricted in occurrence near faults and are ignored because of their relatively small scale.

The final modeling assumption is that cover-layer segments originated from positions of lower structural relief than they presently occupy (Fig. 1.17). This assumption limits the ways in which faulted fold limbs can be reconstructed in the absence of having a standard planar reference for reconstruction (such as the passive-margin wedge). Many restored alignments are still possible for adjacent segments of cover folds after applying the structural-relief assumption. However, palinspastic alignment of F1 structures is further constrained by limiting the profile thickness of basement within a thrust sheet to the interpreted thickness between the upper (basement-cover contact) and lower (sole thrust) boundaries (t_0 in Fig. 1.17).

Tectonic aspects of the regional cross-section interpretations are presented in Table 1.1. The strain values are partitioned into strain components that include (1) horizontal foreland contraction from thrust translation, (2) the cross-section contraction ratio, and (3) negative extension (e) from pre-thrust folding. The translation strain is

measured linearly from the hinterland most basement-cover cutoff showing reverse displacement for each section between the current and restored positions in a horizontal plane relative to the erosion surface. The folding strain values are sinuous bed lengths along the basement-cover contact in the restoration diagrams and do not include penetrative volume-loss strains. The 8° - 11° range of wedge taper values for the current sections are close to other subaerial accretionary wedges (Davis and others, 1983).

Other geophysical and structural data support these current interpretations. Calculated gravity and magnetic models show close agreement with the geometry of the thrust system between cross sections A-A' and B-B' (Fig. 1.18) and define the 3-D geometry of the Beemerville intrusive complex in the northeast Kittatinny Valley (Jagel, 1990; Ghatke and others, 1992). The intrusive complex is shown in cross section A-A' as having been translated northwestward by Alleghanian thrust faults (Fig. 1.17). Spink (1967) proposed that the intrusive complex acted as a tectonic buffer showing stratigraphic contacts and fold axes systematically deflected around it. Also, the Paulins Kill thrust belt has a fault-displacement-length scaling ratio of 1:14 or about 7 %, which agrees closely with values for other fold-and-thrust belts (Boyer and Elliott, 1982). Length-displacement scaling ratios for the JJCS and fault systems in the New Jersey Highlands are more elusive because faults extend into adjacent areas lacking detailed mapping, and fault systems having many branching faults are awkward to process for determination of fault-scaling ratios (Elliott, 1976). Nevertheless, an estimate of the fault displacement-scaling ratio for the JJCS was made to test the results of constructing 'blind' cover-layer folds that satisfy the 'minimal thrust-translation' assumption. The estimated scaling ratio was derived by substituting the strike length of the Cambrian-Ordovician carbonates in the thrust belt (Fig. 1.1) for the fault-length value. This substitution is used because the length of outcropping Cambrian-Ordovician carbonates in the Paulins Kill thrust belt is approximately the same as the map trace of outcropping faults (Fig. 1.11a).

This approach produces an estimated scaling ratio of 1:19 (about 5%) for the JJCS. This ratio is about 2% lower than the ratio for Paulin Kill thrust belt, suggesting that translation strain reported for the JJCS may be slightly underestimated, and blind cover folds may extend a few kilometers beyond those shown in cross section. This also suggests that the length of the outcrop belt may only be used to constrain the order of magnitude for regional fault-translation values, and is probably not an accurate substitute for fault-length when determining length-displacement scaling ratios for a regional fault system.

Discussion

The regional fault system is portrayed here as a subaerial accretionary wedge with a basal detachment entirely contained in basement (Fig. 1.19). Mapped faults in the New Jersey foreland are shown here to be linked to blind faults beneath the Pocono Plateau. The relative lack of structural relief beneath the plateau or its foreland restricts the origin of any structures that could accommodate regional allochthonous transport to the mapped fold-and-thrust belt. Balanced cross-sections of the fold-and-thrust belt show that cover rocks occur as localized, segmented fold sequences in the footwall of subsidiary splay thrusts that are soled in Proterozoic basement. Moderate-dipping reverse faults mapped at the surface in the New Jersey Highlands presumably correspond to Paleozoic faults rooted in basement as interpreted from regional seismic-reflection data (Fig. 1.19). These findings demonstrate that prior allochthonous interpretations for this region depicting hundreds of kilometers of translation strain accommodated by foreland structures (Drake, 1978; 1980; Lytle and Epstein, 1986; Hatcher et al., 1990) are geometrically inadmissible and improbable. The foreland structure depicted here restricts the involvement of Lower Paleozoic rocks to occurring within subsidiary fault slices splayed from a master decollement rooted in Proterozoic basement. This reinterpretation does not preclude

allocthonous transport from occurring elsewhere in comparable rocks along strike. It defines a region marked by parautocthonous tectonic contraction in the foreland with more allocthonous roots preserved along the margin and beneath the New Jersey Piedmont. This interpretation points to the need for more work to be conducted in adjacent regions to understand how the allocthonous and parautocthonous regions merge or overlap.

These cross sections depict a set of consecutive structural stages for the upper crust. The uncertainty of the interpretations increases with each palinspastic step and with higher degrees of cover-layer erosion. Near-surface structures are considered most accurate, followed by deeper structures based on seismic-reflection and deep-well data. Other parts of the overall section are based on the extrapolation of variably-plunging surface structures, and therefore show one of several possible geometric arrangements that are kinematically admissible. These structures depicted in cross section are the preferred interpretation because they agree with observed seismic-reflection, well-bore, gravity, and magnetic data. Still, many interpretive aspects of this model remain unresolved. For example, reconstructed d2 structures assume basement-rooted structural relief prior to Alleghanian thrust faulting. However, it is unclear to what extent cover folds and associated basement deformation occurred in the foreland during the Taconic Orogeny except along the Taconic unconformity and the central part of the Green Pond syncline. It is also unclear how the shear zones from the early tectonic episode relate to later tectonic stages. Shear zones that are assumed to have produced F1 cover folds are not well exposed in the New Jersey Highlands and are therefore poorly understood and omitted in all the cross sections. However, shear zones of the type mapped at Morgan Hill (Fig. 1.14) may also produce Paleozoic antiforms and synforms in Proterozoic basement where its foliation occurs subparallel to cover bedding before shearing. This helps explain why many open and upright basement folds in the southwest part of the New Jersey Highlands show subparallel alignment with nearby cover folds (Monteverde and

others, 1994). The geometric link between cover folding and basement shearing needs to be more closely examined and may lead to reinterpreted ages for many of the folds mapped in Proterozoic basement.

The geometry of F1 folds in d2 reconstructions are based on a restored Cambrian-Ordovician stiff layer and only stylize restored d2 structures for the Martinsburg Formation. The cross sections are derived using spatial constraints and do not address many incremental strains accumulated in the crust. As many as five incremental strains generally require consideration for finite strain analysis of faulted and folded rocks (Beutner, 1978). The palinspastic reconstruction of d2 structures is straightforward for the stiff layer and addresses tectonic compaction, limb rotation, and assumes negligible penetrative strains from S2 cleavage. d2 structures in the 'stiff layer' reflect the finite state of other pre-thrust incremental strains stemming from sedimentary compaction, pre-cleavage LPS, and S1 LPS. Incremental S1 penetrative strains are difficult to account for because they display spatial variability in both the tectonic transport direction and vertically with the cover. S1 may have formed first in more hinterland parts of the region during the Taconic orogeny and developed into the foreland through the Kittatinny Valley during Alleghanian thrust faulting (Drake and Lyttle, 1980). Slaty S1 cleavage in the Bushkill Member claystone is more pervasive than spaced S1 pressure-solution cleavage in overlying graywacke and sandstone of the Ramseyburg and High Point Members. The relative abundance of S1 lower in the formation may indicate the dispersion of strain upwards into the Martinsburg in response to underlying contraction faults and result in having localized, concentrated shear strain at the base of this sequence (Fig. 1.10). This strain profile is consistent with having upward-diverging cleavage geometry in the hinge of the Stone Church syncline (Fig. 1.13).

S1 is sparse in Martinsburg Formation hornfels near the Beemerville intrusive complex in the northeast Kittatinny Valley (Drake and Monteverde, 1992) and at places

along the Taconic unconformity. Therefore it is inappropriate to use an average regional value of about -50 percent (Beutner and others, 1977; Beutner, 1978; Wright and Platt, 1982) of compressive (shortening) strain when palinspastically accounting for S1 penetrative LPS strains throughout the region. Localized variations in S1 shortening probably span a range of values reported throughout the central Appalachians (-7 percent, Wright and Platt, 1982 to -75 percent, Sherwin and Chapple, 1968). d2 structures for those areas where Martinsburg Formation occurs therefore include the finite state of most S1 penetrative strains because line lengths and layer thicknesses were retained during section balancing.

In the Highlands regions where most of the cover has been eroded or overthrust, d2 cover structures are stylized to depict an Ordovician foredeep developed over a rumpled Lower Paleozoic shelf (Fig. 1.16). These methods and assumptions result in a d2 reconstruction portraying cover structures just prior to thrust fault movement and therefore only serve to constrain the geometric admissibility of present structures by helping ensure that individual thrust sheets fit together in a kinematically admissible manner. d2 structures do not intend to portray the continental margin at a specific time because thrust systems typically develop incrementally through time as they break forward.

d1 structures depict the Lower Paleozoic carbonate shelf as broadly arching upwards. This alignment partly stems from the d2 structures retaining a northwestward inclination relative to the position of the sole fault after accounting for d3 fold and thrust-translation strains. The d1 arching also stems from extrapolating the restored position of the foreland sequence southeastward beneath the keels of the d2 synclines in conformance with the structural-relief modelling assumption. More work is needed to determine if this positive crustal flexure is a geometric artifact of imposed modelling constraints or if this flexure approximates the architecture of the early Paleozoic

peripheral bulge that probably marked this region.

Conclusions

This work demonstrates that the northwestern margin of the New York recess contains a parautochthonous thrust system of Paleozoic age composed of Proterozoic basement through Middle Paleozoic cover. The regional thrust system is probably soled by a master fault within basement rocks. Likely estimates of foreland orogenic contraction for those areas presently underlain by Paleozoic cover range from about 30 km in the southwest to about 10 km in the northeast. Tectonic contraction in the foreland stemming from the Alleghanian thrust faulting dies out rapidly northeastward from the Pennsylvania Salient into the New York Recess. This strain gradient was accompanied by progressive steepening of basement faults northeastward along strike in the New Jersey Highlands and a concomitant transition from foreland-directed thrusting in the Valley and Ridge to crustal transpression in the Highlands. The partitioning of bulk strain between the Taconic and Alleghany orogenies varies in the region with proportionately higher Taconic strains recorded in directions toward the map traces of the Taconic allochthons. Tectonic strain in the Kittatinny Valley (Appalachian Great Valley) attributed to the Taconic Orogeny is minimal whereas most strains probably stem from Alleghanian processes. More work is needed measuring incremental strains related to S1 with respect to both lithology and structural position to gain a better understanding of the palinspastic geometry of the Ordovician foredeep and the Taconic foreland.

TABLE 1.1 REGIONAL CROSS SECTION
TECTONIC DIMENSIONS

Cross section	minimum foreland translation (km)	minimum contraction ratio *(L_1 / L_0)	e (F1) (km)	wedge taper angle
A - A'	7.3	0.80	-.05[1.6]	8°
B - B'	13.8	0.71	-.08 [2.8]	8°
C - C'	21.8	0.64	-.04 [1.6]	11°
D - D'	20.9	0.58	-.11 [5.5]	11°
* L_1 , current length; L_0 , restored length.				

Figure 1.1. Generalized bedrock geology of the New York Recess showing the location of the study area, regional cross sections, and nearby seismic reflection data. Modified from Williams (1978). The distribution of Cambrian-Ordovician rocks at the Jenny Jump-Crooked Swamp (JJCS) thrust belt serves to approximate the fault length when calculating a length-displacement scaling ratio.

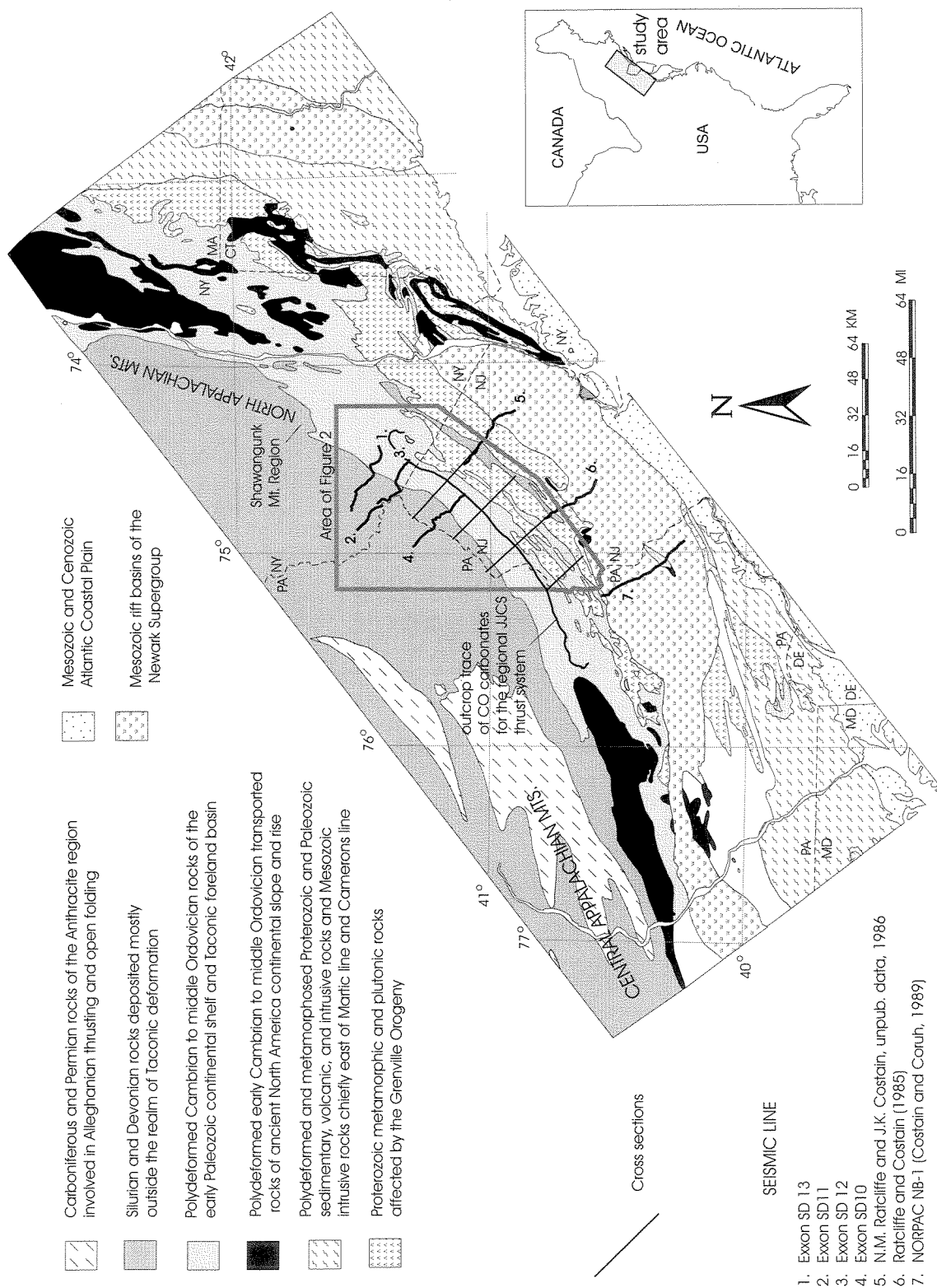


Figure 1.2. Generalized bedrock geology of northern New Jersey and adjacent area showing location of cross sections, seismic reflection lines, and deep petroleum-exploration wells. Geology modified from Drake and others (1994). Tectonic zones in the Hudson Valley adapted from Epstein and Lyttle (1987). MH - Morgan Hill, SM - Scotts Mountain, GPS - Green Pond syncline, SC - Stone Church syncline, HK - Hope klippe, HS - Halsey syncline, PKV - Paulins Kill Valley, ns - nepheline syenite, hf - Martinsburg Formation hornfels.

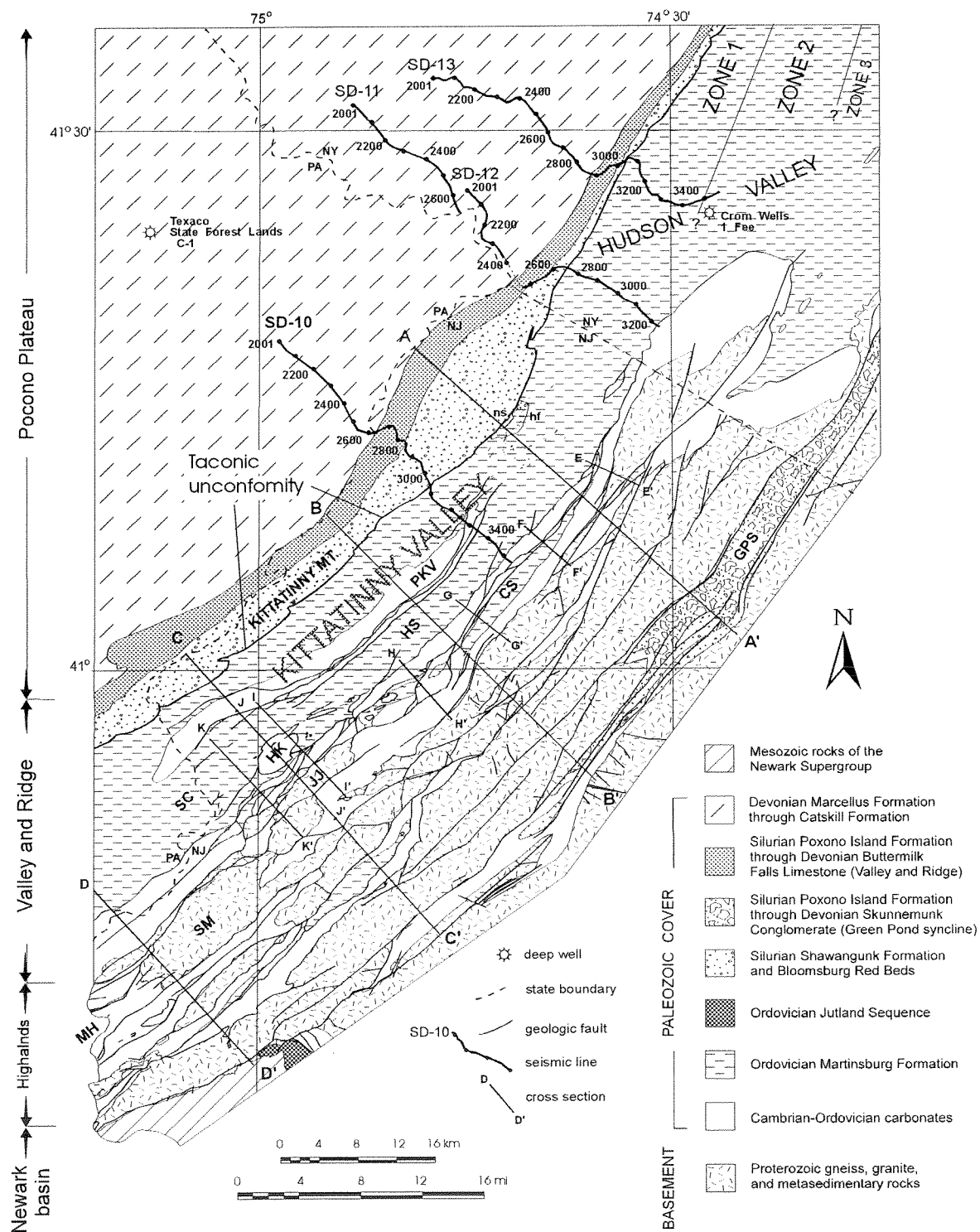


Figure 1.3. Fence-panel diagram summarizing the distribution and thicknesses of the Paleozoic rocks in the study area. Thicknesses are shown above the basement-cover contact. Data compiled from Sherwood (1964), Davis and others (1967), Offield (1967), Sevon and others (1989), Sanders (1983), Herman and Monteverde (1989), and Herman and Mitchell (1991).

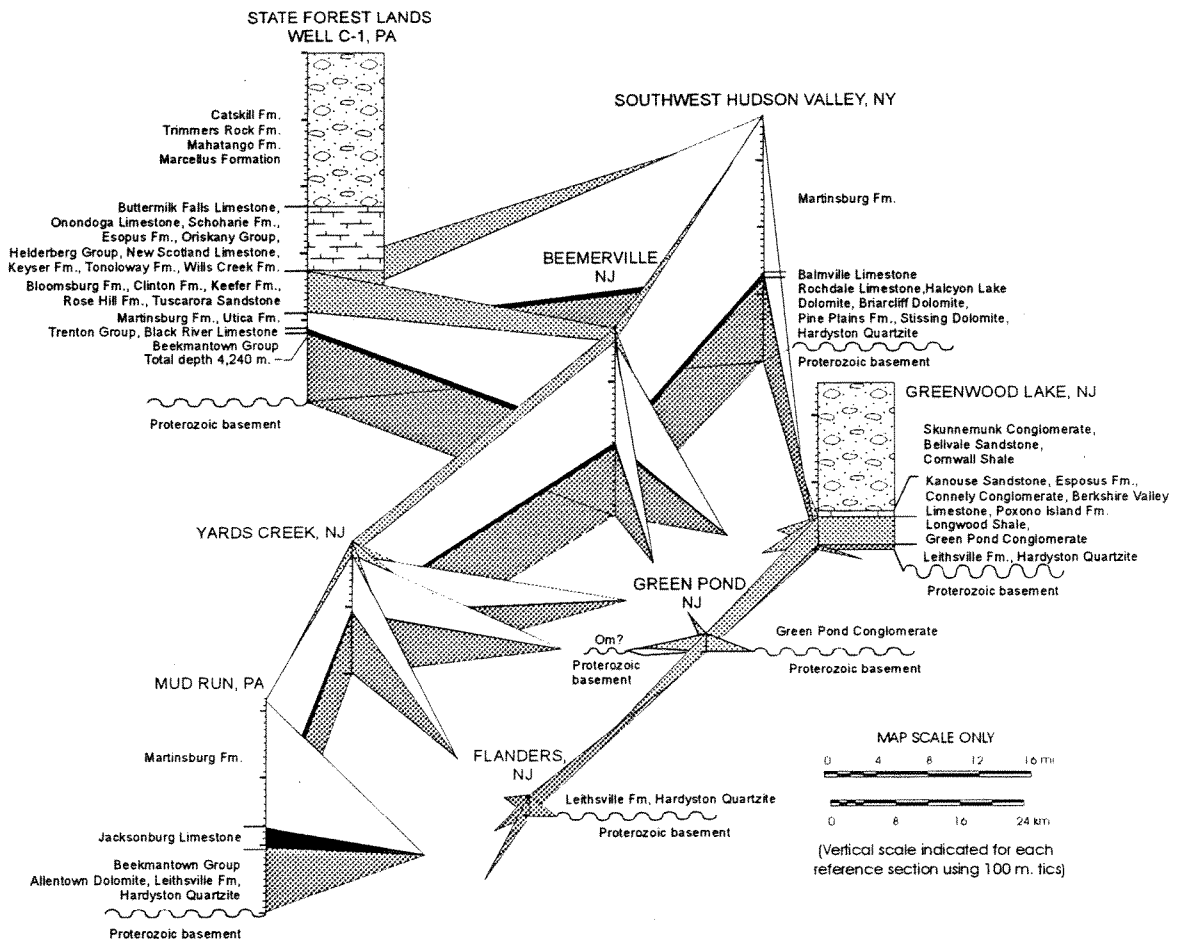


Figure 1.4. Exxon seismic-reflection profiles SD-10, SD-11, SD-12, and SD-13. Profiles show a maximum 64-fold CDP migrated data on the central foreland of the New York Recess in New Jersey, Pennsylvania, and New York. The shot-point locations are shown in Figure 1.2.

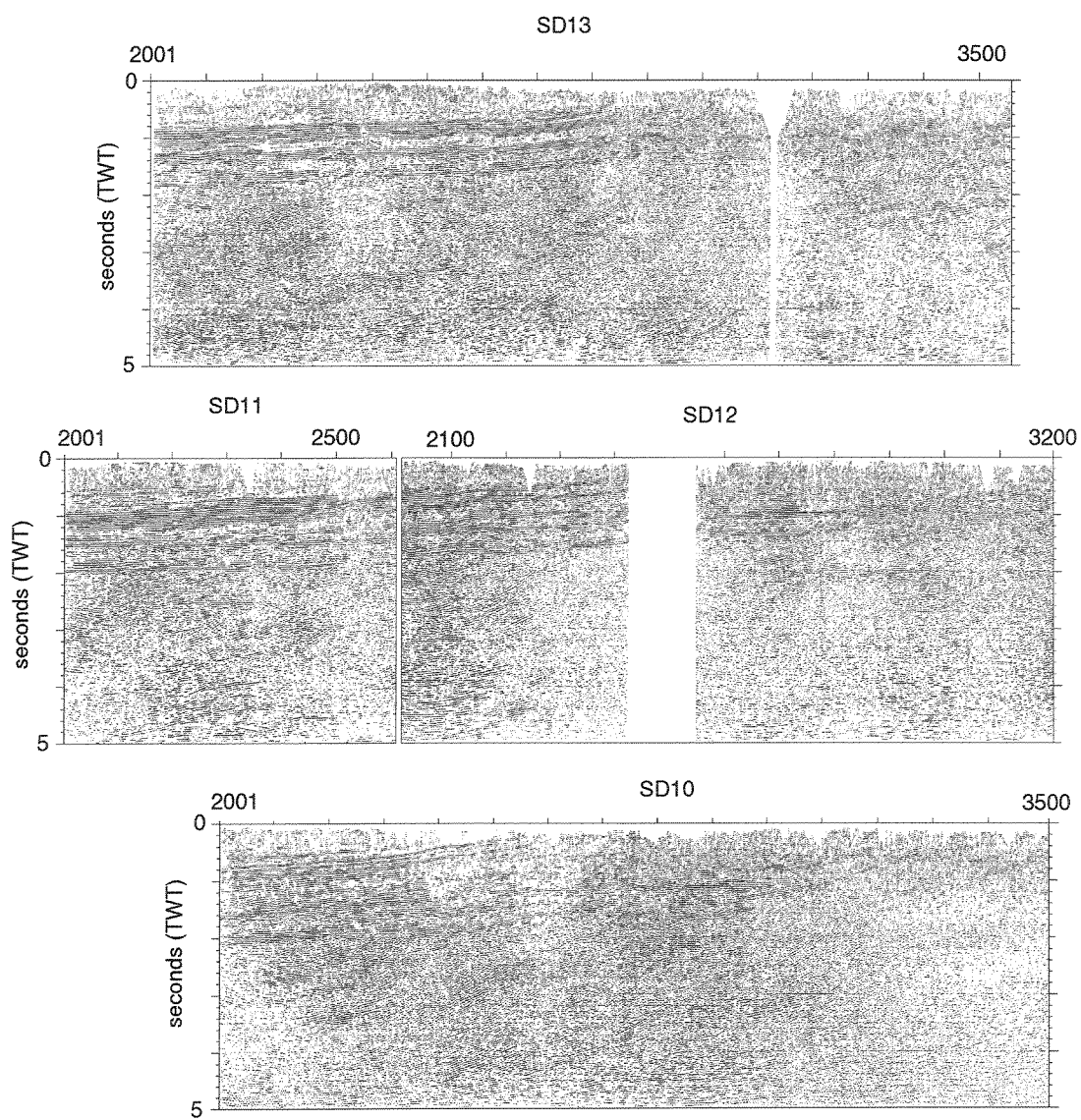


Figure 1.5. A summary of the ages, compositions, and thicknesses of the rock units in the study area, the corresponding seismic units, key reflection horizons, and characteristic seismic-reflection configurations used for interpretation of the seismic-reflection data.

Age	Seismic units, rock types, and reference reflector horizons (unit boundaries)	Reference sections, lithic groups, formations, and group thickness values (meters)			Stratigraphic notes and characteristic seismic reflection configurations	
		Texaco State Forest Lands well C-1	New Jersey Valley and Ridge			
DEVONIAN	D - Sandstone, conglomerate, siltstone, shale, quartzite	Catskill Formation, Trimmers Rock Formation, Mahantago Formation, Marcellus Formation	2316 *	Marcellus Formation	274	Coarsening-upward flysch to molasse. Simple-layered reflectors lower in unit generally become more chaotic upwards.
	H	Buttermilk Falls Limestone, Schoharie Formation, Esopus Formation, Oriskany Group, Helderberg Group, New Scotland Formation, Keyser Formation, Tonoloway Formation, Willis Creek Formation	948	Buttermilk Falls Limestone, Schoharie Formation, Esopus Formation, Oriskany Group, Helderberg Group, Rondout Formation, Decker Formation, Bossardville Limestone, Poxono Island Formation	616	Mostly calcareous rocks. Pronounced, simple-layered reflectors become more chaotic eastward and at shallow reflection depths.
SILURIAN-DEVONIAN	SD - Limestone, dolomite, calcareous siltstone, and shale					
SILURIAN	S - Sandstone, siltstone, shale, quartzite	Bloomsburg Formation, Clinton Formation, Keefer Formation, Rose Hill Formation, Tuscarora Formation	622	Bloomsburg Red Beds and Shawangunk Formation	884	Coarse- to fine-grained siliceous rocks with simple, oblique, and sigmoidal reflection configurations. Truncated reflectors and pinch outs.
	SB					
ORDOVICIAN	O - Siltstone, shale, sandstone	Martinsburg Formation, Utica Formation	259	Martinsburg Formation	1372	Fine- to coarse-grained siliceous clastics with minor carbonates. Complex reflectors resembling stratigraphic onlaps and pinch outs.
	OS					
CAMBRIAN-ORDOVICIAN	CO - Dolomite, limestone 'stiff layer'	Trenton Formation, Black River Formation, Beekmantown Group	109*	Jacksonburg Limestone, Sequence at Wantage, Beekmantown Group, Allentown Dolomite, Leithsville Formation, Hardyston Quartzite	1220	Carbonate rocks with minor siliceous interbeds. Continuous simple-layered reflectors towards top of unit. Generally discontinuous reflectors in lower part of unit.
	T					
B	Proterozoic gneissic and granitoid Grenville basement. Generally chaotic reflectors locally showing simple-layered configurations. Local intervals with reflectors arranged in broad and open arches resembling 'roll over' in the hanging wall of normal faults.					

* total thickness penetrated in well

Figure 1.6. Borehole data for Texaco well C-1 showing stratigraphic correlation to northwest end of Exxon profile SD-11. The BHC sonic log and conventional velocity analysis are by Texaco. The synthetic seismogram was generated by Exxon. See text for further discussion.

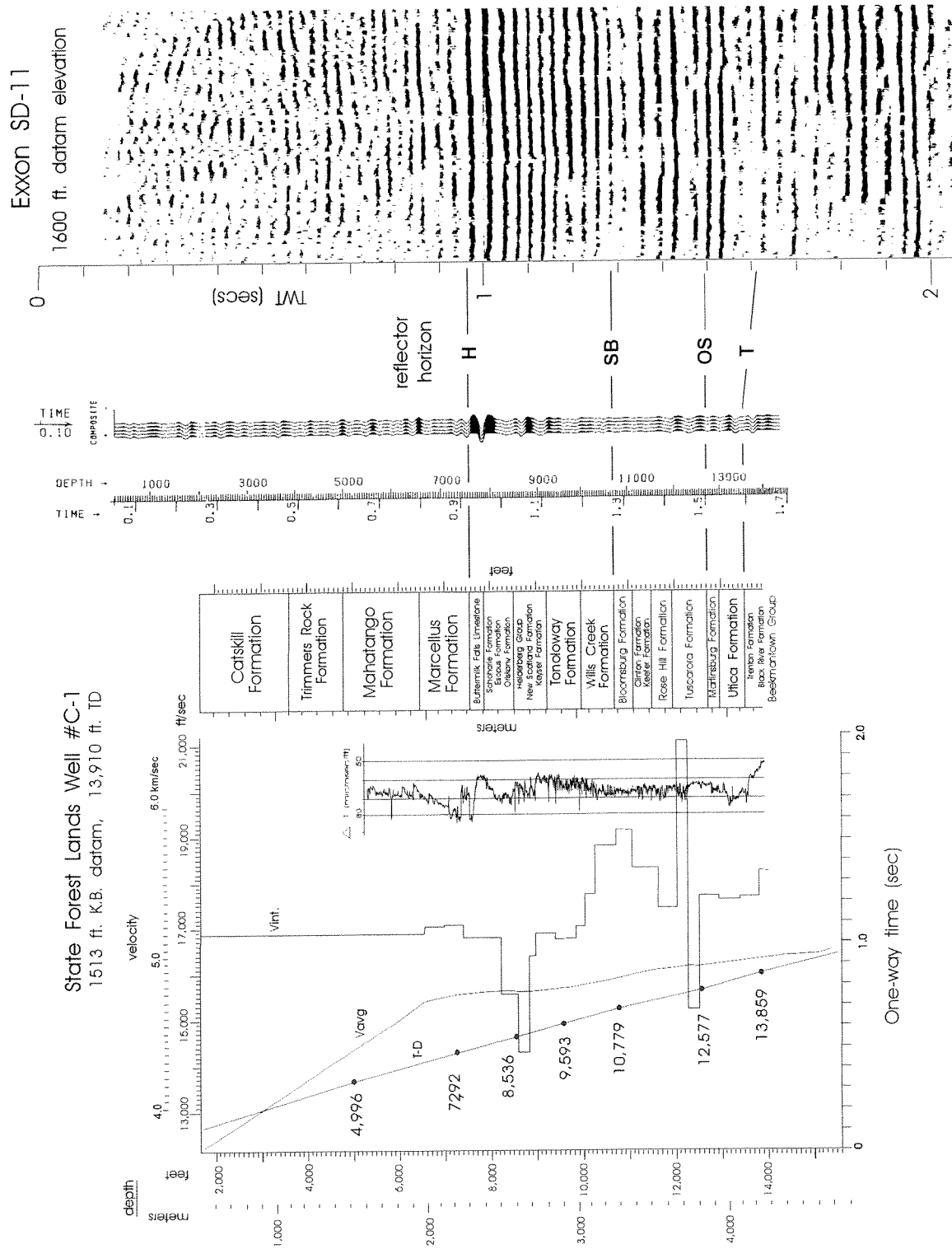


Figure 1.7. Exxon seismic-reflection profile SD10. Geologic interpretations shown for both the migrated, full-display (top) and conventional line drawing of the unmigrated profile (bottom). PZ - Proterozoic, CO - Cambrian-Ordovician carbonates, O - Ordovician flysch, S - Silurian molasse, SD - Silurian-Devonian undivided, D - Devonian undivided. Reflection horizons H, SB, OS, T, and B correspond to the seismic unit boundaries shown in figure 1.5. r - rollover reflection configuration, ol - onlap reflection configuration. po - pinch out reflection configuration. SO is the map location of the Silurian-Ordovician contact. Heavy lines show faults.

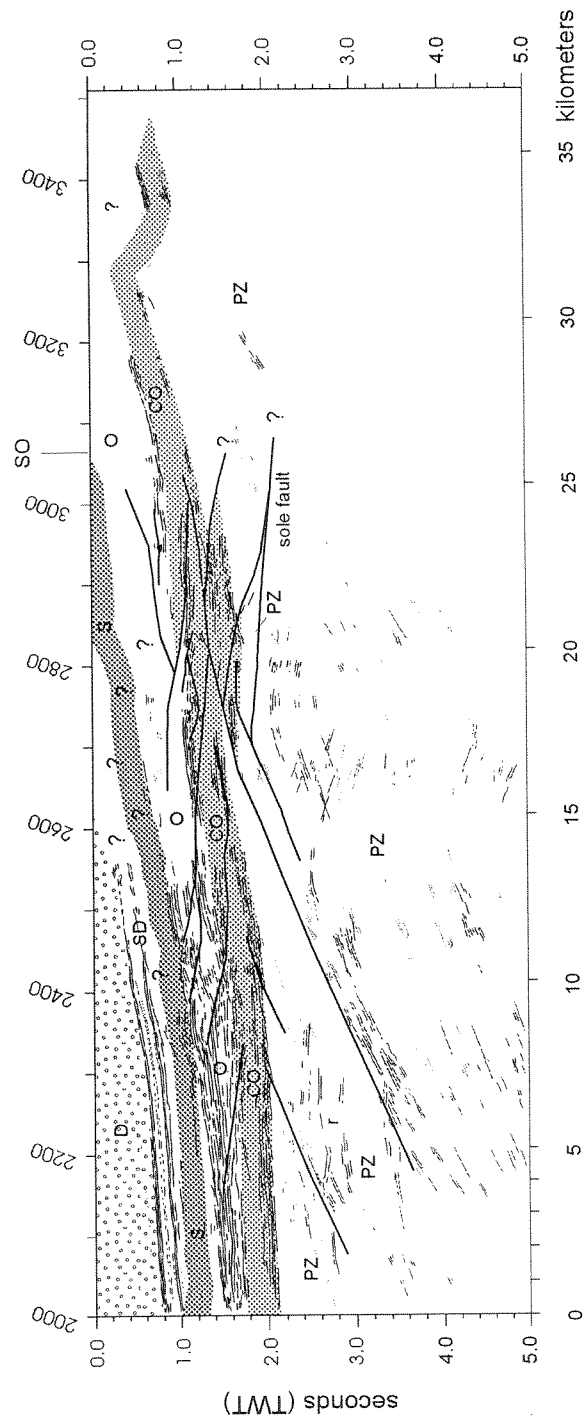
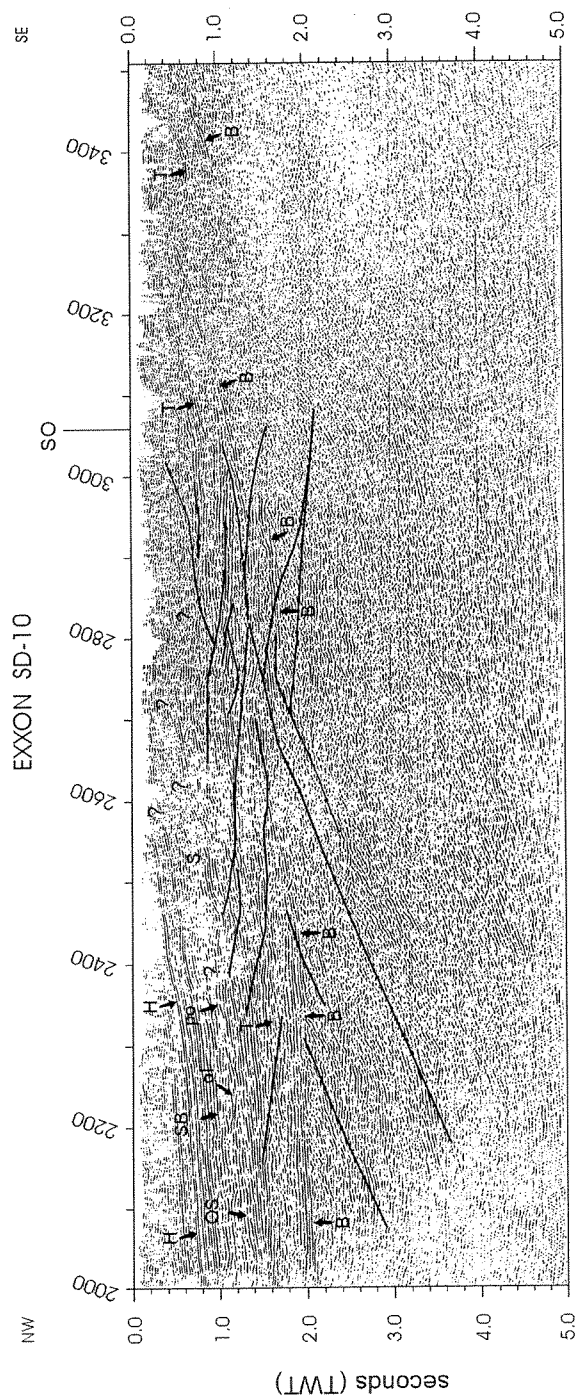


Figure 1.8. Exxon seismic-reflection profiles SD-11 and SD-12. Geologic interpretations shown for both the migrated, full-display (top) and conventional line drawing of the unmigrated profile (bottom). Abbreviations and symbols as in figure 1.7 except, tr - truncated reflectors, cl - complex layering reflection configuration.

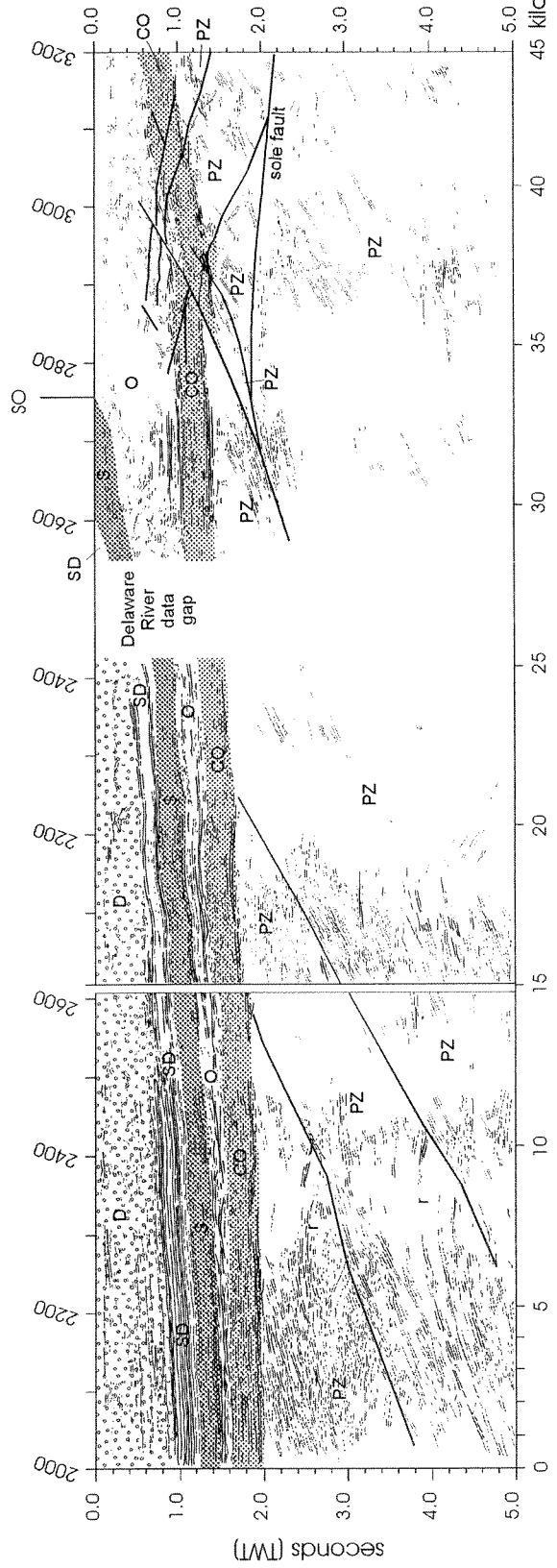
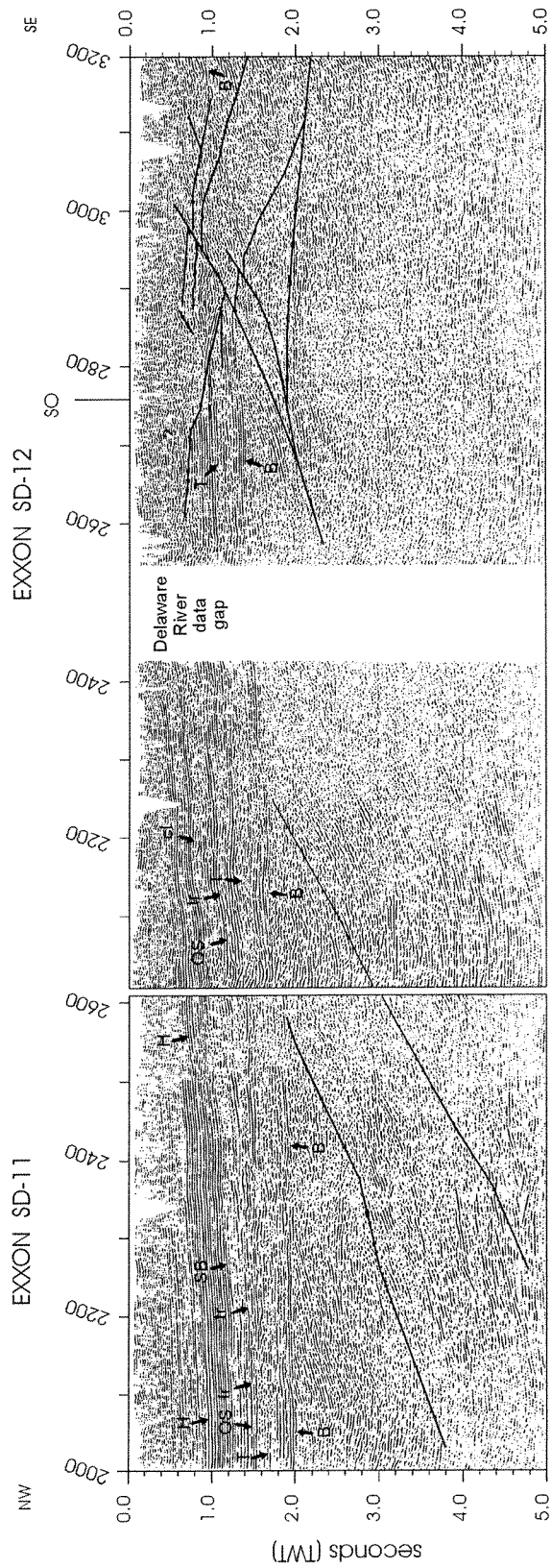


Figure 1.9. Exxon seismic-reflection profile SD13. Geologic interpretations shown for both the migrated, full-display (top) and conventional line drawing of the unmigrated profile (bottom). Abbreviations and symbols as in figures 1.7 and 1.8.

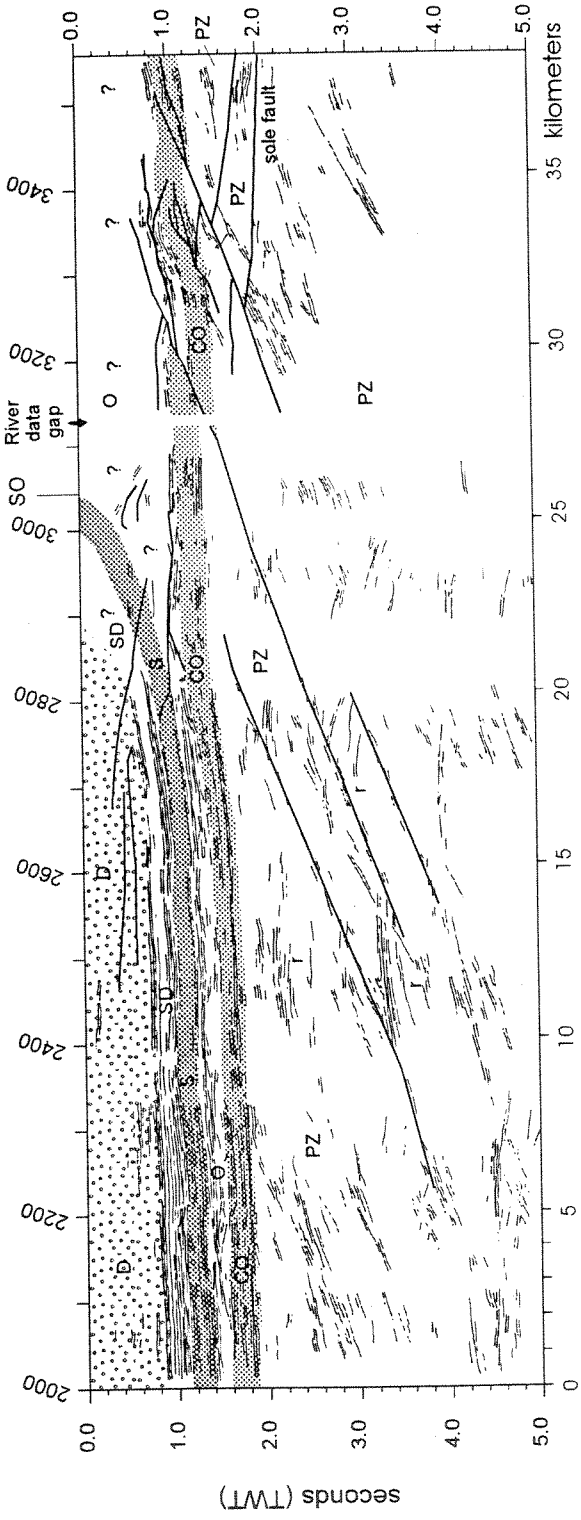
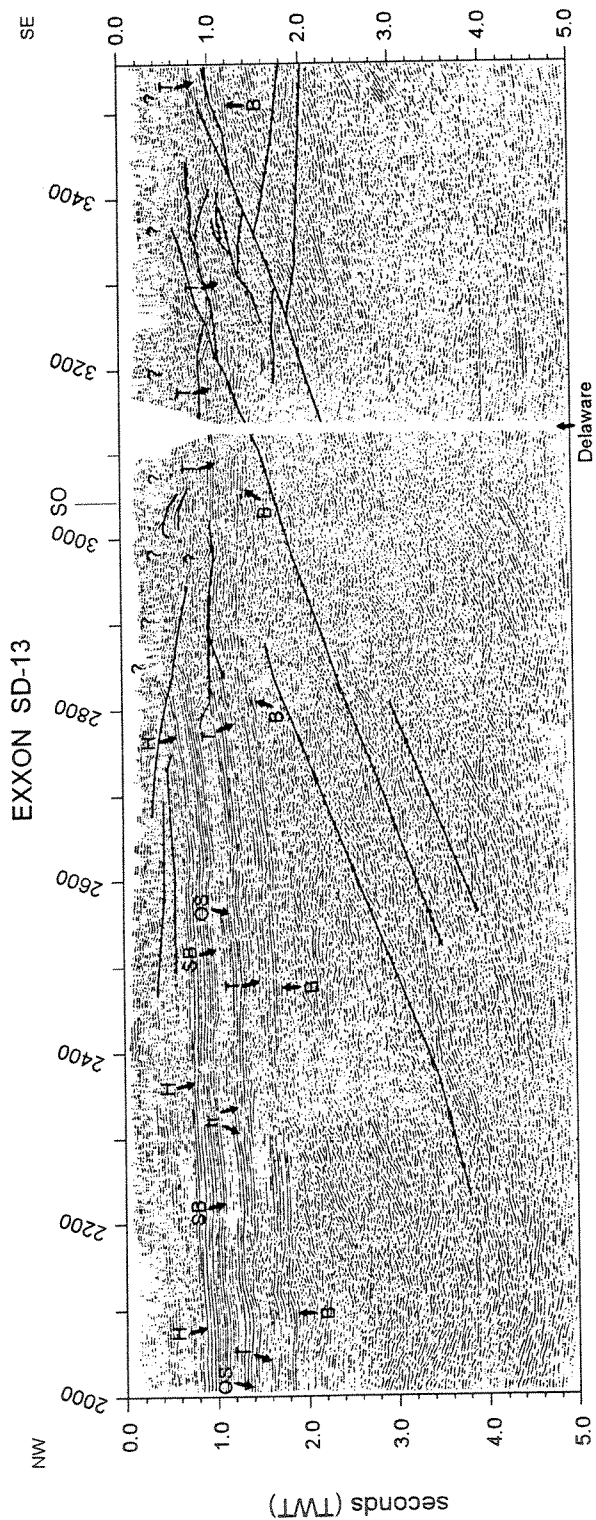


Figure 1.10. Geologic interpretations of the Exxon seismic-reflection profiles shown in serial arrangement. Profiles are aligned to the map trace of the Taconic unconformity (SO). Abbreviations and symbols as in figure 1.7

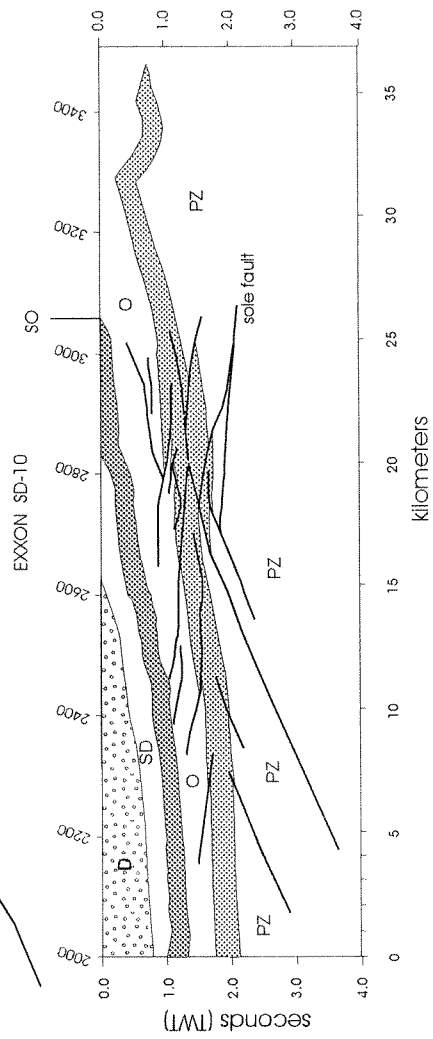
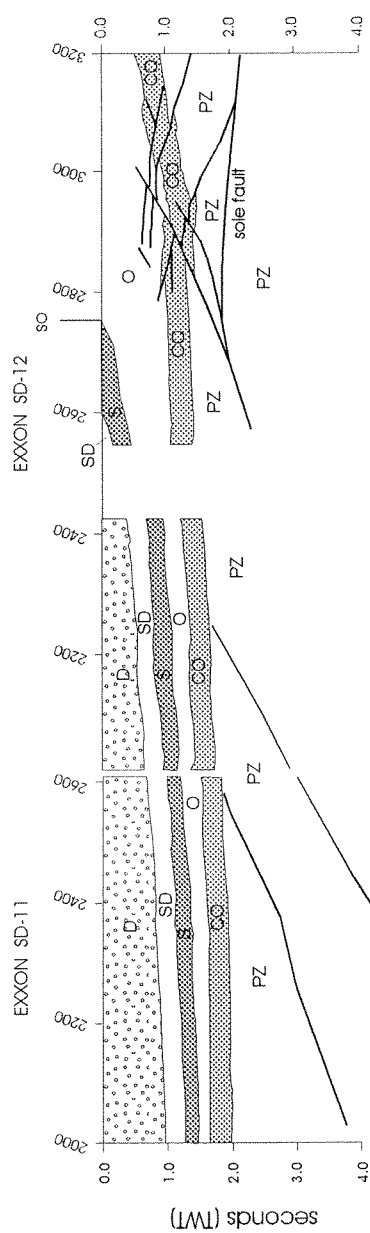
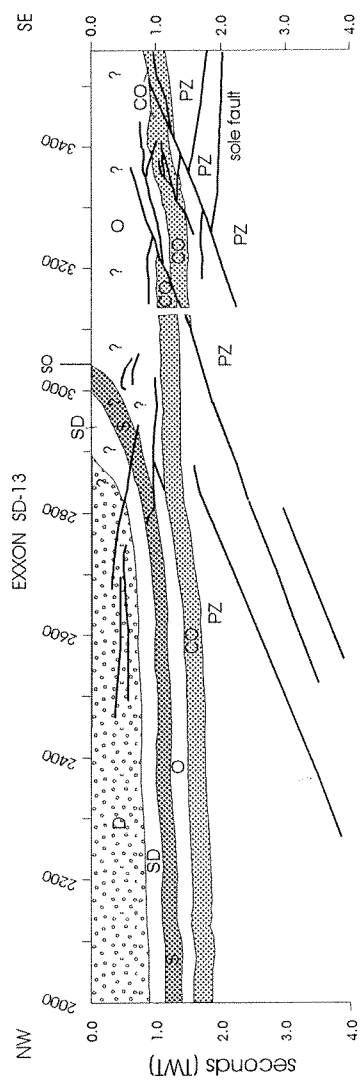


Figure 1.11a. Tectonic map of the Kittatinny Valley, N. J. Geology modified from Herman and Monteverde (1989) and Drake and others (1994). PKF - Paulins Kill foreland, ns - nepheline syenite, hf - Martinsburg Formation hornfels, HK - Hope klippe, SCS - Stone Church syncline, HS - Halsey syncline.

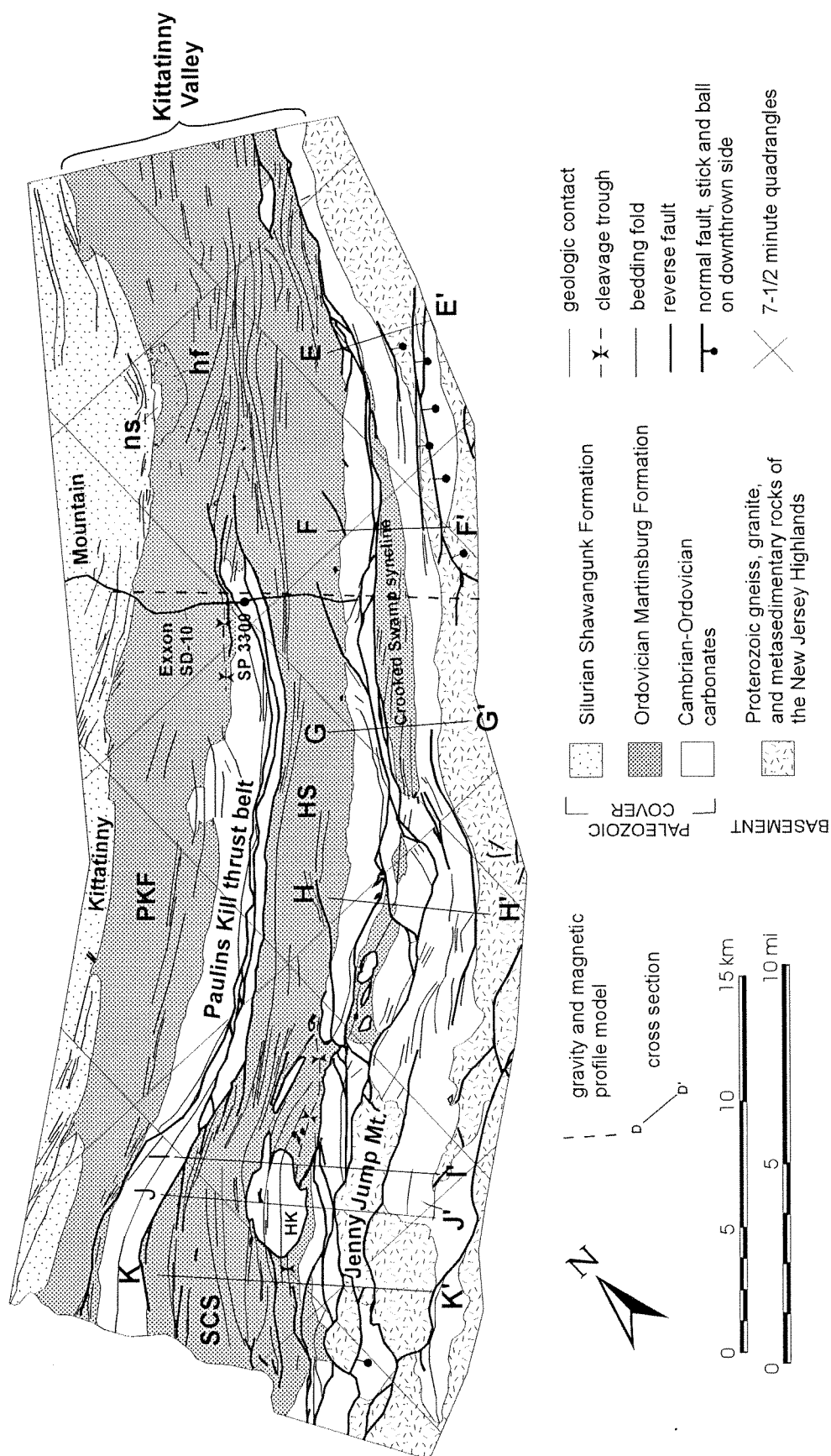


Figure 1.11b. Aeromagnetic map of the Kittatinny Valley, N. J.
Aeromagnetic data modified from Snyder (in press).

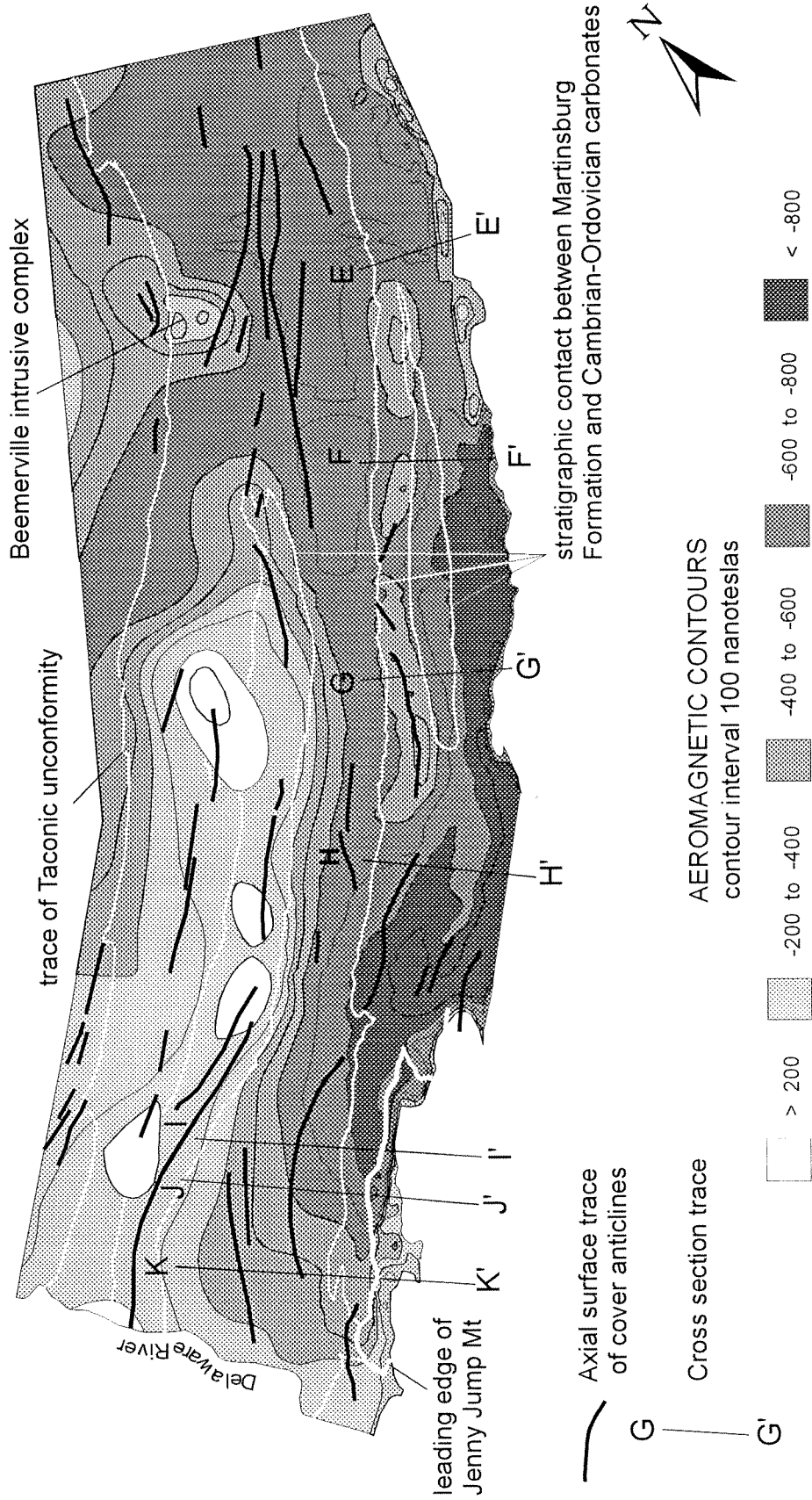
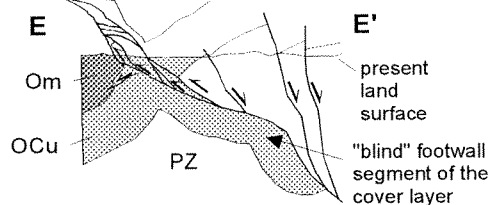
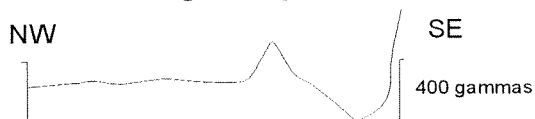
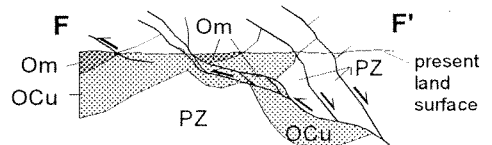
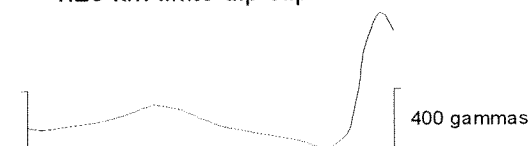


Figure 1.12. Balanced cross sections of the Crooked Swamp thrust belt, northeast Kittatinny Valley, N.J. Locations of the profiles show in Figures 1.2 and 1.11a. Aeromagnetic data from LKB resources (1980). Om - Martinsburg Formation, OCu - Cambrian-Ordovician carbonates and Hardyston Quartzite undivided, PZ - Proterozoic basement undivided.

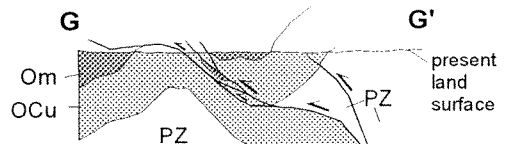
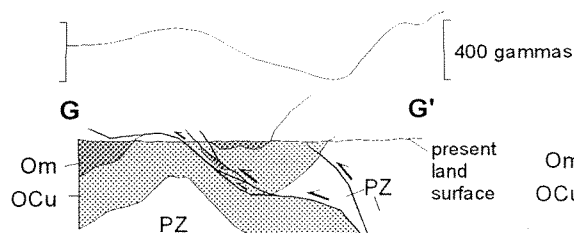
Current structures with aeromagnetic profiles



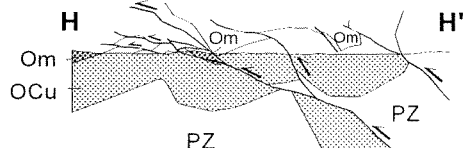
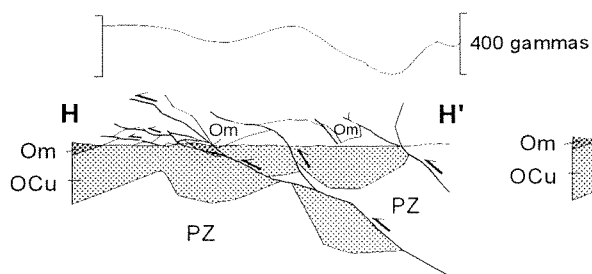
4.20 km finite dip-slip



2.68 km finite dip-slip

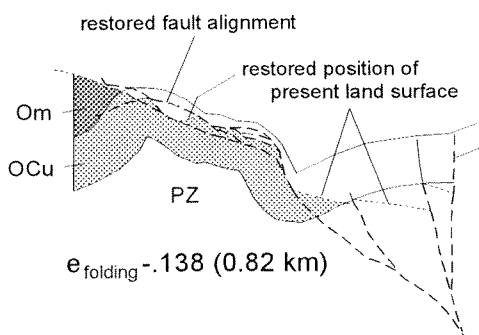


3.46 km finite dip-slip

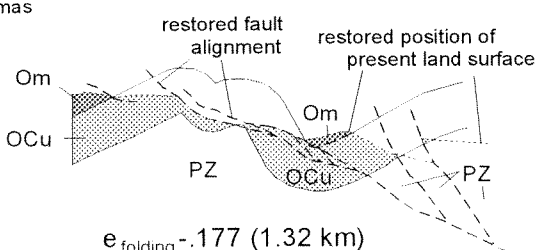


3.65 km finite dip-slip

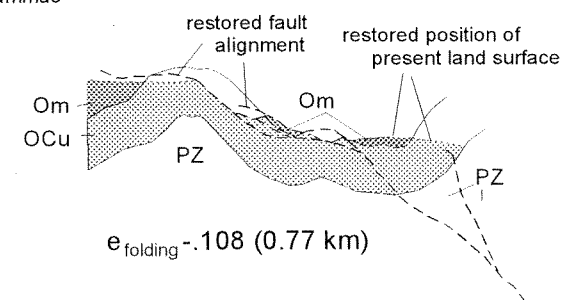
Structures restored to pre-thrust (F1) folds



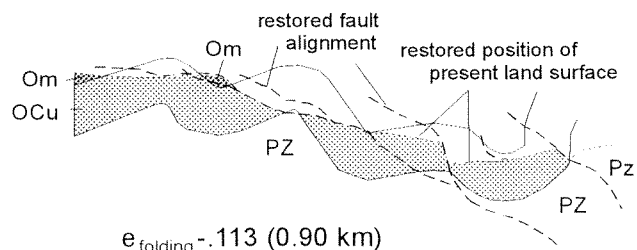
$e_{\text{folding}} = -.138$ (0.82 km)



$e_{\text{folding}} = -.177$ (1.32 km)



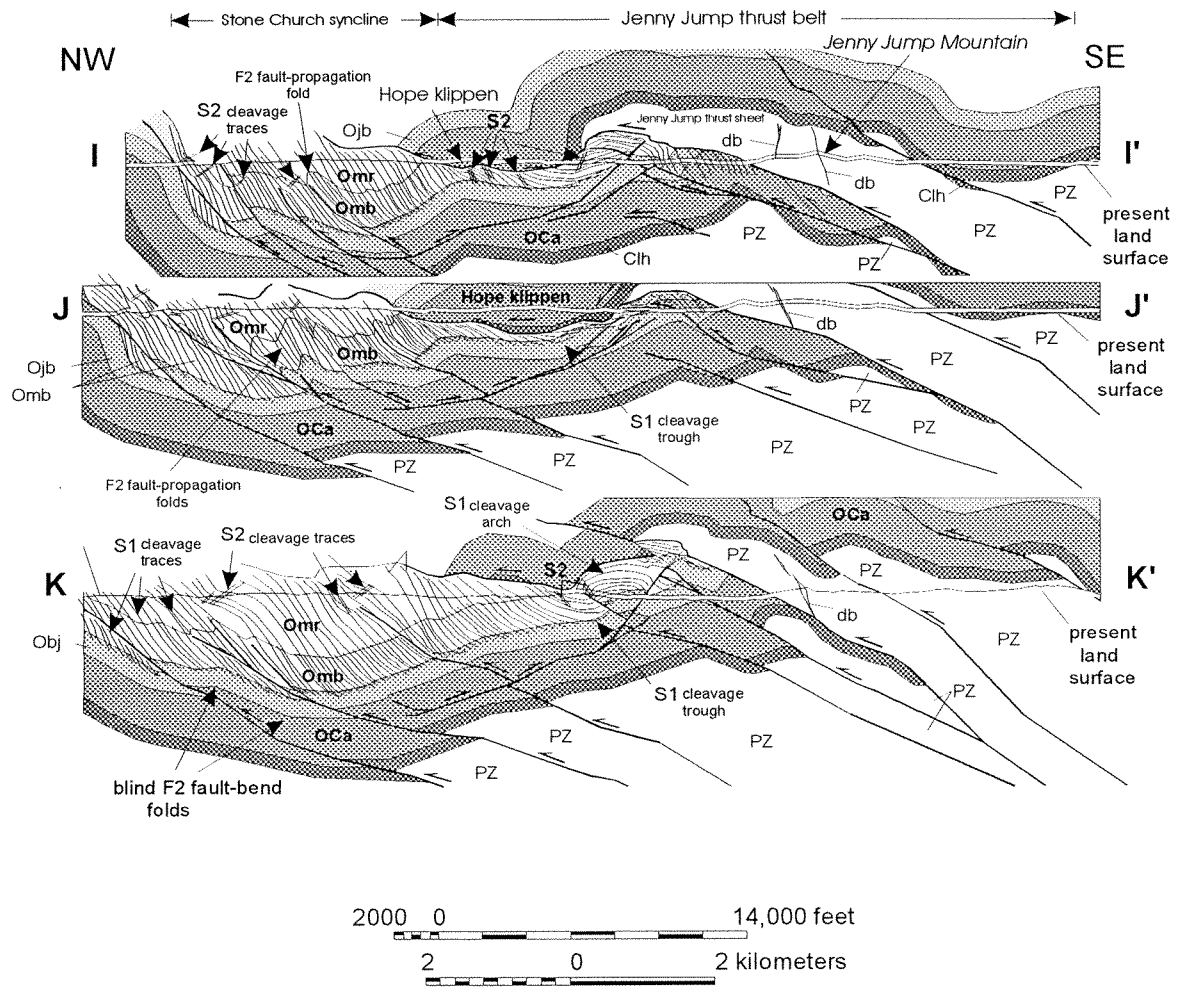
$e_{\text{folding}} = -.108$ (0.77 km)



$e_{\text{folding}} = -.113$ (0.90 km)

0 5 km

Figure 1.13. Cross sections of the Jenny Jump thrust belt and Stone Church syncline in the southwest Kittatinny Valley showing structural details associated with of emplacement of the Hope klippen. The broad and open Stone Church syncline and "blind" cover antiform beneath Jenny Jump Mt. are interpreted as F1 folds. F1 folds are assumed to include S1 cleavage. All faults and associated bedding (S0) and F2 folds in cover are interpreted as d2 structures along with S2 cleavages. Location of the profiles and the Hope klippen shown in figures 1.2 and 1.11a. J-J' is palinspastically restored in figure 1.16 as part of regional cross section C-C'.



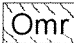




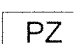
 Ramseyburg Member of Martinsburg Formation	 Allentown Dolomite
 Bushkill Member of Martinsburg Formation	 Leithsville Formation and Hardyston Quartzite
 Jacksonburg Limestone and Beekmantown Group	 Proterozoic gneiss, granite, and metasediments

Figure 1.14. Diagram showing geometric link between cover-layer folding and basement shear zones at Morgan Hill, Pa along the Route 78 road cuts. The location of Morgan Hill is shown in Figure 1.2. The similar orientations of the cover-layer fold axis enveloping the northeast end of Morgan hill (Fig. 14b) and underlying basement shear zones (Fig. 14c) demonstrate their structural link. Lower diagram (1.14a) shows a 2-1/2-dimension rendering of the basement-cover contact, based on six outcrops located with arrows. The basement shear zones are traced in the east-bound face cuts. The stereographic digrams are lower-hemisphere, equal-angle projections. The cover-layer fold axis is plotted as the pole to 17 great circles for bedding mapped around the termination of Morgan Hill. The intersection maximums of the basement shear zones are shown for 14 planes measured along the base of the east-bound face cut. The structural maximums were determined using a contouring algorithm based on multiples (1, 2, 5, or 7 times) of the average relative density of points (poles) plotted on a sperical surface (Gray and Lewis, 1985).

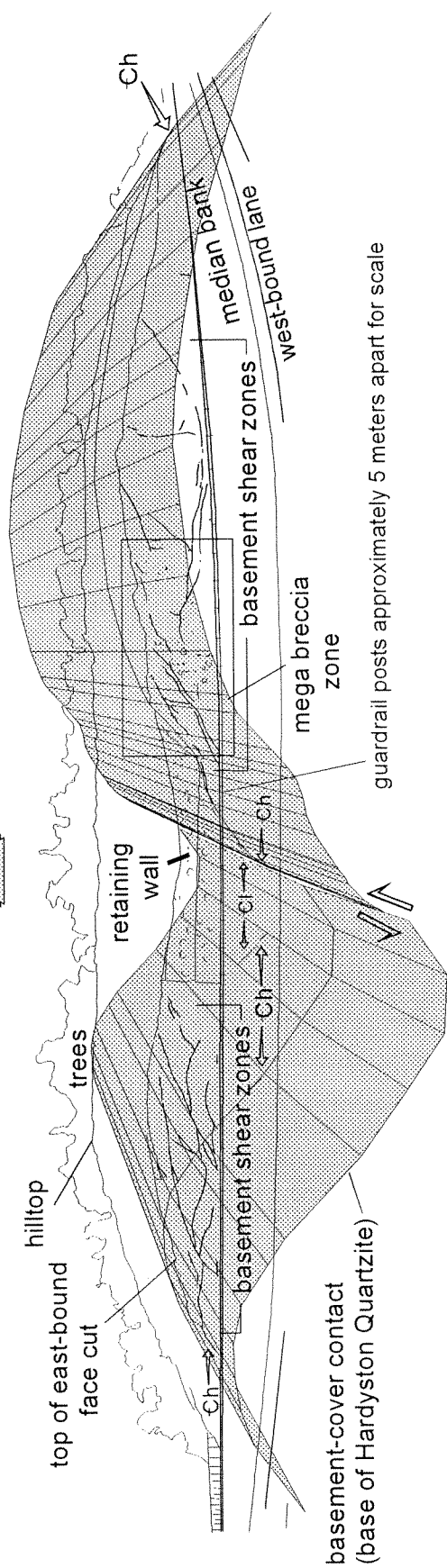
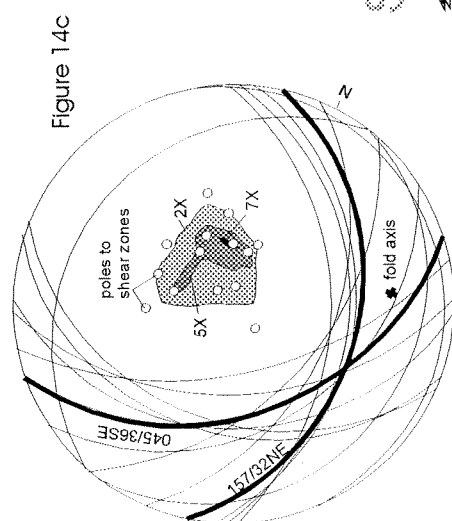
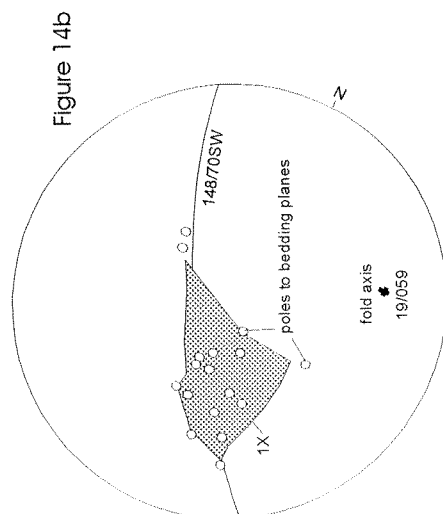


Figure 1.15. Present-day cross sections A-A' to D-D' in the foreland region of the New York Recess. Structures are area and line-length balanced with respect to earlier structures shown restored in Figure 16. The location of the cross sections is shown in figures 1.1 and 1.2. DSu - Devonian and Silurian undivided. Sbs - Silurian Bloomsburg Red Beds and Shawangunk Formation. Slg - Silurian Longwood Shale and Green Pond Conglomerate. Om - Ordovician Martinsburg Formation, Oj - Jacksonburg Limestone (section D-D' only). Ockj - Ordovician Jacksonburg Limestone, Cambrian-Ordovician Kittatinny Supergroup and Cambrian Hardyston Quartzite. PZ - Proterozoic basement. bic- Beemerville intrusive complex. db -diabase dike. MZu/OCu/PZ - undivided Mesozoic, Paleozoic, and Proterozoic rocks southeast of the Newark basin border fault.

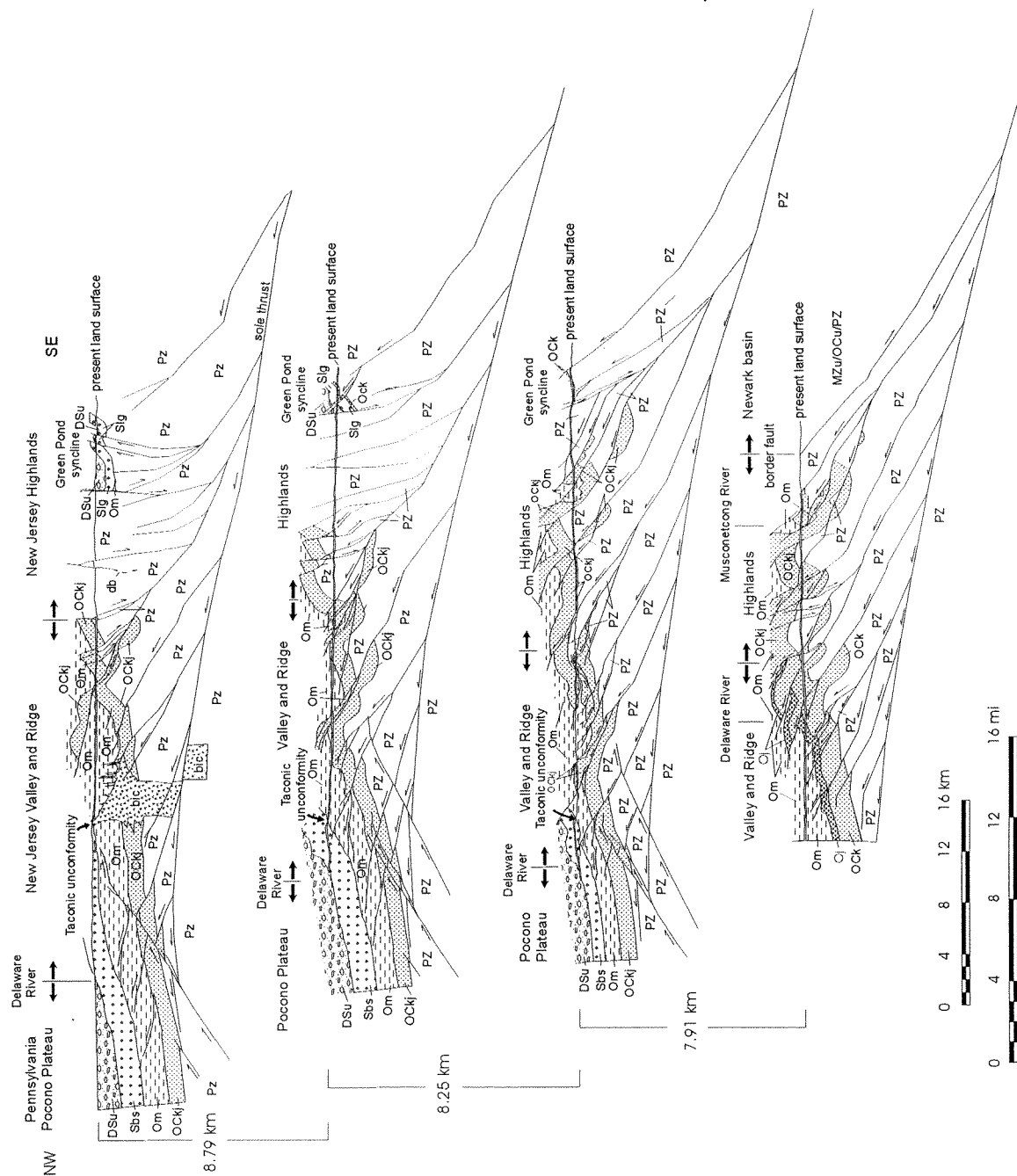


Figure 1.16. Retrodeformed cross sections A_r-A_r' to D_r-D_r' structures (d2 and d1) in the foreland region of the New York Recess. d2 structures reconstruct d3 (Alleghanian) thrust-fault trajectories and related F2 fold and S2 cleavage strains. d2 structures with F1 cover folds include the finite state of S1 penetrative strains. d1 structures depict the alignment of the basement-cover contact from which shortening related to F1 folding was calculated. d1 arches upward beneath the keels of F1 synclines and constrains the amount of basement shear strain accompanying F1 cover folding. t_0 is the difference in depth between the sole fault and d1. t_0 decreases in thickness towards the foreland. Rock-unit abbreviations as in figure 1.7 except Oj - Jacksonburg Limestone, Ow - sequence at Wantage.

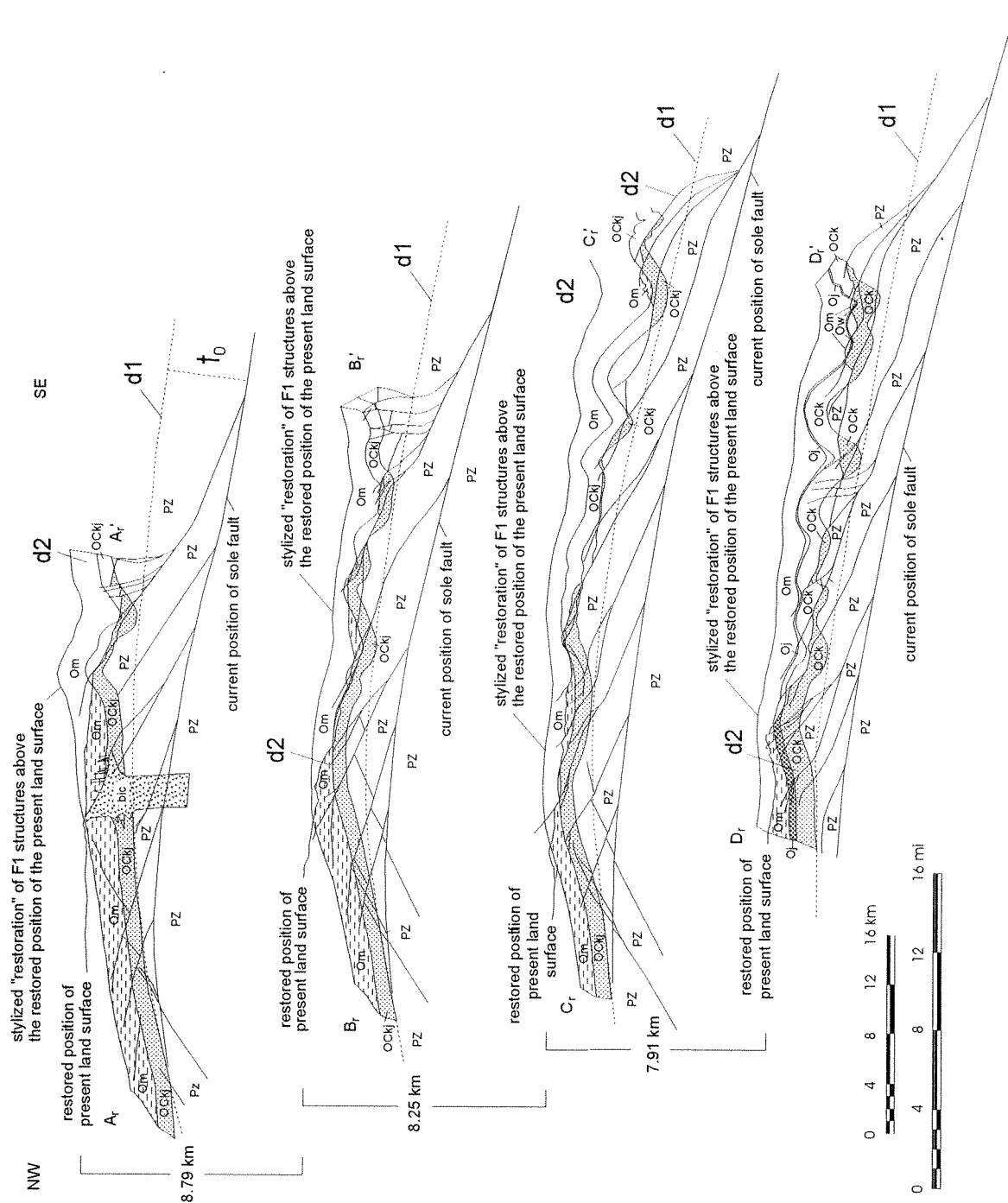


Figure 1.17. Cross section A-A' showing present-day and reretrodeformed structures and the methods for deriving tectonic dimensions (Table.1). The d2 position of the basement-cover is shown superimposed on d3 (upper figure) to illustrate the structural-relief modeling assumption explained in the text. Rock-unit abbreviations as in figure 1.7.

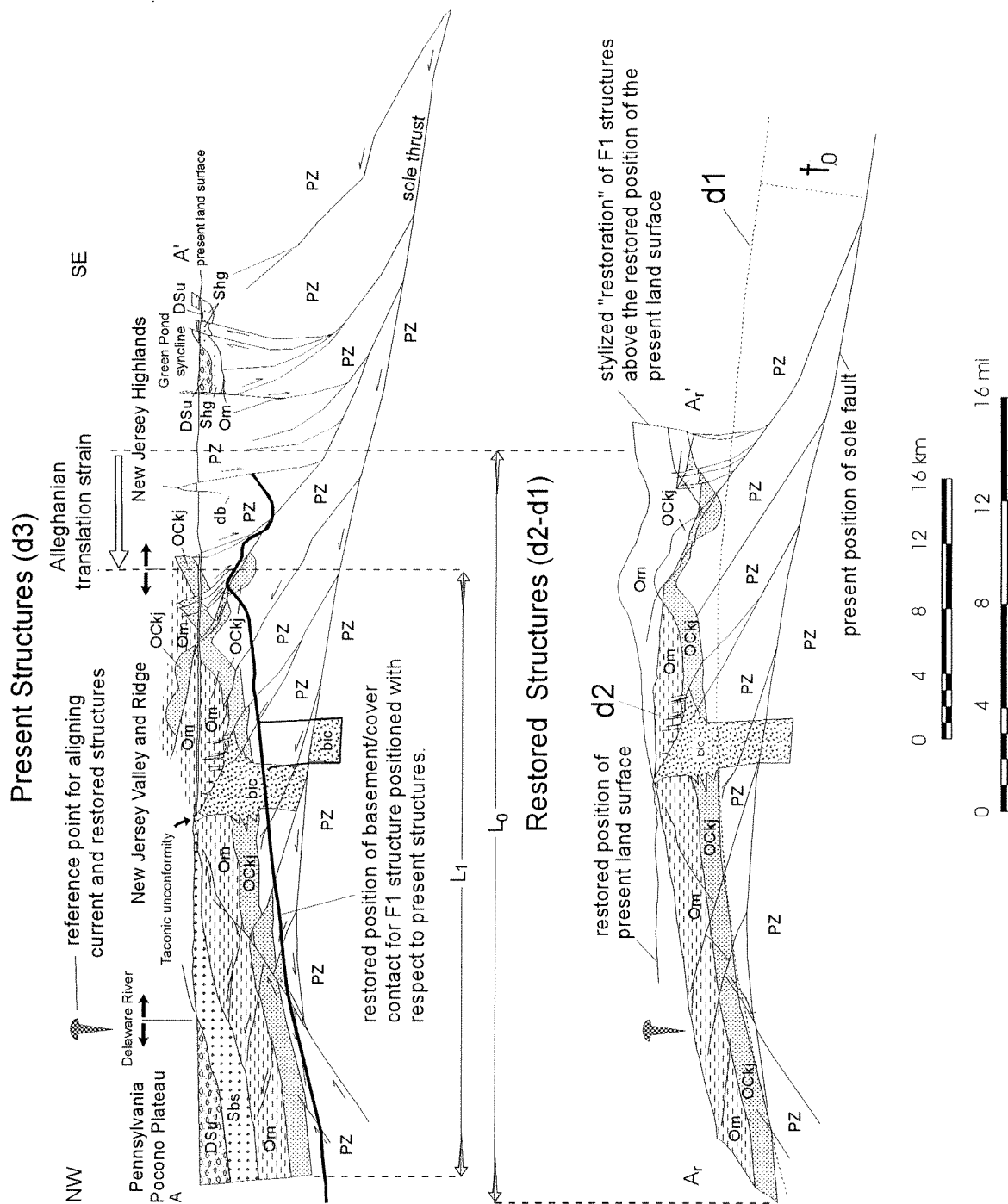


Figure 1.18 Bouguer-gravity-anomaly and total-intensity-magnetic-anomaly model for the north-central part of the Kittatinny Valley, NJ. Location of profile shown in Figure 1.11a. Observed gravity and magnetic data from Jagel (1990) and Ghatge and others (1992). Bouguer residual values derived from the regional gravity gradient of Jagel (1990). Calculated anomalies based on two-dimensional, nonlinear, least-squares, inversion modeling using commercial software. Polygon-model values shown with density-contrast and magnetic-susceptibility model values (ex. $-.35/.00020$). Density contrasts are shown in g/cm^3 relative to an average model density value of 2.67 g/cm^3 .

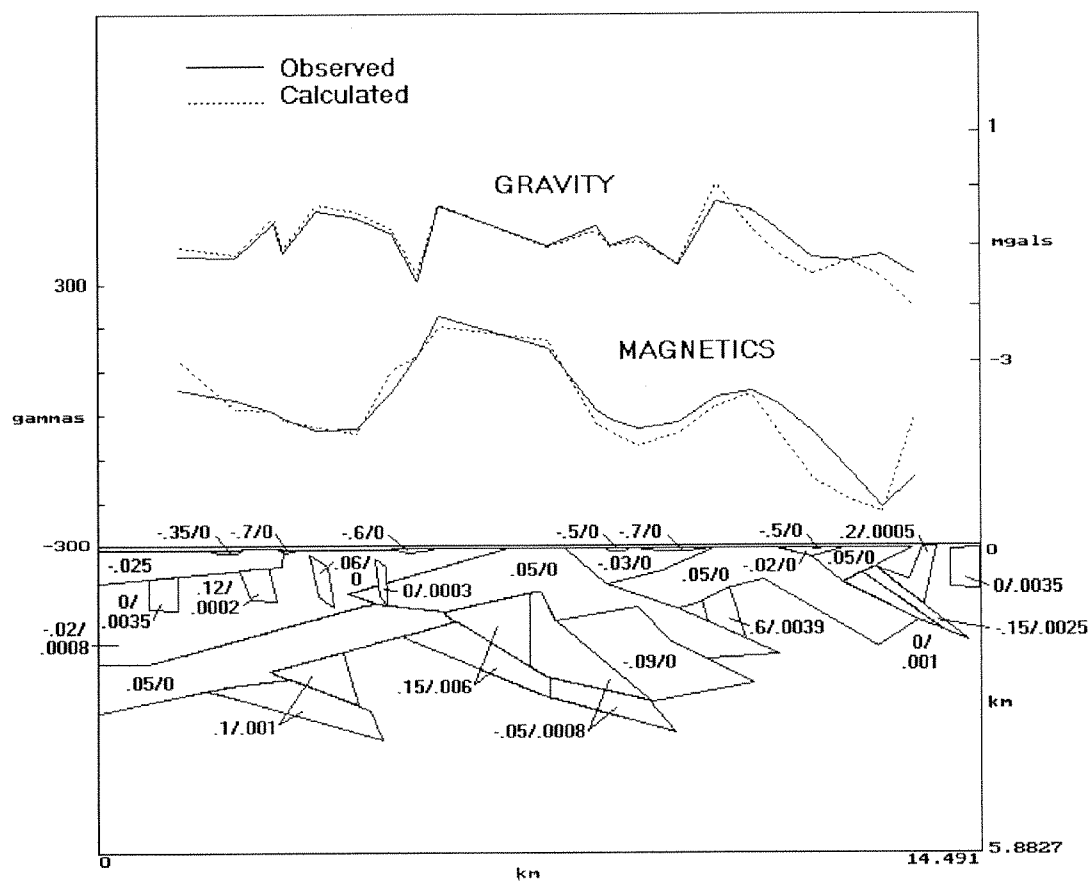
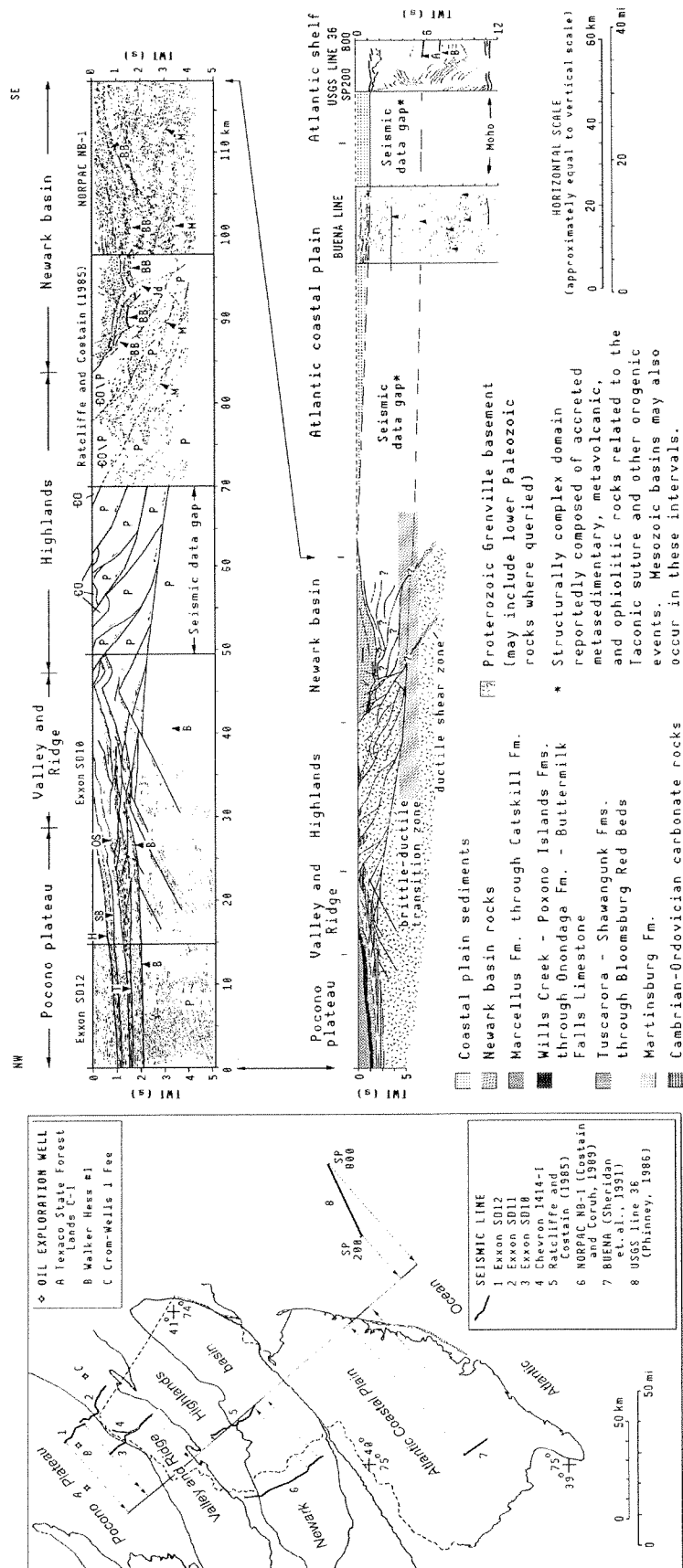


Figure 1.19. Physiographic-province map and schematic regional cross section of the New York Recess modified from Herman (1992). Line drawings from seismic-reflection data are composited northwest of the Atlantic Coastal Plain. Lines of profile projection shown on the map. Regional cross-section shows current data gaps for seismic-reflection database and the location of the brittle-ductile transition based on normal geothermal gradients (Sibson, 1977). Abbreviations as in figure 1.5, and BB = bottom of the Newark basin, Jd = Jurassic diabase, M = mylonitic fault zone.



CHAPTER 2. NJGS BEDROCK GEOLOGY DIGITAL DATA MODEL; FIELD DATA MANAGEMENT, ARC/INFO GIS, DIGITAL CARTOGRAPHY, AND ELECTRONIC DATA PUBLISHING

Introduction

This chapter explains the methods used by the N.J. Geological Survey for generating, managing, analyzing, displaying, and distributing digital geologic data. These methods include the use of personal computer (PC) software for managing outcrop and remotely-sensed structural geology data and a geographic information system (GIS) running on Sun microcomputers to produce digital maps and georeferenced data. The geological data layers (coverages) are documented according to federal standards, archived as electronic data, and distributed to the public through a publication sales office and the Internet. A summary of these methods is a basis for comparing aspects of data management and attribution used by the NJGS to methods used by others. A brief explanation of the vocabulary and notation used to describe the computer-based methods is first given for reference. A brief history of the NJGS organizational environment explains why these methods were developed. An application of the methods explained here is given in Chapter 3.

Document Notation and Software Trademarks

Different styles of text annotation are used in this chapter to help elucidate computer-software functions. An asterisk in a computer file name denotes a set of computer files having the same file-name extension. For example, *.SRT denotes all files with the .SRT extension. PC-DOS files and programs are identified with capital letters whereas UNIX files use lower-case letters in bold typeface, for example **meso.aml**. The following commercially-available computer-software programs also use capitalized or

italicized letters to denote trademarks. ARC/INFO, ARCEDIT, and ARCPLOT, and AML are registered trademarks of Environmental Systems Research Institute, Inc. UNIX is a registered trademark of AT&T Bell Laboratories. MS-DOS is a trademark of Microsoft Corporation. *PowerBASIC* is a trademark of SPECTRA Publishing. Sun SPARCstation is a registered trademark of Sun Microsystems, Inc.

The series of programs, scripts, and data files comprising the NJGS Field data Management System (FMS) are not trademark registered and may be freely obtained, used, and redistributed. The use of FMS for the remainder of this work denotes version 2.1 unless otherwise indicated. FMS program files are capitalized below and use bold type face. File-name extensions are not included when using this notation (for example, **FIELDATA** versus FIELDATA.PBC).

Background

I began working as a field geologist in the NJGS Bureau of Geology and Topography in 1985 at the start of the COGEOMAP program. After conducting several studies with outcrop-based structural data using manual methods of data selection and graphic analysis, I researched computerizing these data and methods to facilitate structural analyses. LOTUS spreadsheet and dBASE relational-database software were evaluated for managing the data, but found to be inadequate for sorting data consisting of complex character strings. Spreadsheet data files also resulted in unnecessarily large files containing many vacant data cells. Maggie Kaeding of the NJGS offered to help create a custom field data management program using the BASIC program language. Our combined efforts resulted in the first version of the Field Data Management System (Kaeding and Herman, 1988). This software consists of uncompiled BASIC programs that provide a flexible, compact database and database-management program for sorting and rearranging structural data collected throughout the region.

In 1992 after COGEOMAP I transferred to the NJGS Bureau of Ground Water Resources Evaluation and began supervising the Data Management and Analysis (DMA) Section. The DMA section began designing a digital geologic database for the COGEOMAP data using ARC/INFO Geographic Information Systems (GIS). We also modernized the GIS laboratory with Sun SPARCstation microcomputers (workstations) connected to desktop PCs using an ethernet local-area network. This effort included adding an E-format (34 inch-wide media) optical scanner, raster-to-vector conversion software, and an electrostatic plotter. By 1994 the NJGS had a modern GIS laboratory for creating and maintaining digital geological databases and publishing geological maps using digital cartography. More recent efforts include the development of an electronic information archive with a distribution outlet on the Internet's World-Wide Web at <http://www.state.nj.us/dep/njgs/>.

The NJGS started building 1 to 24,000 scale bedrock geology coverages using COGEOMAP as a digital cartographic tool in 1992. Mark produced mylar sheets of machine-drafted lines representing geologic contacts and oriented map symbols in lieu of scribing lines on peel coats as part of the standard cartographic process for producing geologic maps. Mark also developed ARC Macro Language (AML) scripts in ARCPLOT for automatically plotting oriented geologic-map symbols. His work formed the basis for other digital-cartographic tools that the NJGS later developed to produce full-color, bedrock geologic maps (Herman and others, 1993; 1994). The advance of these digital-cartographic methods also spurred the development of other PC-DOS data input/output (I/O) and structural-analysis programs for the FMS. I upgraded the FMS strating in 1994 by restructuring the original programs and integrating new ones. The second version of the FMS now includes a set of MS-DOS programs written and compiled in *PowerBASIC* and another set of ARC/INFO AML scripts and ARCPLOT form menus (Herman and others, 1993; 1996).

Overview of the NJGS FMS

The data management and analysis functions of the FMS were developed by the NJGS to facilitate digital-geologic-map production and for use in characterizing the structural framework of fractured-bedrock aquifers. Brief explanations are given for many of the FMS functions including how geologic and geographic data are managed and how FMS-DOS and FMS-UNIX interrelate. A user's guide is available for the FMS that provides full explanations and examples of the programs (Herman and others, 1996). Uncompiled version of the FMS-DOS programs and the set of AML scripts and ARCPLOT form menus are on file at the offices of the NJGS and are available upon request.

The original set of FMS (ver. 1.0) programs were rewritten and compiled using *PowerBASIC* language during 1993 to 1996. FMS-DOS now includes 15 programs compiled as executable (*.EXE) and chained (*.PBC) PC-DOS files (Fig. 2.1). These include 2 software-control programs, 1 database-management program, 3 data-sorting programs, 5 data-analysis programs, and 4 file I/O programs. The utility of the software-control, database-management, data-sorting, and data-analysis programs are summarized below showing examples of data-file structure. The utility of the data I/O programs are explained in the FMS User's Guide (Herman and others, 1996).

FMS-DOS has been used on desktop MS-DOS PC's with 386 and 486 processors, a minimum of 4 Mb RAM, and VGA monitors. FMS-DOS programs are controlled by keyboard entry in response to command-line prompts. FMS-DOS is started by typing <FMS> at the DOS prompt within the directory where the programs reside. The executable FMS.EXE program calls the FMS program-control menu (**FMSMENU**) that provides a link to the other chained programs as illustrated in figure 2.2. The FMS-DOS programs are designed to use a specific set of directory paths that minimize keyboard

responses to program queries. Using the following set of DOS directory paths when setting up the FMS will often allow a single keystroke to be issued in response to a command-line prompt within a program rather than having to type multiple characters that specify file I/O directory paths:

- C:\FMS\AML - Directory holds output files from **FRACGEN** for generating ARC/INFO GIS line coverages
- C:\FMS\DAT - Directory holds output files from **STERCONV** for input to Rockware's STEREO program
- C:\FMS\DOC - Directory contains FMSDOC.WRI (User's Guide for Windows 3.1)
- C:\FMS\FD - Directory holds **FIELDATA** and **EZSORT** data files
- C:\FMS\LIN - Directory holds **LINSORT** data files
- C:\FMS\MES - Directory holds mesostructure sort files (*.MES)
- C:\FMS\LUT - Directory holds mesostructure statistics files output from **ROSESTAT** for input into **DATASORT**.
- C:\FMS\SRT - Directory holds sorted structural geology orientation data files output from **DATASORT** program used for input into **ROSESTAT**
- C:\FMS\STA - Directory holds data files generated within INFO that contain spatial coordinates used by **FRACGEN**

FMS-DOS Data Files

FMS data files mostly use comma- and space-delimited ASCII-text characters arranged in a sequential format (Tables 2.1 and 2.2). The **FIELDATA** file (*.FD) is the standard data file. Each *.FD file uses a STATION variable for noting the beginning and end of a data record for an individual field station or outcrop (Table 2.1). Alphabetic variables are used for the types and kinds of structural features (Table 2.3) and the location variable recording a structural province or domain (Table 2.1). Integer variables are used for structural-orientation data and station numbers. The stratigraphic variable can be integer based or alphabetic (Appendix A).

*.FD files can be created through use of the FMS database manager (**FIELDATA**) or can be generated by typing data with an ASCII text editor. The second

kind of **FIELDATA** file (*.FDZ) uses an abbreviated data format for organizing presorted structural-orientation data for one kind of structure from a set of field stations. The *.FDZ file only contains variables delimiting field stations and specifying station number integers and corresponding structural-orientation readings (Table 2.1).

*.FD files can be sorted and reassembled into other *.FD files using combinations of geographic, stratigraphic, and structural variables with **VARISORT**. They can also be sorted to output files containing structural-orientation data for a subset of geologic units, geographic locations, or a set of station numbers using **DATASORT**.

The **DATASORT** program outputs two kinds of data files. The first is a sort file (*.SRT) containing structural-orientation data for the strike and dip of planes or the trend and plunge of lineations (Table 2.2). The *.SRT file is input into the **ROSESTAT** and **STERCONV** programs for conducting orientation-analyses. Another kind of sort file is the mesostructure file (*.MES) that contains a station number, corresponding values of structural-orientation data, and a variable used for setting the size of a graphic marker symbol used for automated digital cartography (Table 2.2). The *.MES file is used in the FMS-UNIX **meso.aml** digital-cartography process (Fig. 2.3) and in the FMS-DOS orientation-analysis programs **FRACGEN** (Fig. 2.4) and **ARCAZMTH** (Fig. 2.6). **EZSORT** is another data-sorting program used in conjunction with *.FDZ files to produce *.SRT and *.MES files.

FMS-DOS Analysis Programs

The FMS-DOS analysis programs include **ROSESTAT**, **ARCAZMTH**, **FRACGEN**, **LINCALC**, and **LINSORT**. **ROSESTAT** generates structural bearing and inclination statistics and DOS-VGA graphics display of circular histograms using simple 1° , 5° , or 10° histogram bins or petals (Fig. 2.5). **ROSESTAT** also produces data-output files (*.LUT) used within **DATASORT** for statistically setting the length value of

ARC PLOT markersymbols to conduct automated structural-data plotting (Table 2.1 and Fig. 2.3).

ARCAZMTH reads the vertex coordinates for chord or polyline segments from AUTOCAD drawing exchange files (*.DXF), calculates each line's azimuth and length, then summarizes the azimuth angle versus percent occurrence of line length for the entire data set using fixed radial sectors of either 1°, 5°, or 10° (Fig. 2.6). **ARCAZMTH** generates VGA-graphics to display the relative frequencies of map-based structural trends using standard-histograms and allows point-based trends input from mesostructure (*.MES) files to be displayed simultaneously (Fig. 2.6). **ARCAZMTH** is used by the NJGS to analyze the orientations of geologic contacts, faults, and fold traces from map coverages to be graphically compared to outcrop-based structural trends. **ARCAZMTH** imports *.DXF files output from ARC/INFO using the **arcdxf** command (Herman and others, 1996).

FRACGEN generates ASCII files containing sets of geographic coordinates corresponding to end points of lines (fracture traces). Each line trace is drawn at an user-specified length from the center of the outcrop location along the map or profile trend. Output files are assigned an *.AML file name extension and are formatted for generating line coverages (Fig. 2.4) using the **&run** command in ARC/INFO.

FRACGEN uses data-input files containing geographic coordinates in state-plane-coordinate feet for the northwest global quadrant, x-coordinate increasing westward and y-coordinate increasing northward. Two types of ASCII-based input files are required. The first input file contains field-station numbers and both x- and y-coordinate values (ex. 45708,785006,500000). This file requires the *.STA file extension and can be generated from within INFO using the **<LIST STATION, X-COORD, Y-COORD PRINT>** command for a pre-existing ARC/INFO bedrock-outcrop theme containing point topology and station numbers (Table 2.4). The

second input file is a mesostructure (*.MES) sort file generated within the **DATASORT** program. Two program-output options are available within **FRACGEN**. The first option generates line traces for the map view corresponding to the structural bearing of planar (strike) or linear (trend) structures. The second output option generates lines of apparent inclination (dip) for planar structures viewed in the vertical profile (cross section). This option requires mesostructure (*.MES) files to contain structural data using the dip-azimuth format (Table 2.2). The apparent inclination of profile structures can be calculated along a map trace specified through keyboard entry of paired coordinates for the profile-trace end points, or along an azimuth (0° - 179°) calculated through the center of the map data. Each outcrop point is projected into cross section along a direction normal to the map trace of the profile. A user-prompted, projection-angle variable determines the depth at which the centers of lines are plotted relative to the location of a zero-elevation datum (map trace). A projection angle of 0° results in all lines centered along a horizontal datum whereas a projection angle of 90° results in lines centered at their respective map coordinates. **FRACGEN** can also plot selected ranges of apparent-dip or map-azimuth values for either views (Fig. 2.4). The line traces generated for the VGA graphics display can be saved to an output file (*.AML) for generating ARC line coverage. Each fracture trace is assigned a line-identification integer (line id) equal to the dip (map) or apparent dip (cross-section) value of the fracture trace.

The **LINCALC** program calculates the plunge and trend of the linear intersection of two planes. Data-input options include manual keyboard entry of orientation values for any two planes or automatic data input for multiple planes from a **FIELDATA** (*.FD) file. The latter option allows the user to input up to three types of planes and calculates the intersections of all planes based on multiple-variable sort criteria (Herman, 1996).

The **LINSORT** program sorts azimuth-orientation data for sets of lineations based on user-specified stratigraphic variables (Table 2.1). Data-input files must have the

*.DAT file-name extension, and must contain an integer variable denoting planar strike (0° - 179°) and an associated character string specifying the stratigraphic units that a lineation intersects. The stratigraphic variable string should have the youngest stratigraphic unit listed first and subsequent units ordered in descending age. The output file name is assigned the file name extension *.LIN. The **LINSORT** program is designed to summarize the frequency of occurrence and azimuth trends of lineations that intersect several lithologic units. **LINSORT** was written as a class exercise to examine the probable age and orientation of fault traces cutting a Late Tertiary volcanic field in El Salvador. *.DAT data files are generated outside of FMS using ASCII text editors and data from a standard map analysis.

FMS-UNIX

FMS-UNIX is a set of uncompiled ARC/INFO (ver. 7.0) AML scripts and form menus written for ARCPLOT that facilitate the graphic display and analysis of geological map structures for either remotely-sensed or outcrop-based structural data (Herman and others, 1994;1996). FMS-UNIX runs on Sun Workstations using Solaris 2.x operating systems and has not been tested on other platforms or different operating systems. These programs use both mouse and keyboard control of program functions. They are organized under the **meso** "root" directory shown in Figure 2.7.

The primary function of FMS-UNIX is automated plotting of graphic-marker symbols on digital maps using the ARCPLOT **meso(.aml)** script. The **meso** script initiates other AML scripts (Fig. 2.7b.) and form menus (Fig. 2.8) that provide options for plotting oriented structural-geologic symbols corresponding to individual graphics files (Fig. 2.9) within ARCPLOT map compositions (Fig. 2.3). An ARCPLOT map composition is converted into an ARC/INFO graphics metafile (*.gra) for peripheral output when plotting hard-copy maps. FMS-UNIX therefore does not generate

ARC/INFO symbol themes or point coverages. It only generates digital-graphics files organized as file directories. However, ARCPLOT graphic metafiles can be converted to other data-exchange formats (*.DXF, *.PLT files) for display of hardcopy graphics using commercial desktop-publishing software.

meso.aml uses the custom ARCPLOT marker-symbol set **bedrock.mrk** that contains 144 structural-geology symbols. **bedrock.mrk** uses the custom ARCPLOT font set **fnt034** (Fig. 2.7a) that was digitized by the NJGS. Some of these geologic symbols are used in the custom ARCPLOT lineset **bedrock.lin** that contains 40 line symbols used by the NJGS for digital geologic map production. Most of these cartographic symbols and lines are based on U.S. Geological Survey standards. Others were created for geologic features that are not available from current USGS standards (for example recumbent fold traces and custom fracture-trace symbols).

NJGS Digital Cartography using FMS-UNIX (ARCPLOT)

The FMS-UNIX programs are started by typing and entering the **&run meso** command at the ARCPLOT command-line prompt within a user's workspace (ARC/INFO directory). The **meso(.aml)** script must reside in the workspace from where the command is issued or the full directory path to the script must be entered following the **&run** command (for example **&run /home/gregh/meso/meso.aml**). The **meso** script automatically sets the ARCPLOT markerset file and global variables designating the directory paths where GIS point coverages and ARCPLOT files reside. These global 'path' variables are summarized below:

.fpath - specifies the directory containing mesostructure files *.MES files
(/home/gregh/meso/mes of Fig. 2.7a).

.spath - ARC/INFO workspace containing the station (point) coverages

.mpath - directory containing the ARCPLOT map composition

.expath - ARC/INFO workspace containing the GIS coverages that will be used
for setting the ARCPLOT map extent

.amlpath - directory path containing the program AMLS

(/home/gregh/meso/amls of Fig. 2.7b)

.ipath - directory containing the program icons (/home/gregh/meso/amls/icons of
Fig. 2.7c.)

.hpath - directory containing the program help files (/home/gregh/meso of
Fig. 2.7a.).

The **meso** script calls the **startup(.mnu)** menu (Fig. 2.8a.) that provides mouse-controlled clickable links to other scripts and menus for setting the ARCPLOT map composition (Fig. 2.8b) and initiating the **Location & Drawing Menu** (Fig. 2.8c). The **Map Composer Setup Menu** (Fig. 2.8b) provides mouse-activated variable fields for setting the ARCPLOT session parameters **Mapextent**, **Mapunits**, **Mapscale**, and **Pagesize**. Most of these variables can be manually set at the ARCPLOT command-line prompt before starting **meso**. However, it is critical to always activate the **Mapscale** variable in this setup menu because it's a global variable used for positioning structural-inclination values next to oriented structure symbols (Herman and others, 1996).

The **Location & Drawing Menu** provides scrolling selection frames and push buttons for setting ARCPLOT variables related to plotting graphics (structural) symbols (Fig. 2.8c). Frame-selection variables include choices for the GIS point themes (**STATION COVERAGES**), mesostructure files (*.MES), and graphic symbols (**STRUCTURE SYMBOL**). The GIS point themes are listed from the ARC/INFO directory specified in the **.spath** global variable. The ***.MES FILES** frame shows the list

of mesostructure data files in the directory set by the **.fpath** global variable. The **STRUCTURE SYMBOL** variable frame displays the marker-symbol choices corresponding to structure and point symbols (Fig. 2.8c). The structural symbols are linked to ARCPLOT markersymbol numbers from **bedrock.mrk** in the **draw.aml** script.

The **Draw** button on the **Location & Drawing Menu** runs the **draw.aml** script (Fig. 2.8b). This script uses INFO cursor processing to sequentially read each string variable from a *.MES file (Table 2.2), split the *.MES variable into a subset of string variables used for selecting a station point from the ARC/INFO spatial coverage, and setting other ARCPLOT variables designating the graphic symbol orientation and size. The **draw.aml** script sequentially establish a one-to-one relationship between the designated station number from the *.MES file and the corresponding ARC/INFO point location, then plots a geo-referenced and oriented graphic symbol in a map composition at the map coordinates of the selected point location.

Other buttons on the **Location & Drawing Menu** are used for varying the color, size, and orientation of graphics symbols. The **MARKERCOLOR** button provides black, red, green, and blue color options from the menu, or any custom color can be specified by editing the **location.mnu** and **draw.aml** files (Fig. 2.8b). The **ORIENTATION** button is used for positioning structural-inclination labels next to structural symbols. Planar structures requiring inclination annotation use the **dip azimuth** button. The **MARKERLENGTH** button sets the size of all structural symbol to the specified value. The **weighted** variable will automatically uses the size-variable substring from the *.MES file (Table 2.2b) to set the size of the graphics symbol to be plotted. The **MARKERLENGTH** variable must beset after choosing a **STRUCTURE SYMBOL** in order to override default markersize values. The **DIP/PLUNGE VALUES** button controls how **draw.aml** organizes the set of structural-inclination labels. The **none** button results in having only structural symbols drawn with no inclination labels. The **group**

button results in sequential plotting of an inclination label immediately after each structural symbol. The **separate** button results in having all structural symbols plotted before the sequence of inclination labels. The **colored** button is used to automatically set the color of the graphics symbol based on the inclination value read from the *.MES file. For this options, structural symbols are colored based on their inclination values but the actual values are not plotted. Default colors and inclination values include green ($< 30^\circ$), blue ($30^\circ - 60^\circ$), and red ($61^\circ - 90^\circ$). This option is used for helping delineate structural domains based on the inclination values for sets of structures (for example, identifying domains containing gently-dipping cleavage from moderate- to steeply-dipping cleavage). The **meso** script uses similar ranges of structural inclination for plotting customized flag symbols representing inclined or vertical bedrock fractures (Fig. 2.3). Default plot symbols for gently-inclined fractures ($< 30^\circ$ dip) use an unfilled flag, moderately-inclined fractures (30° to 60° dip) use a diagonally-filled flag, and steeply-inclined joints (61° to 89° dip) using filled (solid) flags. Vertical joints use bisected, unfilled flags. The flag mast originates from the outcrop location and the unattached end of the flag points in the direction of dip for inclined structures. This approach is used to alleviate crowding normally resulting from plotting multiple structural features and their inclination values at each outcrop point.

Other buttons on the **Location & Drawing Menu** include check boxes and individual buttons for increasing the size of weighted marker symbol (Fig. 2.8c), for generating an ARC/INFO **annocoverage**, and for grouping all graphics symbol plotted during a single draw session into a single graphics element (**mgroup** button). Annotation coverages are generated using the values of the structural inclination variable from the *.MES files. If annotation are generated from a plot session, the user must temporarily exit the form menu immediately after a plot session and issue the ARCPLOT command **annocover none** at the command line to signal the end of the annotation-generation

process. The **&return** command returns program control back to the **Location & Drawing Menu**.

After all session parameters have been set and the user starts the **draw.aml** by clicking the **Draw** button, ARCPLOT re-selection processes are echoed to the command tool and scroll upwards to reflect the repeated cursor-processing steps. The **Location & Drawing Menu** also includes the **Msel ***, **Mmove ***, **Mwho ***, **Minfo**, and **Mdelete** buttons that are used to select, reposition, identify, and delete graphic elements within a map composition after a plot session. The **Help** button calls help text file that provides details describing form menu functions and control. The **Cancel** and **Done** buttons exit the menu and return program control to the initial startup menu.

Bedrock Geology GIS Coverages

NJGS bedrock-geology coverages are geo-referenced sets of points, lines, and polygons stored as electronic data in computers running Geographic Information Systems software. Bedrock coverages are developed for both map and cross-sectional views. Point coverages are built for sets of field stations (outcrop locations). Line themes are built for stratigraphic and structural contacts, fold axial-surface traces, and fracture traces. Polygon coverages are built for areas denoting stratigraphic or structural continuity. Stratigraphic-thickness (isopachous) maps and structure-contour maps are less commonly built and usually stem from localized aquifer-framework and tectonic studies.

Digital Processing of Bedrock Geologic Coverages

Most geologic coverages produced by the NJGS are initially generated in NAD27 State Plane Coordinate (SPC) feet because USGS 7-1/2' topographic maps are based on this datum and the because the NJDEP uses SPC feet as the default geographic projection. Each map is geo-referenced (registered) to the NAD27 projection grid using at least four

corresponding reference points (tics) for each map. The tics usually correspond to the corners of 1 to 24,000 scale, 7-1/2' quadrangles, or 2-1/2' gradicules corresponding to the corners of 1 to 12,000 scale quarter-quadrangles. A reference set of tics is maintained by the NJDEP Bureau of Geographic Information Analysis.

All archived data sets at the NJGS are projected into NAD83 SPC feet upon completion. This projection typically results in map rotations of about $\pm 0.5^\circ$, and translation shifts up to about .015" (± 120 SPC feet) for 1 to 100,000 scale coverages scanned and traced from NAD27 base maps. A statewide study of the standard deviation between the NAD27 and NAD83 projection grids at the 1:24,000 scale would be very useful for quantifying limitations of using NAD27-based geology coverages with other NAD83 data generated using Global-Positioning-Systems and Digital Orthophotquads.

The NJGS normally maintains a maximum root-mean-square (RMS) error of .006 (about 12 ft. at the 1:24,000 scale) for coverage development. An estimated 85% of the archived geologic and hydrogeologic coverages are accurate to within .003 RMS deviation. Quality assurance is conducted by comparing proof plots of each coverage to the original base maps. Any line that deviates from the original position by more than .012 inch (about 1 to 1.5 line widths) is re-digitized, re-plotted, and corrected until acceptable results are obtained.

Bedrock geology coverages are digitized using either a digitizing tablet and/or an optical scanner in conjunction with raster-to-vector (R-to-V) conversion software. Point themes are typically generated using a digitizing tablet. The NJGS uses CalComp 9100 and 9500 digitizers with a reported accuracy of ± 0.005 in. (± 0.127 mm). A set of at least four points (tics) are used for registering map sheets on a digitizing tablet at the beginning of each editing session.

Line and polygon themes are often built by optically scanning a map as a raster image, then tracing linear arrays of image cells (pixels) with R-to-V conversion software.

The NJGS uses a CalComp ScanPlus II roll-feed, E-format, two-camera scanner for scanning maps larger than legal-sized documents. Most maps are scanned using a 400 dots-per-inch (dpi) image resolution. The scanned image accuracy is reported as $\pm 0.25\%$. The NJGS has obtained the best imaging results from scanning either translucent or clear mylar separates with drafted neatlines of black rapidigraph ink. Acceptable results have been obtained from using soft-lead pencils (at least a No. 2, or HB pencil lead) on white paper or mylar.

R-to-V coverage development usually require more time preparing media for reproduction than normally spent when using a digitizing tablet, but an estimated 50% of the time developing a coverage can be saved using the R-to-V approach if the coverage is physically large or detailed. The R-to-V approach allows a uniform coverage to be developed without having to worry about errors stemming from repeatedly registering maps on a digitizing tablet at the start of consecutive digitizing sessions. This concern frequently arises when digitizing large maps drafted at intermediate (1:100,000) and small (1:250,000 or less) scales. The R-to-V method works best with maps having continuous lines requiring no ornamentation. Separate mylar sheets should be prepared for each set of points, lines, and polygons to be individually generated from a pre-existing map. The scanned coverages are usually edited using a digitizing tablet.

The NJGS uses CADCore Version 2.0 R-to-V software. Original maps or mylar separates are scanned and saved using a TIFF 5.0 image format. The TIFF image is imported into CADCore where it is converted into a CADCore image format (*.hrf) used for image display, processing, and line tracing. The raster image is center-line or outline traced with vector-line segments measured in inches. The vectors are saved as a CADCore drawing file (*.drw) and exported as an input file for use with ARC/INFO **generate** command. The output files are generated as lines in ARC/INFO and built into line or polygon coverages having inch units. The map is then transformed from inch units

into NAD27 or NAD83 coordinates using the standard reference tics or other sets of links in the map-transformation process. Coverages are subsequently edited using ARC/INFO ARCEDIT.

Bedrock Coverages and Coverage Attributes

The NJGS has developed a standardized reference set of coverage items (database fields) and item variables for developing the various point, line, and polygon bedrock coverages (Table 2.5 and Appendix A). Point coverages are built for sets of outcrop locations (or field stations) for each 7-1/2 minute quadrangle. An outcrop-location coverage contains the field-station numbers and geographic coordinates needed to produce fracture-trace coverages using **FRACGEN** and to work the **meso.aml** symbol-drawing program (Fig. 2.3). Outcrop locations are digitized from field maps, built solely as point coverages, and assigned unique, six-integer numbers (STATION variable, Table 2.4). The first three digits of the STATION variable correspond to a quadrangle reference number (001 to 077) and the remaining three digits specifying the station number. For example, station number 055106 is the 106th station in quadrangle number 055. The ARC command **addxy** must be issued for each field-station coverage in order to add the geographic coordinates for each station to the coverage's point-attribute table (*.PAT file). These coordinates are read by **meso.aml** as part of the data-plotting algorithm and are needed for producing the *.STA file used by **FRACGEN** (Table 2.4).

Line coverages contain 2-dimensional traces of inclined, 3-dimensional, curvilinear or planar surfaces for the map and cross-sectional views. Bedrock line coverages containing sets of fold-axis traces are called **folds** coverages. They are built only as a line coverage and have an arc-attribute table. Fracture-trace coverages are also built as line coverages as previously discussed for the **FRACGEN** program.

Polygon coverages contain 2-dimensional traces of inclined, 3-dimensional solids

for the map and cross-sectional views. Bedrock polygon coverages containing areas of stratigraphic continuity are called **contacts** coverages. Stratigraphic units are labeled using the primary **geonum** variable (Appendix A). The linear boundaries of each stratigraphic unit can either be structural (fault) or stratigraphic and therefore a **contacts** coverage is built and coded with both line and polygon feature attributes. Line attributes are used for separating different coverage features such as faults, stratigraphic contacts, and geographic boundaries when drafting maps and cross sections. The **folds** and **contacts** coverages are built and maintained separately from one another but spatially coincide (fig. 2.10).

Cross sections represent a special case for GIS coverage development because they depict subsurface geologic information based on the vertical (z) dimension relative to the map (x and y) dimensions. The standard ARC/INFO programs (ARC, ARCEDIT, and ARCPLOT) are limited to working with x- and y-coordinate data and therefore do not allow complete integration of cross section data with map-based information. Other GIS modules such as TIN and GRID are designed to work with irregular-surface data and allow z-coordinates to be added as items in a map database for generating triangulated-network surfaces and generating planimetric display of 3-D data. Cross-section coverages are currently unable to be georeferenced in ARC/INFO because they are built using the standard GIS programs and only contain x and y coordinates. They are built at the scale in which they are drafted, digitized or scanned. Serial cross sections can be digitized separately and translated into serial arrangement using either ARCEDIT or ARCPLOT. Cross section coverages use the same item fields and attributes as for the map-based bedrock coverages.

N.J. Geological Survey Metadata

Metadata is defined by the Federal Geographic Data Committee (FGDC) as data

that describe the content, quality, condition, and other characteristics of data, or in other words "data about data". Metadata is required as an integral part of a complete GIS coverage in order to convey details surrounding the origin and use of the data. These details include important information such as a citation, the physical limitations, and scope of the data.

The NJGS produces and archives geologic, hydrogeologic, and geophysical data as digital data files for electronic distribution to the public. One method of electronic-data transfer uses the Internet mail protocol from the World Wide Web (WWW) home page for the NJGS (<http://www.state.nj.us/dep/njgs/>). Because the Web reaches a global market, the NJGS developed a metadata-file format (Appendix B) based on the content standards for digital geospatial metadata proposed by the Federal Geographic Data Committee (FGDC). These content standards were evaluated with respect to their completeness, applicability, and content for use with geologic data produced by the NJGS. A comparison was also made to the NJDEP data dictionary file which currently serves as the NJDEP metadata standard. An ASCII-text format was chosen as a document template due to its broad user base and because of the need to develop metadata files using the many different computer platforms (DOS, Windows, Apple, and UNIX). A prototype NJGS metadata format was submitted for review and comment to the NJGS staff and others at the NJDEP Office of Information Resources Management in June, 1995. The review product included the outline in Appendix B and two examples of its implementation. The few critical comments received back were addressed and the abstracted version of the FGDC standard was adopted for use by the NJGS in June 1996. This standard is applied to all electronic files intended for distribution over the Web and all GIS coverages to be archived by the NJGS. The NJGS currently archives ARC/INFO coverages and related dBASE relational data files as part of their Digital Geodata Archive. Compressed data files containing less than 1.4 Mb information are also being made

available as Digital Geodata Series (DGS) publications. The NJGS DGS products are designed for use by ESRI's ARCVIEW2 software. The NJGS metadata documents therefore focus on ARC/INFO coverages and dBASE files. However, metadata are also being generated for other products that include ASCII-text document files and computer-software programs such as the NJGS FMS.

Discussion

GIS coverages are developed by digitizing and coding points, lines, and polygons. Documented methods of coding geologic features range between those using only numeric codes (Reynolds and others, 1995) to those based mostly on alphabetic codes (Walker and others, 1996). The NJGS uses both integer and alphabetic variables for coding feature attributes depending on the circumstance (Table 2.5). Table 2.6 illustrates three different coding systems using a geologic fault line requiring three descriptive attributes as an example. The advantages and disadvantages of each coding system are discussed below.

The USGS data model was recently published as an open-file report by Reynolds and others (1995). This model was built for global applications, requires the combination of two independent variables to describe a single coverage feature, and requires a set of lookup (reference) tables relating integer codes to their corresponding feature descriptions. This system is the most comprehensive of the three data models reviewed, requires the most time coding coverage features, and is therefore probably the most expensive system to employ for coverage development. The strict use of integer codes provides the advantage of using algebraic expression when selecting classes or groups of geologic features. However, this system appears to be somewhat inflexible and cumbersome. For example, there are no codes available in the USGS system to note whether a fault plane is steeply or moderately inclined. Also, this model may prove difficult to use because the data developer or user needs to be constantly aware of the

pairing of major and minor codes when selecting, editing, or illustrating coverage features. There are also no suggested codes within this scheme to denote geographic or political entities that usually form coverage boundaries. Separate coding of these features is usually necessary during the data development process and for digital cartographic display.

The data model published by the University of Kansas (Walker and others, 1996) appears to have been built for regional applications as it lacks the comprehensive detail required for a national data model. Of the three data models reviewed, it requires an intermediate number of feature items and mostly uses alphabetic variables (Table 2.6). The main advantage of using this model is that feature descriptions are flexible, direct, and easily understood. There isn't a need to rely upon supplemental reference tables for feature identification as for the USGS model. However, this model cannot use logical operators based on algebraic expressions to sort data and therefore requires complex data-selection processes when separating individual coverage features or groups of similar features for analysis or graphic representation. The University of Kansas model also illustrates point-based geologic data for single structures only and does not specify how to display multiple structural readings at a single point. This model also provide a comment field that can be used for separately identifying geologic features from other geographic or political features in a data layer.

The NJGS data model was also built for regional applications and requires the fewest number of feature items of the three reviewed data models (Table 2.6). It therefore has the least overhead and is probably the least expensive to employ. This model also requires a set of lookup tables for some feature codes that relate integers to alphabetic descriptions of coverage features. This can can complicate coverage development as previously discussed for the USGS model. The NJGS model also includes codes for noting geographic and political entities and therefore facilitates coverage development for

GIS technicians. A major difference between the NJGS data model and the other models is the manner in which structural-geology data for the outcrop are handled. Whereas all point-based structural information are developed as part of a GIS coverage in the preceeding two models, the NJGS model handles this information outside of the GIS using the NJGS FMS. Only the locations of outcrops and the field-station-numbers are developed in GIS coverages. This approach allows structural data to be managed and analyzed outside of GIS to take advantage of the many PC-based geologic data-analysis utilities in the marketplace. The NJGS is currently focusing on linking outcrop-based structural geology data stored in a relational database or spreadsheet format to corresponding point locations in GIS for access and viewing. Data will be linked to the outcrop using the field-station number in a manner similar to that depicted in figure 2.3. Problems associated with the graphics display of structural geology data using popular GIS viewing tools such as ESRI's ARCVIEW (v. 2.x) are generally unresolved at this time and have recently been the focus of informal technical discussions within the GIS community.

Another disadvantage of using the NJGS data model stems from it's reliance on ARCPLLOT for digital cartographic production. ARCPLLOT imposes a 999 graphic-element limit to the number of graphic elements within a map composition. This limitation requires extensive data management for each set of plotted geologic structures. Each set of strcutres needs to be grouped as a single graphic element for subsequent combination with other structures. For example, all bedding strike and dip readings are first plotted individually, then subsequently grouped for display and used as a basis for positioning subsequent data layers such as rock cleavage, mineral lineations, etc. Each type of structure must be therefore be prioritized, plotted, grouped, and combined with each subsequent data layer for effective display of complex, multi-layered data sets in order to compose a complete digital geologic map. Furthermore, ARCPLLOT is currently

being supplanted by ARCVIEW as the most popular GIS graphic-production tool. Many of the digital geologic maps produced in the past by the NJGS with ARCPLOT have not been able to be reproduced using "new" technologies. For example, the NJGS has successfully used an electrostatic plotter for transparently integrating topographic base-map imagery with GIS-based geology data. We have not yet been able to adequately reproduce these effects using ink jet technology for E-format digital geologic maps.

The use of GIS for conveying geologic information within the earth-science community is becoming increasingly popular but is hampered by the lack of standardization, centralization, and certification. There are currently no standards for quality assuring or certifying data so that competing data sets can be compared and chosen for use based on their accuracy and applicability. The development and release of national standards for digital geologic maps and databases will promote the use and proliferation of GIS within the earth-science community and may help alleviate some of the problems surrounding the growth of this relatively new industry. However, problems arising from the development and circulation of competing data sets, and the lack of understanding surrounding GIS, particularly regarding cost effectiveness, will continue to hamper these efforts for the immediate future. In order for digital geologic information to become more broadly accepted and useful, the federal and state government should standardize basic data layers such as political and geographic boundaries and devise certification procedures to ensure that complimentary data are compatible and accurate.

The USGS is currently coordinating the development of a National Cooperative Geologic Mapping Program with the American Association of State Geologists in response to public law establishing the National Geologic Mapping Act of 1992. One of the priorities of this national program is to develop a national geologic data model that includes digital data standards to facilitate the efficient search, transfer, and use of digital geologic data by the public (Soller and Berg, 1995). In August 1996, representatives from

many state geological surveys met with USGS representatives in a second organizational meeting to identify relevant issues and to proceed to develop a digital data model and standards. The future development of standardized digital geological data in the U.S. will primarily rely upon this type of organizational framework.

TABLE 2.1 FMS-DOS DATA-INPUT FILES

2.1a. Standard FIELDATA (*.FD) file		2.1b. Easy FIELDATA (*.FDZ) file*	
<u>Variable</u>	<u>Explanation</u>	<u>Variable</u>	<u>Explanation</u>
STATION*	beginning of file or station (station delimiter)	/	beginning of file or station (station delimiter)
B	primary structure (bedding plane)	023134	station (outcrop) number
123,34,S**	strike, dip, and dip direction of bedding	N45E,60,S**	strike,dip, and dip-direction
P***	primary structure (user-specified plane)	NS,40,W	strike,dip,dip-direction
JUC2	secondary structural variable (kind of plane)	/	station delimiter
40,69,N	strike, dip, and dip direction of plane	007465	station number
SP	primary structure (shear plane)	123,88,N	strike,dip,dip-direction
NORL	secondary structural variable (kind of shear plane)	45,67,S	strike,dip,dip-direction
179,23,N	strike, dip, dip direction of shear plane	/	station delimiter
SL	primary structure (slickenline lination)		
NORL	secondary structural variable (kind of slickenline)		
4,45	trend and plunge of slickenline		
C	primary structure (cleavage plane)		
JMC3	secondary structural variable (kind of cleavage)		
0,50,E	strike, dip, and dip direction of cleavage		
JTRP	lithologic variable for the outcrop		
FFZ	locational variable for the outcrop		
58023	station (outcrop) number		
STATION	end of file or station (station delimiter)		
<p>*The FIELDATA(*.FD) file and each field station must begin and end with the STATION variable.</p> <p>**The map-bearing for planes uses strike-azimuth of 0° to 179° whereas lineations use trend-azimuths of 0° to 359°. The inclination of all structures use 0° to 90° but planar inclination (dip) requires a single variable denoting a hemisphere toward which the plane dips (N,S,E,W).</p> <p>***Some primary structures require secondary structural variables denoting the kind of primary structure. Refer to Table 2.3 for a list of the primary and secondary structural variables used in the FMS.</p>		<p>* The *.FDZ files are designed for use with one type of pre-sorted structure.</p> <p>**Structural-orientation data can use either quadrant or azimuth convention for planes (striking 0°-179°) or lineations (trending 0°-359°).</p>	
		<p>2.1c. LINSORT (*.DAT) file</p>	
		<u>Variable</u> *	<u>trend/stratigraphic variable(s)</u>
		123CHB	NNNAAA\$
		009CH	NNNAAS\$
		179B	NNNA\$
		000CHB	NNNAAA\$
		177CHB	NNNAAA\$
		045H	NNNA\$
		<p>* The LINSORT variable contains both the lineation trend (0°-179°) and a sequence of stratigraphic variables denoting the unit that the lineation intersects.</p>	

TABLE 2.2. FMS-DOS DATA-OUTPUT FILES

TABLE 2.2. FMS-DOS DATA-OUTPUT FILES					
2.2a. DATASORT (*.SRT) OUTPUT FILES CONTAINING ONLY STRUCTURAL ORIENTATION DATA				2.2c. ROSESTAT.PBC STATISTICS FILE (*.LUT)*	
Plane data*			Lineation data**		
strike	dip	dip direction	trend	plunge	
30	71	N	10	64	.108
45	80	N	135	17	.086
26	65	N	124	48	.259
87	24	S	110	66	.086
25	85	S	325	16	.086
76	51	N	305	39	.086
30	89	S	136	61	.237
70	76	N	315	11	.302
*Planes uses strike-azimuth of 0° to 179° and need a single variable denoting a hemisphere toward which the plane dips (N,S,E,W) **Lineations use trend-azimuths of 0° to 359°.					.194
					.216
					.129
					.065
					.000
					.086
					.065
					.086
					.108
					2.2b. DATASORT (*.MES) OUTPUT FILES USED FOR MAKING MESOSTRUCTURE PLOTS WITH meso.aml
file containing markersize values		file with no markersize values			
01750220971.108*		02400316046.000			
01750422521.259		02400315035.000			
01750621481.302		02400316026.000			
01751028585.065		02400300120.000			
*The first six characters denote the field-station (outcrop) number, the seventh through ninth characters the structural bearing, the tenth and eleventh the structural inclination, and the last three, the size of the ARC PLOT plot symbol (markersize in inches). Note that there cannot be any spaces within the numeric string (null values in the variable string must be filled with zeros), and that either planar (0°-179°) or linear (0°-359°) structural bearing can be used. *.MES files used with the profile option of the FRACGEN program require planes to be specified using the dip azimuth (0°-359°)					
*Plane data using strike require length variables for 18 sectors whereas lineations and planes using dip azimuth require variables for 36 sectors. Note that the statistics values are used as the last three characters in the *.MES files shown in Table 2.2b.					

TABLE 2.3. FMS PRIMARY AND SECONDARY STRUCTURAL VARIABLES USED IN THE FIELDATA (*.FD) FILE

2.3a. PRIMARY STRUCTURAL VARIABLES		2.3b. SECONDARY VARIABLES USED BY THE NJGS FOR MODIFYING THE KIND OF PRIMARY STRUCTURE*	
Planar Structures Not Requiring Secondary Variables		Variable	Explanation
Variable	Explanation	Variable	Explanation
B	Bedding	JM	mineralized joint
BDZ	Brittle Deformation Zone	LL	left lateral
DDZ	Ductile Deformation Zone	MI	mica
KB	Kink Band	MY	mylonite
KBB	Kink Band Boundary	NO	normal
J	Joint	PM	prominent/primary
TG	Tension Gash	PX	pyroxene
TGA	Tension Gash Array	QZ	quartz
Planar and Linear Structures Requiring Secondary Variables		RL	right lateral
Variable	Explanation	RV	reverse
C	Cleavage	SB	subordinate
F	Fault	SC	secondary
FI	Fiber	SD	spaced
FO	Foliation	SI	slip
FR	Fracture	SY	slaty
LAY	Layering	TO	tool and groove
L	User-defined Linear Structure	T0	short, discontinuous trace length
P	User-defined Planar Structure	TN	trace length to about N meters
SP	Shear Plane	XX	unspecified secondary variable
SZ	Shear Zone		
SL	Slickenline (Lineation)		
SS	Slickenside (Shear plane)		
ST	Stylolite		
V	Vein		

*This list of two-character variables is suggested for use within FIELDATA files. Any combination of these variables or any other user-specified variables can be used provided that they are two characters long and they do not duplicate the primary variables in Table 2.3a.

**TABLE 2.4. ATTRIBUTES OF ASCII FILES GENERATED USING THE INFO
<LIST PRINT> COMMAND FOR GIS POINT COVERAGES OF OUTCROP
LOCATIONS AND EDITED FOR USE AS FMS-DOS INPUT FILES**

Table 2.4a. INFO *arcns* output file edited to make input file for FDUPDAT.PBC

Unedited INFO *arcns* file generated using the INFO command **LIST PRINT** → Edited *arcns* file saved as *.NSP input file for FDUPDAT.PBC

RECNO\$	STATION	GEONUM	DOMAIN	STATION,GEONUM,DOMAIN
1	57001	8,340	paljt	57001,OJTA,PALJT
2	57003	8,750	yupu	57003,OCA,YUPU
3	57004	8,750	yupu	57004,OCA,YUPU
4	57005	5,450	ffwn	57005,TRSSC,FFFWN
5	57006	8,620	yupu	57006,OBU,YUPU
6	57007	8,340	yupu	57007,OJTA,YUPU
7	57008	8,340	yupu	57008,OJTA,YUPU
8	57009	3,950	ffwn	57009,JTRCQ,FFFWN

Table 2.4b. INFO *arcns* output file edited to make input file for FRACGEN.PBC

Unedited INFO *arcns* file generated using the INFO command **LIST PRINT** → Edited *arcns* file saved as *.STA input file for FRACGEN.PBC

\$RECNO	STATION	X-COORD	Y-COORD	STATION, X-COORD, Y-COORD
1	57289.	366,221.000	652,906.400	57289,366221.000,652906.400
2	57290.	366,072.800	652,903.000	57290,366072.800,652903.000
3	57208.	385,724.600	652,811.100	57208,385724.600,652811.100
4	57293.	370,568.400	652,779.300	57293,370568.400,652779.300
5	57285.	373,439.900	652,754.400	57285,373439.900,652754.400
6	57209.	385,569.000	652,727.300	57209,385569.000,652727.300
7	58213.	417,416.900	652,714.400	58213,417416.900,652714.400
8	57296.	371,176.200	652,698.800	57296,371176.200,652698.800
9	57294.	370,669.600	652,669.900	57294,370669.600,652669.900
10	57295.	370,723.700	652,453.800	57295,370723.700,652453.800

TABLE 2.5. REFERENCE LISTS FOR ARC/INFO GIS LINE ATTRIBUTES
USED BY THE NJGS FOR BEDROCK GEOLOGY COVERAGES

<i>Variable</i>	<i>Description</i>	<i>Variables</i>	<i>Description</i>
lintype (1 1 I) [input width, output width, Integer]		linkind kind (2 2 I) (8 9 C) [Character]	description
0	contact	1	kn known
1	fault	2	al approximately located
2	fold	3	in inferred
3	igneous dike	4	pr probable
4	bed or foliation formline	5	co concealed
5	linear artifact (line necessary to close a polygon)	6	pr primary
6	user-defined variable	7	se secondary
7	quadrangle boundary	8	te tertiary
8	County boundary	9	rv reverse
9	State boundary	10	no no
		11	rl right lateral
		12	ll left lateral
		13	ln left lateral normal
		14	rn right lateral normal
		15	lr left lateral reverse
		16	rr right lateral reverse
		17	au anticline, upright
		18	ar anticline, gently inclined to recumbent
		19	ao anticline, overturned
		20	su syncline, upright
		21	sr syncline, gently inclined to recumbent
		22	so syncline, overturned
		23	pa paleozoic fold
		24	pr proterozoic fold
		25	mz mesozoic fold
		26	ca cleavage arch
		27	ct cleavage trough
		28	gi gently inclined (0° to 29°)
		29	mi moderately inclined (30° to 59°)
		30	si steeply inclined (60° to 89°)
		31	ve vertical (90°)
		32	ot overturned
		33	up upright
		34	ov overthrust
		99	xx user-specified meaning

<i>Variable</i>	<i>Description</i>
lithbnd (1 2 I)	
0	unspecified
1	DS/OCYu lithic boundary
2	Om-Ojt/OCjkx lithic boundary
3	Yu/OCu lithic boundary
4	Mz/OCYu lithic boundary
5	boundary of outcrop
6	boundary of shallow outcrop (<10 ft. thick)
7	(unused)
8	physiographic province boundary
9	structural domain boundary

<i>Variable</i>	<i>Description</i>
incline (1 2 I)	
0	unspecified
1	low-angle dip (<30° dip)
2	moderate- to high-angle dip (> 29° < 60°)
3	high-angle (>60° dip)
4	vertical (90°)

TABLE 2.6. A COMPARISON OF DATA ATTRIBUTES FROM THREE DIFFERENT GIS-BASED GEOLOGIC DATA MODELS FOR A LINE REPRESENTING AN APPROXIMATELY-LOCATED, MODERATELY-INCLINED, NORMAL FAULT

<i>U.S. Geological Survey*</i>	<i>N.J. Geological Survey</i>	<i>University of Kansas</i>
major1 = 060 ¹ minor1 = 0012 ² minor2 = 0001 ³ ¹ primary 3-digit code for line representing intersection of geologic surface with surface of earth ² secondary code combined with major1 to denote normal fault ³ secondary code combined with major1 to denote approximately located *no variable currently set for inclination	lintype = 1 ¹ kind = 'no,al,mi' ² ¹ fault (see Table 2.5) ² 'no' = normal dip slip, 'al' = approximately located, 'mi' = moderately inclined (see Table 2.5)	contacttype = 'fault' quality = 'approximate' type = 'normal' notes = 'moderately inclined'

Figure 2.1. A screen-captured VGA display of a page from the World-Wide-Web site of the NJGS showing the file components of the FMS-DOS. As part of the NJGS Digital Geodata Archive, the FMS-DOS set of programs are assembled into a compressed "zip" file for electronic data transfer using Internet Mail Protocol. **fmsdos.zip** includes an executable DOS program and 14 chained program files.

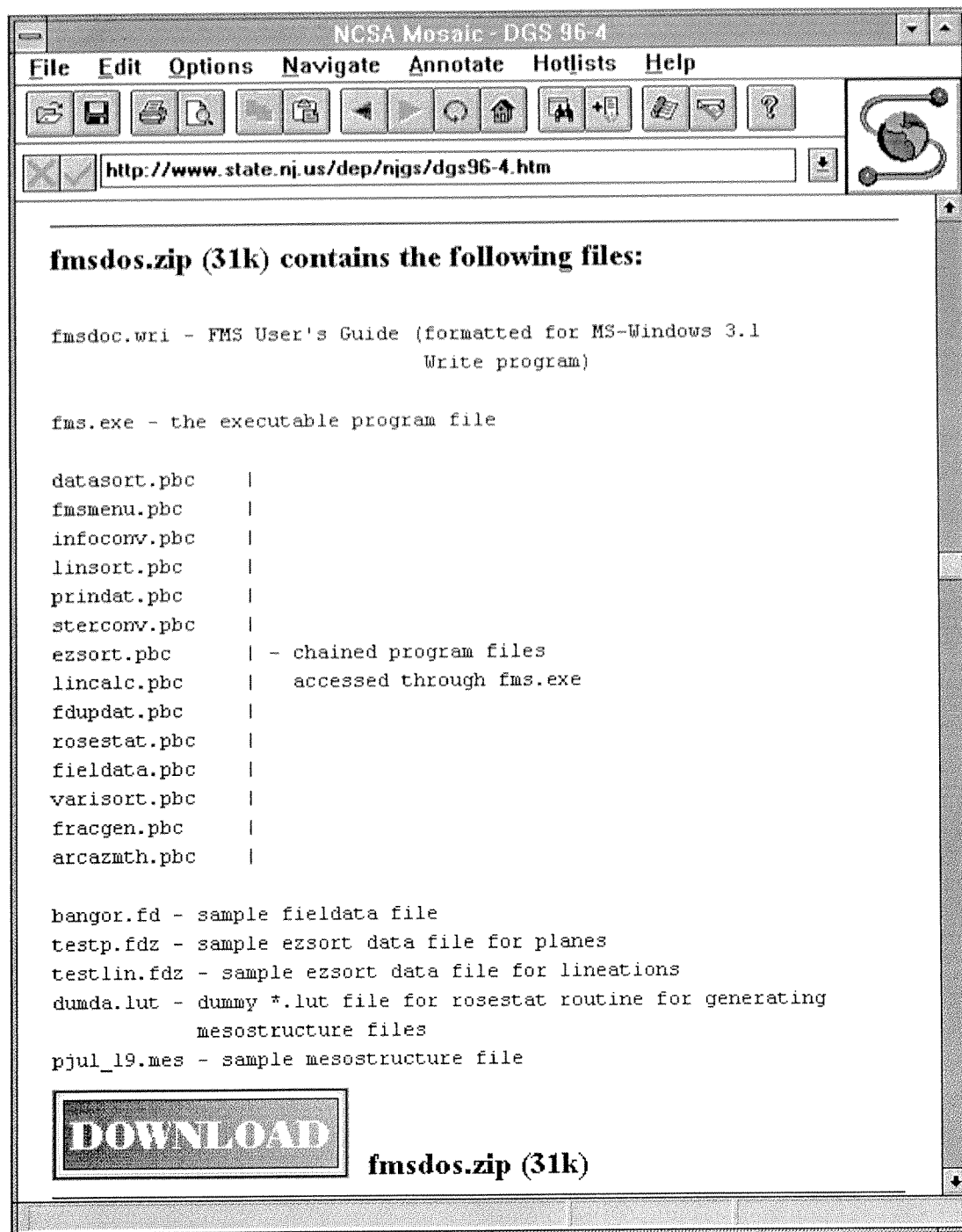


Figure 2.2. A screen-captured VGA display of the opening menu for the FMS-DOS showing the program options and brief explanations.

```

MS DOS Prompt
Field data Management System Ver. 2.1      New Jersey Geological Survey

***** PUT CAPS LOCK ON! *****

Menu of programs for field data management and analysis.  Select a program
option by typing its highlighted letter

ARCAZMTH: calculate line lengths and generate relative frequency histograms
DATASORT: sort FIELDATA files to make structural data (.SRT) & plot (.MES) files
EZSORT:  sort customized field data files (*.FDZ) to make .SRT and .MES files
FDUPDAT: updates location and unit variables for stations in FIELDATA files
FIELDATA: make .FD files containing station attributes and structural readings
FRACGEN: make .AML files for generating ARC/INFO coverages of fracture traces
INFOCONU: converts .FD files (sequential) into .INF files (array)
LINSORT: sorts lineation trends from .DAT (map-lineation) files
LINCALC: calculates intersection lineations for sets of planar structures
PRINIDAT: view or print FIELDATA (.FD) files
ROSESTAT: screenplot a rose diagram of .SRT data or make a .LUT statistics file
STERCONU: converts *.SRT files into ROCKWARE format for use with STERONEIT
UARISORT: extract .FD files from other .FD files based on station attributes
EXIT:     exit program

----- Press (Ctrl Break) at any time to abort the program -----

```

Figure 2.3. Illustration of the link between structural-geology symbols in an ARCPLOT map composition and structural-geology data contained in a FMS-DOS mesostructure (*.MES) plot file. Structural data are shown in conjunction with other GIS-based site data. Structural symbols include bedding strike and dip plotted at the outcrop location and multiple fracture readings showing strike and dip plotted nearby. FMS field-station numbers correlate to part of the string variable in the *.MES file. Oriented graphic symbols are plotted automatically using FMS-UNIX **meso.aml** but placement of symbols for more than one type of structure at one point requires manual repositioning of symbols.

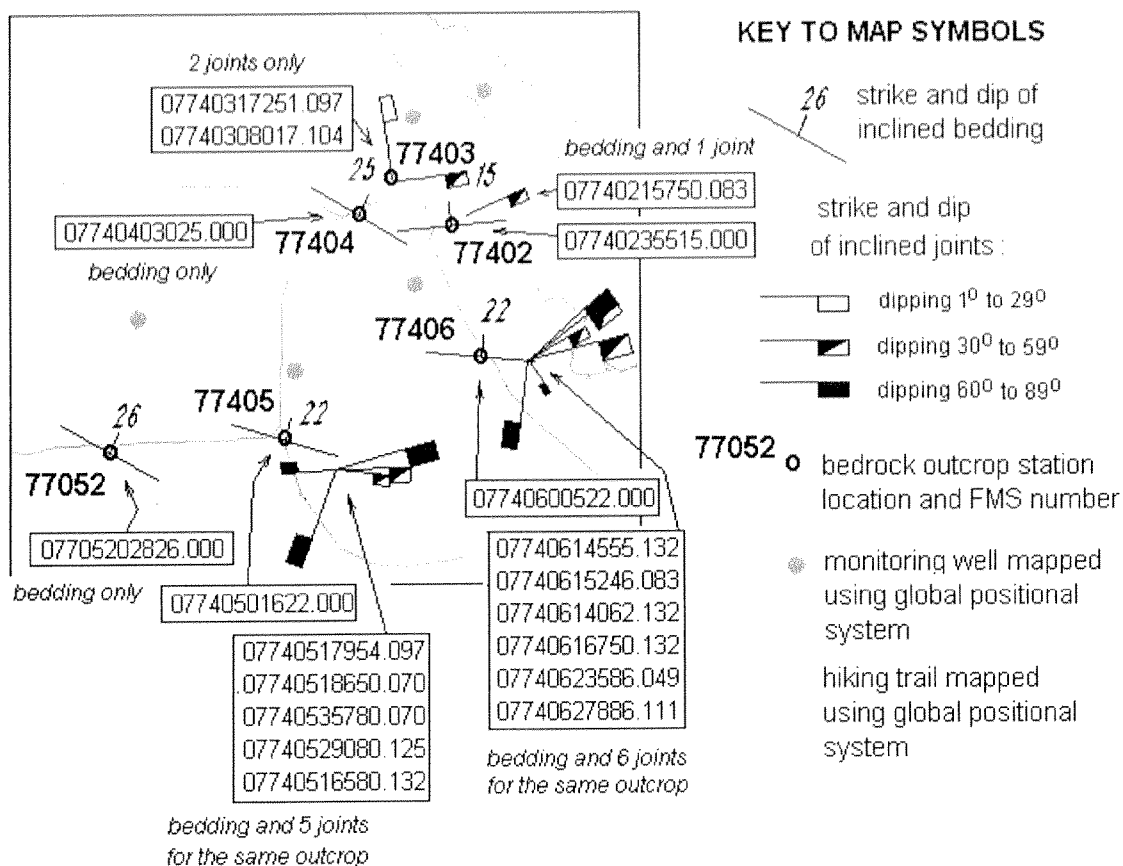
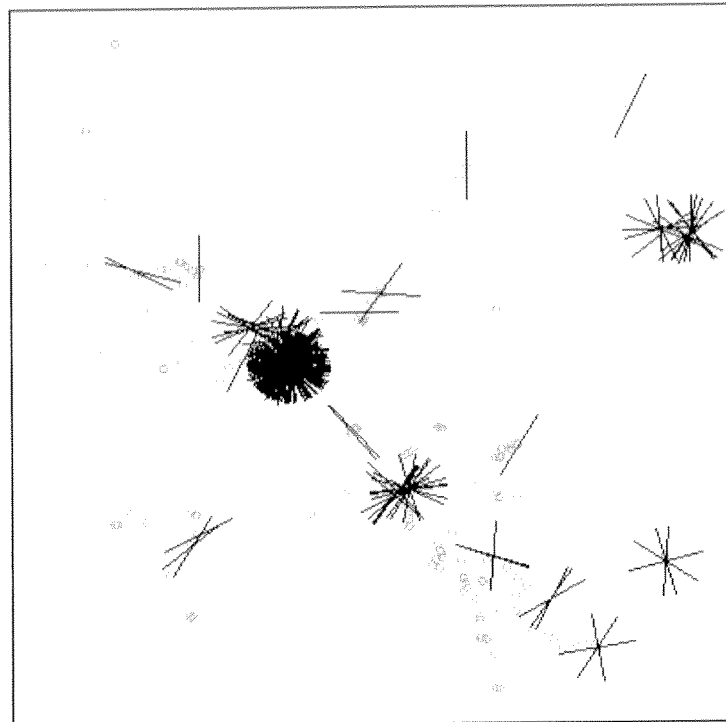


Figure 2.4. Modified VGA graphic displays from the **FRACGEN** program. Fracture-traces are generated from a mesostructure data file (*.MES) for either the map (top) or cross-section (bottom) view. Data can be output from this program to an *.AML file for generating ARC/INFO line coverages. The cross-section view was generated using a profile trace through the center of the data set along an azimuth bearing of 135° and a projection angle of 45°. The length of the fracture traces in both diagrams is 10,000 ft. Diagrams show the orientation of greenschist-facies brittle shear planes in Proterozoic basement across the northeast part of the N.J. Highlands. Lower diagram illustrates that these type of structures mostly dip northwest at moderate to high angles across the region.



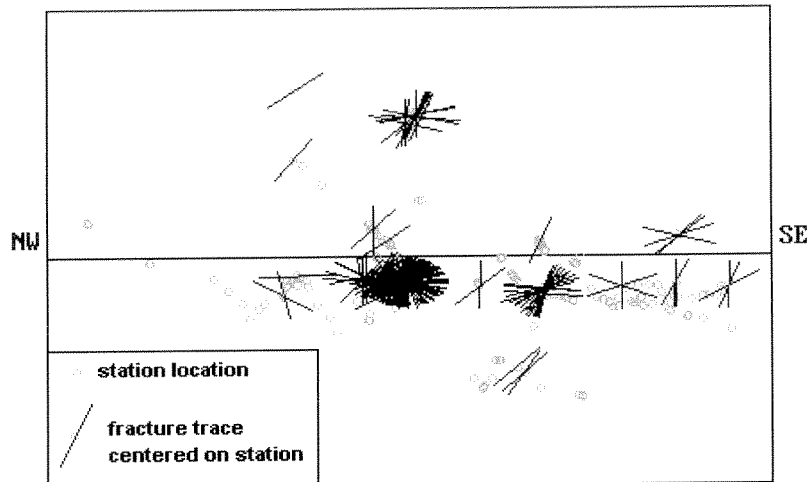
of stations: 44
of traces: 201

Map Coordinates

xmin: 459603.1
xmax: 553608.7
ymin: 760867.3
ymax: 867600.9



Location of study area
in New Jersey



Profile azimuth: 135
Projection angle: 45
Trace length: 10000

View points only
Save *.AML file
Filter by dip
Restart program
eXit program

Figure 2.5. FMS-DOS VGA screen graphics from **ROSESTAT** includes graphics display for 1°, 5°, and 10° bins for half-(Fig. 2.5a) and full-rose (Figs. 2.5c, 2.5d) histograms. Fig. 2.5b. shows simultaneous graphics display of planar strike and dip.

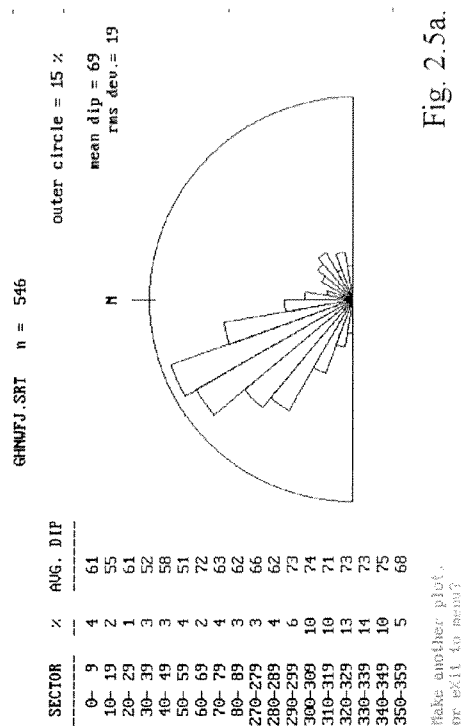


Fig. 2.5a.

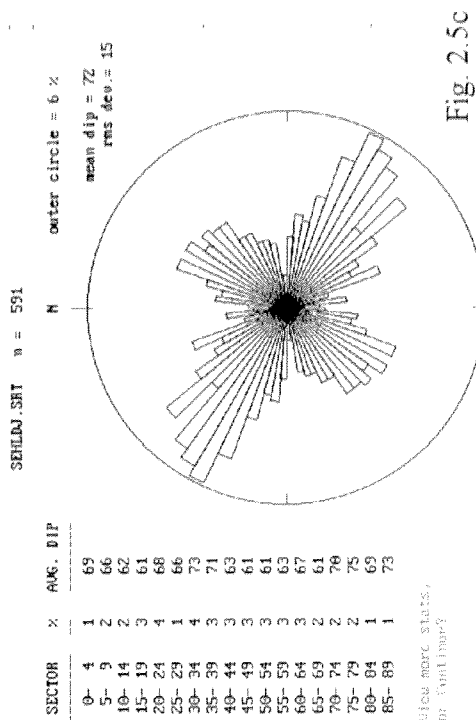


Fig. 2.5c

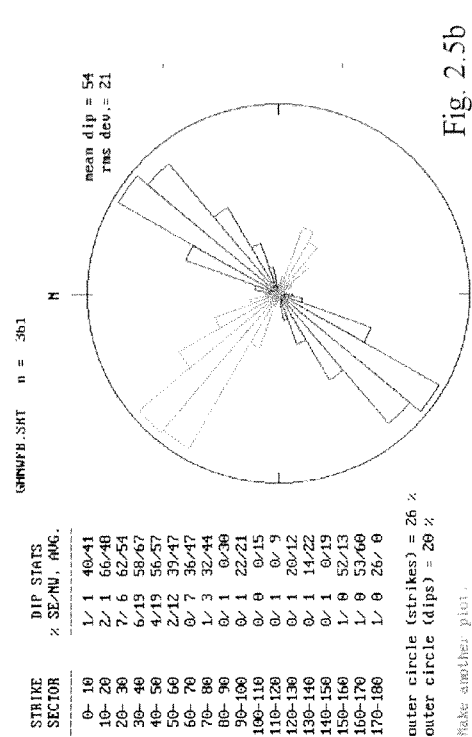


Fig. 2.5b

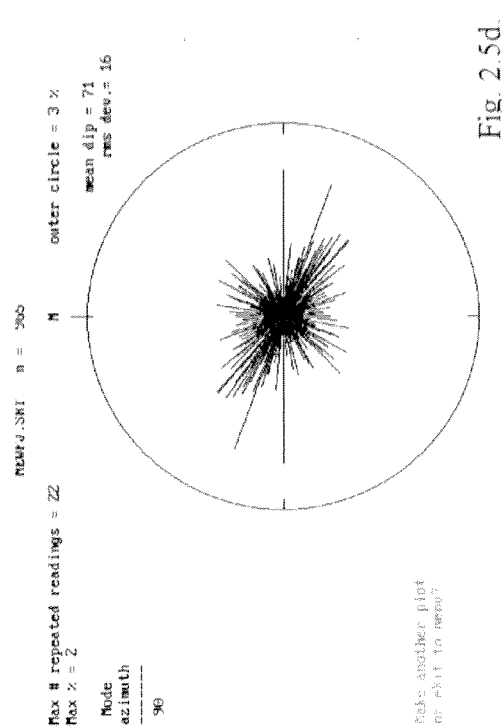
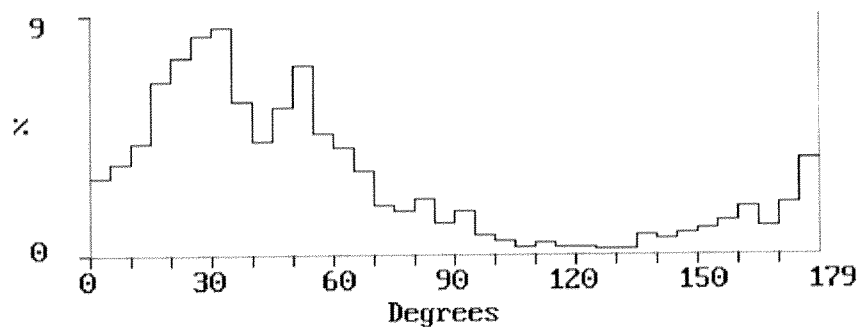


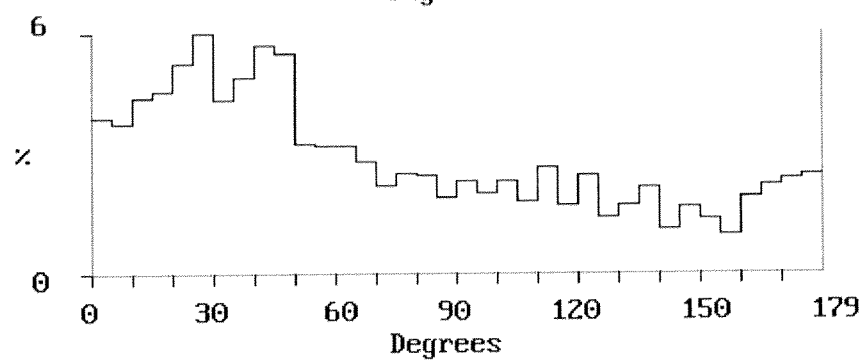
Fig. 2.5d.

Figure 2.6. FMS-DOS VGA screen graphics from **ARCAZMTH**. Top histogram summarizes azimuthal relative frequencies for an AUTOCAD Drawing Exchange File (*.DXF) containing only line and polyline segments. Lower diagram summarizes azimuthal relative frequencies for an outcrop-based structural data file (*.SRT) made using **DATASORT**.



FAULTS.DXF

81 Lines
2115 Polyline
segments
Total length:
746567 feet

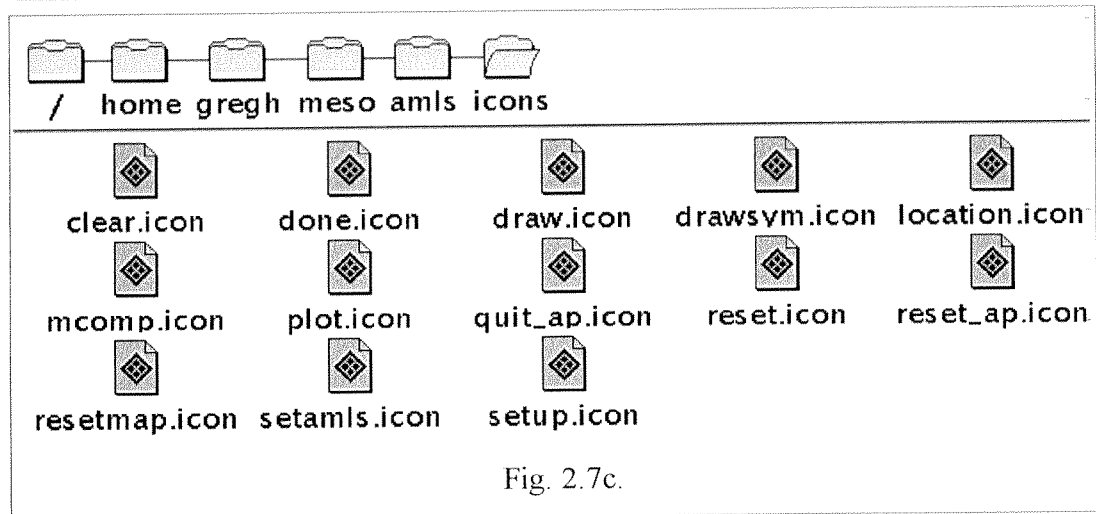
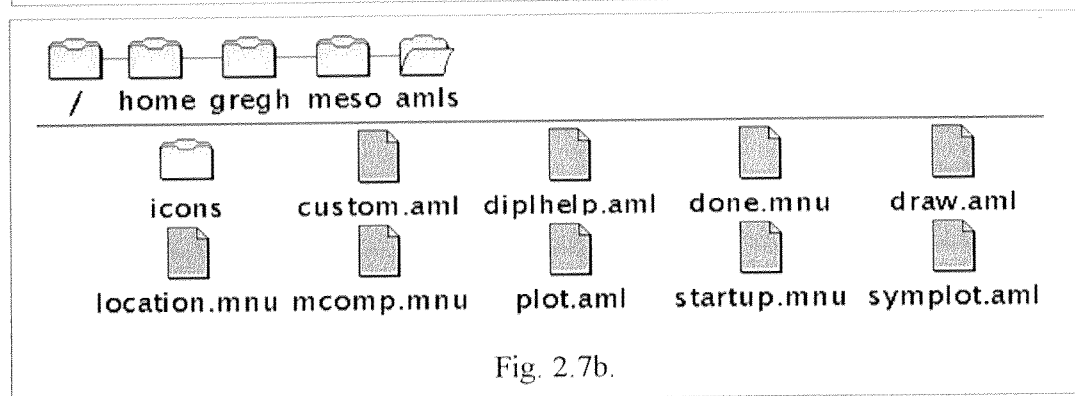
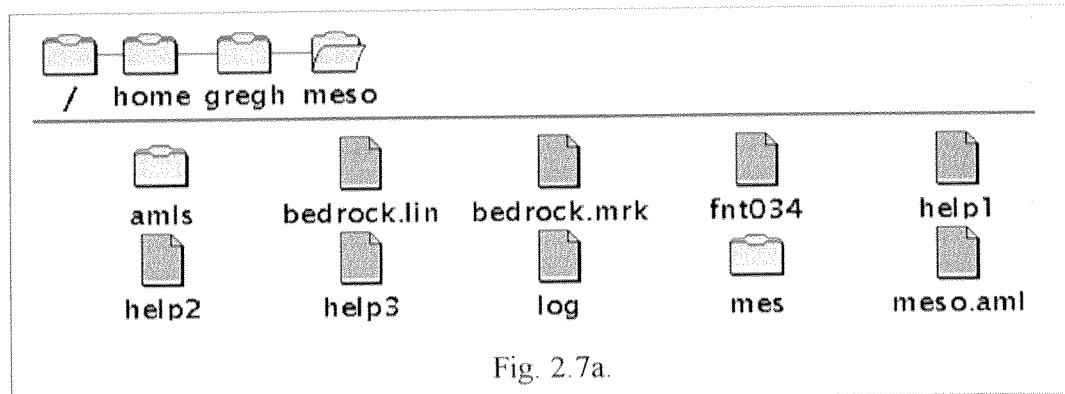


HAZPJU.SRT

n = 2360

Press X to return to the menu

Figure 2.7. The directory paths and contents for the set of files that comprise the FMS-UNIX **meso.aml**. (a). Directory path and file contents of the meso "root" directory. (b). Directory path and file contents of the "aml" subdirectory. (c). Directory path and file contents of the "icons" subdirectory.



KEY TO SYMBOLS:





	directory folder		UNIX file
	open directory folder		UNIX file (icon)

Figure 2.8. The set of ARCPlot form menus accessed through the FMS-UNIX macro **meso.aml**. (a). The opening FMS-UNIX (ARCPlot) form menu. (b)The FMS-UNIX menu for setting the map composition. (c). The FMS-UNIX Location & Drawing menu.

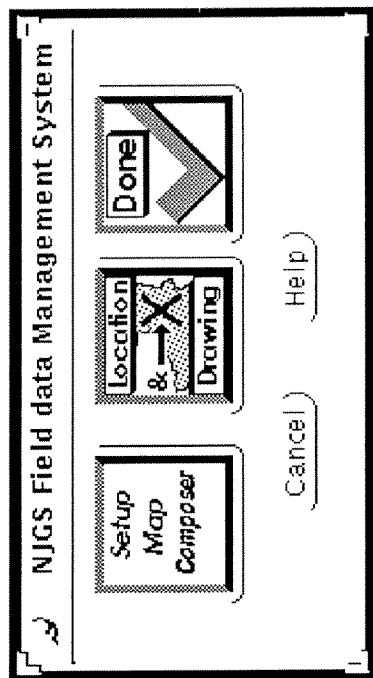


Fig. 2.8a.

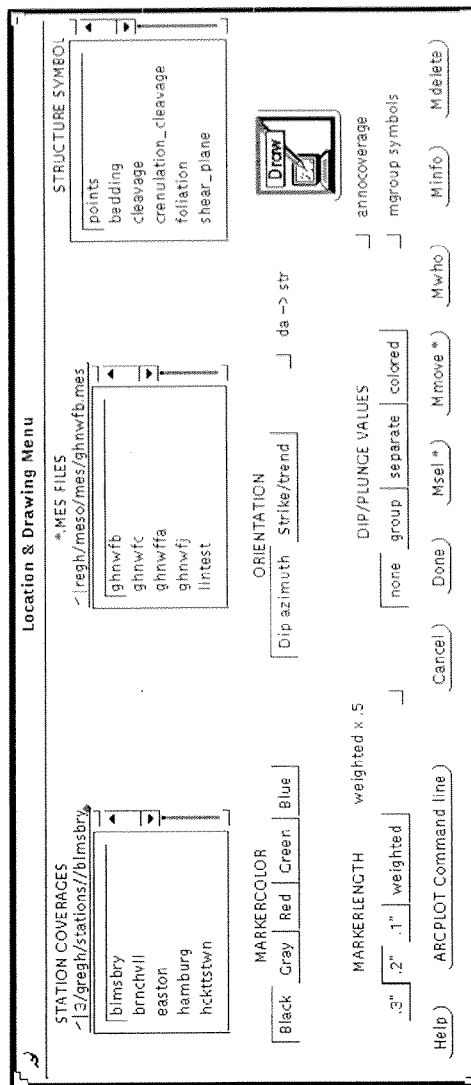
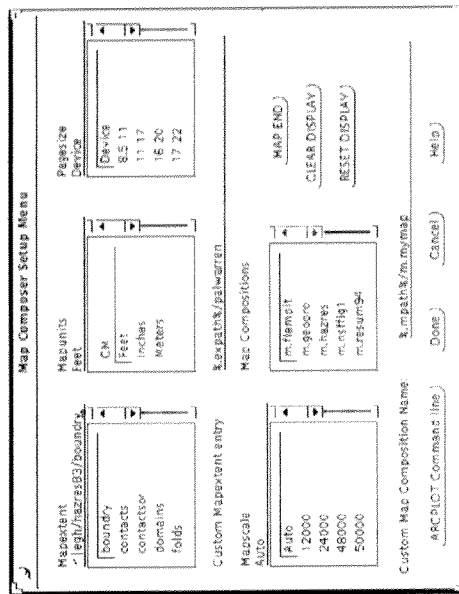


Fig. 2.8b.

Fig. 2.8c.

Figure 2.9. Screen capture of a UNIX file manager showing the directory path (top) to the ARCPLOT map composition **plate1.map** and the graphic files contained in the **plate1.map** directory. Each file within the directory corresponds to a geologic symbol or annotation graphic on the map.

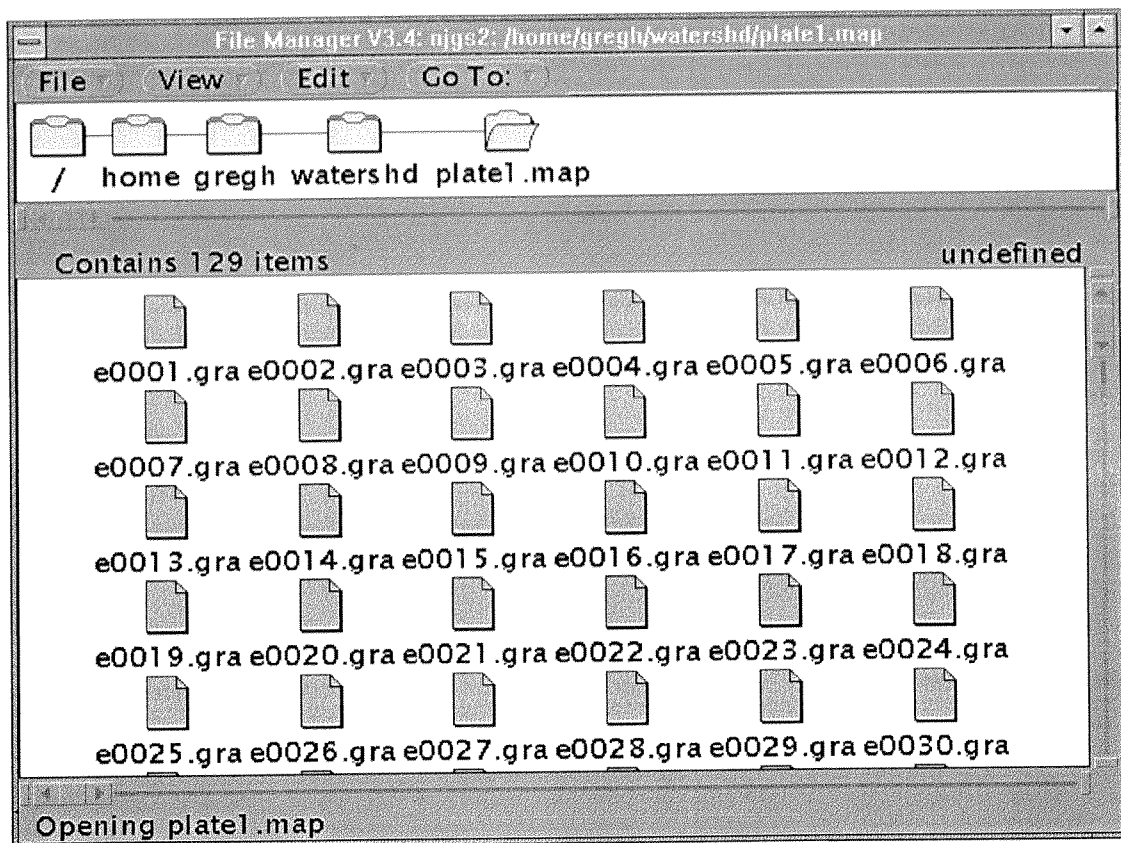
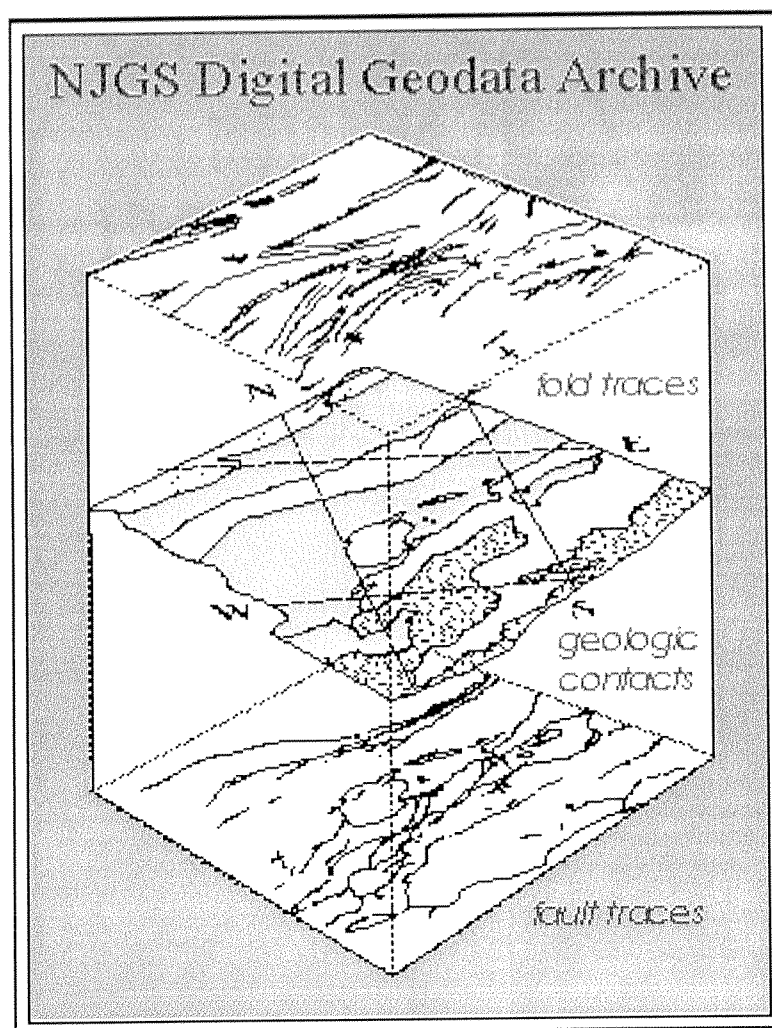


Figure 2.10. A 3-D exploded-block diagram illustrating three data layers generally included as part of the NJGS bedrock-geology coverages. Contacts and faults are built as one coverage with both line and polygon attributes. Folds are built as a separate coverage with line attributes.



CHAPTER 3. DIGITAL MAPPING OF FRACTURES IN THE MESOZOIC NEWARK BASIN: DEVELOPING A GEOLOGICAL FRAMEWORK FOR INTERPRETING MOVEMENT OF GROUND-WATER CONTAMINANTS

Introduction

Bedrock fractures are the principal source of secondary porosity and permeability in most bedrock aquifers. Understanding the distribution and connectivity of fracture sets within the aquifer system is critical for determining the storage capacity and flow direction of ground water and its contaminants. The purpose of this work is to examine the orientations and distribution of bedrock faults, folds, and fractures mapped in a faulted part of the Mesozoic Newark basin to depict the geologic structures resulting in anisotropic flow of ground-water. The study focuses on the orientation and distribution of geologic faults, folds, and unmineralized fractures in a six-quadrangle region (Fig. 3.1). The spatial variability and relative density of bedrock fractures is examined with respect to the location of major fault and fold structures using the NJGS FMS and a GIS. The relationship between specific fracture sets and aquifer characteristics is not directly explored. This paper demonstrates one approach for analyzing and producing digitized structural geology data for use in ground-water studies of contaminated bedrock aquifers and for helping to predict ground-water flow directions.

Geologic Setting

The study area is a six-quadrangle area (about 300 square miles) in west-central New Jersey within the central part of the Newark basin (Fig. 3.1). The Newark basin is the most densely populated physiographic province in New Jersey and the largest and most intensively studied Mesozoic-aged sedimentary basin in a series of such basins extending from Newfoundland, Canada to the southeast U.S.A (Olsen and others , 1996).

The central part of the basin was chosen for analysis because of recent geologic mapping in the area and because the area is traversed by large faults that impart many folds and fractures to the bedrock.

The Newark basin is a rift basin filled with Triassic-Jurassic sedimentary and igneous rocks that have been tilted, faulted, and locally folded (see recent summaries in Schlische (1992) and Olsen and others, (1996)). Most tectonic deformation is thought to be of Late Triassic to Middle Jurassic age (Lucas and others, 1988; de Boer and Clifford, 1988). Multiple tectonic phases are proposed to have affected the basin based on stratigraphic, paleomagnetic, and radiometric data. As summarized by Schlische (1992), a series of small rift basins began to form early in the Late Triassic along several normal fault segments that were probably reactivated Paleozoic reverse faults. As continental extension continued the basin grew in width and length and the sub-basins merged to form the Newark basin. A transition from fluvial to lacustrine sedimentation accompanied basin growth during the Triassic. The variation in thickness of Triassic sediments in the basin reflects syndepositional fault activity and along-strike variation in displacements along both intrabasinal and basin-bounding fault systems. Tectonism probably intensified during the latest Triassic into the earliest Jurassic based on the occurrence of widespread igneous activity and a marked increase in sediment-accumulation rates. Tectonic deformation and synchronous sedimentation continued into the Middle Jurassic at which time extensional faulting and associated tilting and folding ceased. At this stage, the basin likely experienced a period of postrift contractional deformation and localized basin inversion, which have been recognized in other Mesozoic rift basins (de Boer and Clifford, 1988; Withjack and others, 1995; R. Schlische, 1996, personal communication). Subsequent erosion of Mesozoic rocks was followed by flexural loading of the passive margin by Cretaceous sediments of the coastal plain sequence.

Two general structural trends are identified in the New Jersey part of the Newark

basin, one that correlates with the strike of the basin's northwest margin (about N 40°-50° E), and another with the strike of the intrabasinal Hopewell and Flemington faults (about N 10° -20° E). Both trends are dominant within the study area. The border, Hopewell, and Flemington faults are simplified representatives of complex fault systems composed of many fault segments (Fig. 3.2). Many gently-northwest-plunging bedding folds occur close to the Hopewell and Flemington fault systems that are apparently crosscut and offset by smaller faults that splay from the main faults (Fig. 3.2). These transverse folds likely stem from the variable amounts of fault-slip commonly found along the strike of normal faults (Schlische, 1992).

Methods

The bedrock geology was mapped and compiled for a six-quadrangle region of the Newark basin (Fig. 3.2). Structural data were recorded for about 1300 rock outcrops (Fig. 3.3). Multiple readings of structural bearing and inclination were collected at individual outcrops wherever individual measurements varied by more than 5°. Multiple readings of a particular type of structure are included in the statistical analyses and maps. The geologic field data sources for each quadrangle are summarized in Table 3.1. Geologic data recorded at each outcrop includes primary structural and lithologic criteria such as bed orientation and the stratigraphic unit. Secondary structural information includes the orientation and morphology of faults, folds, and fractures as available.

The map traces of stratigraphic contacts, faults, and folds for the six-quadrangle area were built as GIS coverages to use as a basis for examining the spatial relationship of bedrock fractures. Stratigraphic contacts and faults were built as a single GIS coverage having both polygon and line attributes to enable their separate identification (as previously discussed in Chapter 2). Geologic folds and outcrop locations were built as individual GIS coverages having line and point topology respectively. Fold traces were

only assigned default coverage variables from ARC/INFO. Outcrop locations were assigned field-station numbers and geographic coordinates were added to the point attribute table. Other ARC/INFO coverages developed as part of this study include the study area boundary and a set of structural domains (Fig. 3.3).

The fracture classification system for this study was limited in scope because data were collected from outcrops of varying quality and exposure and because field geologists used different methods to map and record the structural information. As a result, similar types of geologic structures of varying genesis and morphology were commonly recorded as a single type of structure. For example, bedrock fractures other than those oriented subparallel to sedimentary bedding were noted as one type of structure even though this classification combines both tension (mode I) and shear (mode II and III) fractures (Engelder and others, 1993). This classification system was necessary because very few field notes were taken on fracture morphology and fracture lengths. However, about half of the field notes contain information about fracture spacing. Therefore, the regional part of this study focused primarily on the distribution and orientation of fractures and inter-fracture spacing.

Geologic data from the geologist's field notes were typed into an ASCII text file using the FMS FIELDDATA (*.FD) file format (Table 2.1). Data entries for each field station include the station number, geologic formation, a structural domain variable, and information for each geologic structure recorded in the geologist's field notes. Geological structures were sorted and organized using a set of primary and secondary structural variables. Four primary variables from Table 2.3 were used to note the type of geologic structure. These included: B (bedding plane), P (user-defined planar structure), SP (mineralized shear plane), and SL (fibrous slip lineation). Secondary variables were used in conjunction with the primary variable for the user-defined planar structure (P) to denote unmineralized (JU) and mineralized (JM) fracture planes. Other secondary variables were

used for categorizing the inter-fracture spacing and trace length of measured fractures (Table 2.3b). All secondary structural variables were combined in strings of two-character variables as illustrated in Table 2.1a. The following structures were recorded in the HAZRES.FD FIELDATA file for 1339 mapped outcrops:

a) bed-parallel fractures sets:	1070 from 990 outcrops
b) non-bedding unmineralized fracture sets:	2361 from 912 outcrops
c) non-bedding mineralized fracture sets:	35 from 23 outcrops
d) mineralized shear planes with slip lineations:	144 from 59 outcrops

Bed-parallel fractures define planes of brittle fracturing that are oriented at small acute angles (10° or less) to sedimentary bedding. Non-bedding fractures include all other fractures in sedimentary rocks and all fractures in igneous rocks. The analysis of mineralized fractures and shear planes is beyond the scope of this study. Mineralized fracture sets often form subparallel to unmineralized fractures in the same outcrop and unmineralized fracture sets occurring in one outcrop may be mineralized in nearby outcrops. A comparative study of mineralized and unmineralized fracture sets is complicated by the near-surface dissolution of the more common mineral precipitates (calcite and quartz). More subsurface information is needed to understand this relationship.

The variables used for noting the fracture spacing (C0 to C5) were patterned after work by Harris and others (1960) for a regional fracture study of bedded sedimentary rocks. However, an expanded range of fractures per unit distance was used for the intermediate class of fracture to address complications arising from measuring both spaced fractures and spaced sets of fractures. Complications arose in employing a linear classification system for fracture spacing (for example 2, 4, and 6 fractures per meter).

because subparallel fractures commonly are grouped in sets or "swarms" that are spaced from one to a few meters apart (Fig. 3.4). Most spaced-fracture sets have about five to twenty-five individual fractures spaced from .5 cm to 2 cm apart within a fracture set or "swarm". It was therefore necessary to broaden the range for the intermediate class of fracture spacing to in order to separately identify fracture sets exhibiting similar spacing for individual fractures (fracture classes C4 and C5). Although the C3 class of fracture cannot convey whether it represents ten equally-spaced fractures in a meter distance or one fracture set composed of ten tightly-spaced fractures, it provides a mechanism to discriminate between broadly spaced, intermediate spaced, and tightly spaced sets of fractures while restricting the number of secondary variables used to denote fracture spacing.

There were no entries made in the FIELDATA file for the spacing or trace length of bed-parallel fractures. There is currently a lack of published information relating lithologic criteria such as grain size to bed thickness and fracture spacing for rocks of the Newark basin. However, other studies examining layering in sedimentary bedrock show direct correlation between fracture spacing and lithologic thickness (Huang and Angelier, 1989; Narr and Suppe, 1991; Gross, 1993). Field notes for this study indicate that laminated siltstone and mudstone of the Passaic Formation generally show closer spacing of bed-parallel fractures and shorter trace lengths of fractures than sandstone and hard shale of the Stockton and Lockatong Formations, respectively. No bedding- or foliation-parallel fracture systems were recorded for any of the igneous rocks. More work is needed to characterize fracture spacing in different lithologies stemming from physical weathering near the earth's surface and neotectonic fracture systems.

The orientation, distribution, and spacing of bedrock fractures was compared to the orientation and distribution of nearby faults and folds for the entire study area, and with respect to a set of subregions, or 'structural domains' (Fig. 3.3). A structural domain

is a subregion of bedrock that is distinguished from other subregions by structural criteria. Each domain either displays a unique structural trend, composes an area where the bedrock is folded or unfolded, or corresponds to a fault zone or fault block occurring next to a fault zone (hanging wall or footwall fault block). Most domain boundaries correspond to the trace of mapped faults whereas others are more arbitrary. The latter include folded panels of rocks separate from panels containing unfolded rocks, or a domain polygon established by extrapolating the map trace of a fault. This study does not focus on lithologic control on fracture orientation and density because different rock types are often combined within a structural domain.

Fracture orientations were analyzed using five different graphical methods:

- 1). The structural bearing of each set of fractures were compared to the structural bearing of faults and folds for the entire study area using standard azimuth frequency histograms
- 2). Bed-parallel and other fracture sets were analyzed for a set of structural domains using circular azimuth frequency histograms.
- 3). GIS coverages of fractures were generated for both bedding and non-bedding fractures using both statistically weighted and unweighted plot symbols. Weighted plot symbols used 10° azimuth ranges from circular azimuth frequency plots for the regional data sets.
- 4). Fracture sets were sorted and mapped based on the spacing of individual fractures in a fracture set.
- 5). Five sets of non-bedding fractures corresponding to ranges of frequency maximums for different geologic structures were separately sorted and mapped to investigate their regional distribution (domain overlap analysis).

Results

Four GIS coverages of fracture traces were generated for the bed-parallel and non-bedding fractures using the FRACGEN program (see Chapter 2). FRACGEN generates ASCII files containing coordinate information corresponding to the endpoints of fracture traces. The ASCII files are used to generate GIS line coverages in ARC/INFO. Two coverages were generated for each data set: one showing unweighted fracture-traces (Figs. 3.5a and 3.6a), and the other showing statistically-weighted fracture-traces based on the azimuthal bearing of a fracture population for the entire study area (Figs 3.5b and 3.6b). The statistical filtering of fracture-trace data allows dominant trends within a region to be graphically emphasized relative to less frequent trends.

Azimuth Histogram Analysis of Mapped Faults, Folds, and Fractures

The map traces of fracture, fault, and fold azimuths were graphically plotted on standard histogram using the ARCAZMTH program, then stacked to compare their similarities and differences (Fig. 3.7). A visual comparison of the data shows that data for all structural features has either primary or secondary population maximums in the 40° to 55° ranges. This range of structural bearings is therefore the dominant structural trend in this part of the Newark basin, and conforms with the azimuth bearing of the northwest margin of the basin, the long axis of the basin, and many fault segments within the intrabasinal fault systems (Fig. 3.1). The coincidence of frequency maximums about the 45°-55° structural bearing for all measured structures demonstrates that the orientation of the system of faults along the northwest border of the basin largely determines regional structural trends. Local structural trends vary widely, most notably for secondary faults, non-bedding fractures, and folds.

Figure 3.7 also shows that non-bedding fracture orientations are generally subparallel to mapped fault traces. Specifically, fault traces and non-bedding fractures

both have two clusters of frequency maximums that are subparallel to one another. The dominant fault-traces have frequency maximums in the 25°-35° and 45°-55° ranges whereas the non-bedding fractures have maximums in the 20°-30° and 40°-50° ranges. These two ranges of maximums coincide with the bearing of the Flemington fault system within the study area, and with the aforementioned primary structural trend in the region. It is interesting that in both cases the alignment of the fracture maximums is shifted about 5° counterclockwise relative to the maximums for the faults. The reason for this shift is uncertain. The coincidence of frequency maximums for the bearing of fault traces and non-bedding joints throughout the study area demonstrates that the development of non-bedding fractures in the region is primarily related to tectonic faulting, and local variation in the strike of non-bedding joints is probably influenced by local variations in the strike of map-scale faults. To test this last hypothesis, the orientation of bedding and other fracture sets were examined with respect to a set of structural domains.

Both groups of unmineralized fractures were statistically summarized for each structural domain using relative frequency circular histogram graphs (rose diagrams) with 10° bins (Fig. 3.3b). Bed-parallel fractures are displayed for each domain in the upper half of each histogram (shaded petals) and non-bedding fractures are summarized in the lower half (unshaded petals). Other statistical data accompanying the histograms include the average inclination (dip) for each set of fractures, the number of recorded fractures and the number of outcrops visited (for example 92:83 respectively), and the percentage value of the maximum frequency bin.

The data show that 1) non-bedding fractures frequently strike subparallel to the trace of local faults and show a subordinate relationship of strike to the orientation of bedding fractures, 2) the average inclination of bedding fractures range between 13° to 26°, with the steepest dips (inclinations) occurring to the north towards the border fault system, and within intrabasin fault zones, and 3) the average dip of non-bedding fractures

ranges between 70° to 79°, with more gently-dipping non-bedding fractures occurring to the north towards the border fault system.

Map Analysis of Non-Bedding Fracture Densities

The spatial relationship between faulting and folding and the distance between subparallel fractures in a fracture set was also examined. The average number of subparallel fractures within a distance of 1 meter in a direction normal to the fracture strike was recorded for 1047 of the total 2361 fracture sets measured in the study area. The structural bearing of fractures of each set of fractures with recorded density values was sorted and plotted on separate GIS map compositions at their respective outcrop locations (Fig. 3.8). Custom plotter symbols were created and used to denote each class of fracture; one line was used to show the location for each fracture set with a low relative density value (fracture density $<1/\text{m}$) whereas symbols with up to five parallel lines were used for fracture sets with higher density values. The results of this analysis show that there is a direct correlation between the spacing of fractures in a fracture set and their location relative to faults, folds, and igneous bodies. The most striking result is the agreement between fracture sets with relatively high densities (short spacing between fractures) and the orientation of nearby faults. Figure 3.8 shows that fracture sets with higher density values (variable C4 with 25 to 50 fractures per m, and C5 sets with >50 fractures per m) are usually restricted to near-fault intervals and show subparallel alignment to local fault traces. Therefore fracture sets with fractures spaced less than 4 cm mostly originate from mechanical processes related to tectonic faulting. Figure 3.8 also shows that the most common fracture density value recorded in the study area was 5 to 25 fractures per meter (density variable C3). This density class has the broadest range of spacing values for the data set and includes subparallel fractures spaced from 4 cm to 20 cm. Most of these fracture sets strike subparallel to nearby fault segments. However,

they also occur with cross-strike orientations near the trace of faults, folds and igneous intrusions. Fractures belonging to this density class have a complex genesis related to the development of faults, folds, and the intrusion of igneous bodies. Fracture sets displaying relatively low density values commonly are oriented both subparallel and sub-perpendicular (cross-strike) to both bedding and fault strikes throughout the study area. Fractures occurring sub-perpendicular to local faults have slightly higher density values (C2 variable for 1 to <5 fractures per m) than cross-strike fractures occurring away from faulted areas (C1 variable for <1 fracture per meter). Fractures with a C2 value commonly strike parallel to intrabasin faults within 8 km of the fault, particularly in the down-thrown side of the fault (hanging wall).

Domain Overlap Analysis

Domain overlap analysis is a graphical technique to identify discrete regions (subarea) within a study area where structural domains having the same fracture azimuths overlap (Mabbe and others, 1994). The distributions of non-bedding fracture orientations for five ranges of azimuth were examined over the study area for the entire data set. The five ranges of frequency maximums were picked by eyeballing five pronounced trends on the standard histogram analysis for fractures, faults, and folds (Fig. 3.7). They include the two principal orientation maximums for fault traces and non-bedding fractures (020°-029° and 040°-049°), the most prevalent range of cross-strike fractures (110° to 124°), and two other ranges of fractures that correspond to subordinate maximums for both fault and fold traces (175° to 004° and 080° to 094°). Data plot files were then produced for each range of azimuths and a corresponding set of plot files were produced which shows the location of each set of fracture that fell within each selected range.

The results of this analysis show that cross-strike fractures are ubiquitous, but the non-bedding fracture sets that strike subparallel to faults are spatially variable (Fig. 3.9).

For example, fractures that strike sub-parallel to the trace of a major fault commonly occur in rocks on both sides of the fault. However, the most frequently mapped non-bedding fractures (040° to 049°) in the study area are absent west of the Flemington fault system. Immediately west of the Flemington fault, the border fault system shows about a 20° clockwise rotation of structural bearing, with an average strike of about 65° . Fractures with a 040° to 049° structural bearing may be absent in this region simply because the bounding fault has a different strike. This suggests that the occurrence of a fracture set within a fault block largely relates to the orientation of the bounding faults. Another explanation for the restricted occurrence of these fractures may relate to the amount of structural movement (strain) that stratum within a fault block are subjected to. For example, the Flemington fault block has been structurally displaced downward towards the east and south by more than 10,000 feet, based on having relatively young Mesozoic strata preserved on the east side of the main fault trace (Fig. 3.2). Strata within the Fleimington fault block were subjected to dip-slip movements along the border fault and both dip-slip and strike-slip movements along the Flemington fault system (Herman and others, 1992). In contrast, Mesozoic strata occupying the footwall of the Flemington fault system (west of the fault) may have only been strained from dip-slip movements along the border fault and have experienced comparatively less strain than rocks in the Flemington fault block. The degree to which fault-subparallel fractures are developed within a fault block may simply be related to the amount of structural displacement of the fault block, with more fractures occurring in more highly-strained rocks. More mapping and research are needed to determine if fracture sets in adjacent blocks also display similar spatial relationships as those observed in this study area.

Conclusions and Discussion

This research shows that the distribution, orientation, and density of non-bedding fractures in the Newark basin are primarily influenced by tectonic faults. Fractures occurring within a fault block are most frequently aligned sub-parallel to the fault systems that bound a fault block and less frequently at moderate angles to the strike of faults and at cross-strike bearings. Furthermore, the structural bearings of faults that form the northwestern border of the Newark basin seem to play the dominant role in determining the strike of the most frequently-mapped non-bedding fracture set in a fault block. Other conclusions from this research are:

- 1) The most frequently mapped fracture sets in the central part of the Newark basin show a range of inter-fracture spacing from 4 to 20 cm.
- 2) Subparallel fractures with an average spacing of 4 cm or less over a distance of a meter (tightly-spaced sets of fractures) are common within 4 km of major fault, become more concentrated approaching the fault, and are most frequently aligned subparallel to the strike of the fault.
- 3) Digital mapping of fractures is an effective approach for characterizing the geological framework of fractured bedrock aquifers

Although these results are restricted in their applicability for tectonic analyses, they provide the environmental community with a general understanding of how fracture orientations and densities in the Newark basin spatially relate to primary geological map structures such as faults and folds. These data are meant to compliment more detailed information collected near ground water contamination sites and may help reduce the costs of characterizing and remediating ground-water contamination by constraining the hydraulic framework of contaminant flow paths and increasing the effectiveness of siting

monitoring and decontamination wells.

Figure 3.1. Index map showing the location of the study area in the New Jersey part of the Newark basin, major geologic faults, 7.5 minute quadrangles, and Counties. Quadrangle abbreviations include PT (Pittstown), FG (Flemington), ST (Stockton), HW (Hopewell), LB (Lambertville), and PN (Pennington). County abbreviations include H (Hunterdon), S (Somerset), and M (Mercer).

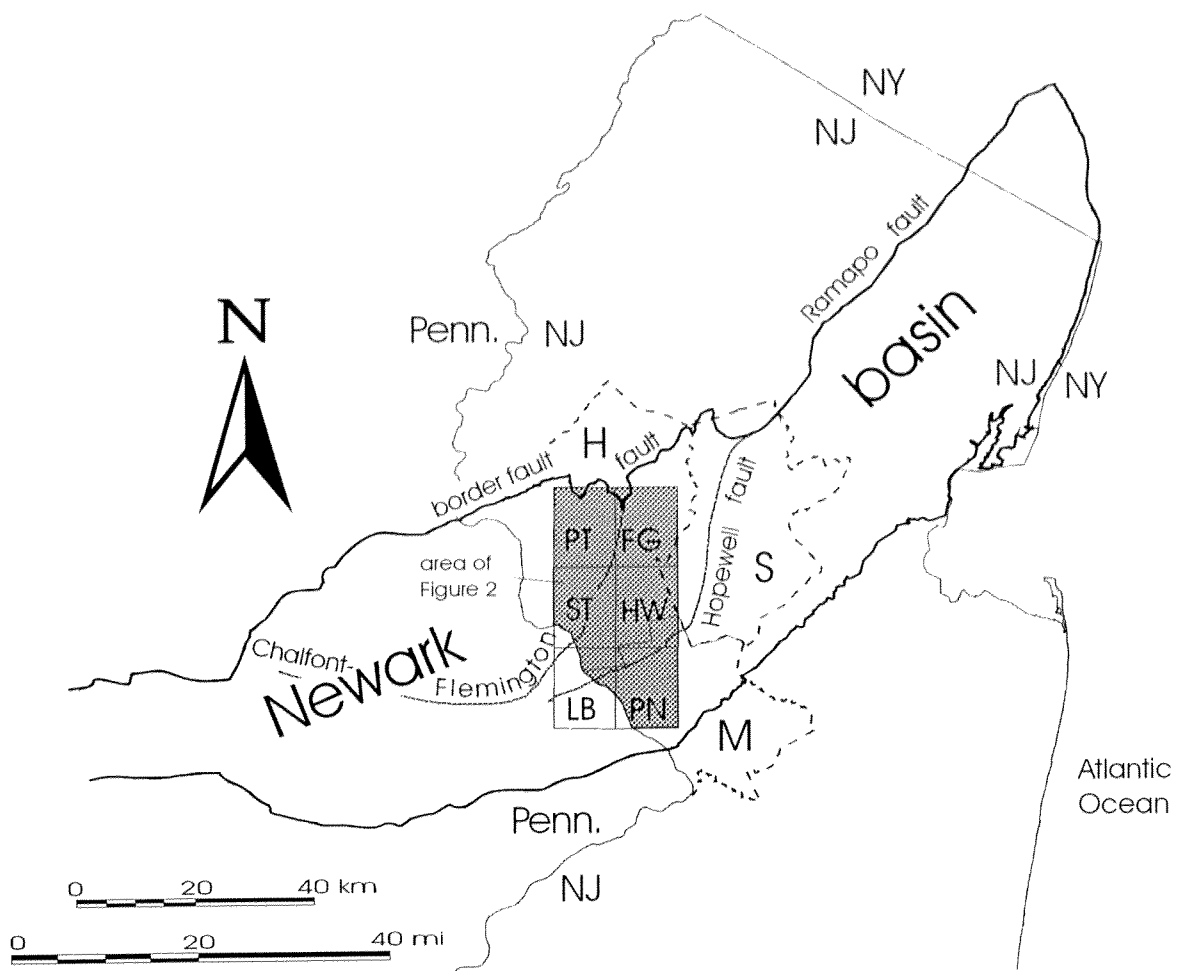


Figure 3.2. Generalized geologic map of a six-quadrangle area in the New Jersey part of the Mesozoic Newark basin. Map modified from Herman and others (1992) and compiled from unpublished geologic mapping by H. B. Kummel (1895-1898, 1:21,120 scale), H. F. Houghton and J. P. Mitchell (1985-1990, 1:24,000 scale), and G. C. Herman and D. H. Monteverde (1990- 1995, 1:24,000 scale).

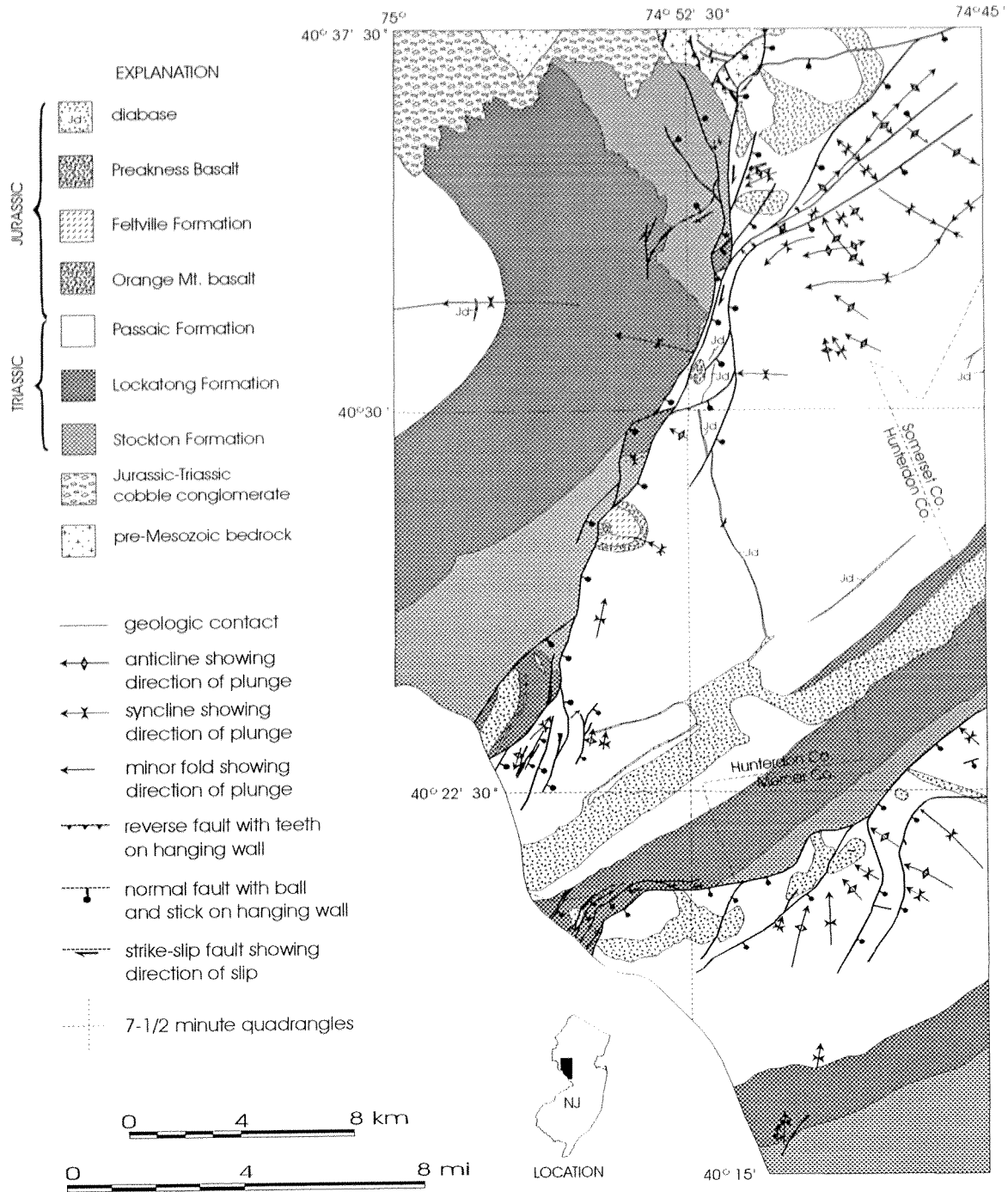
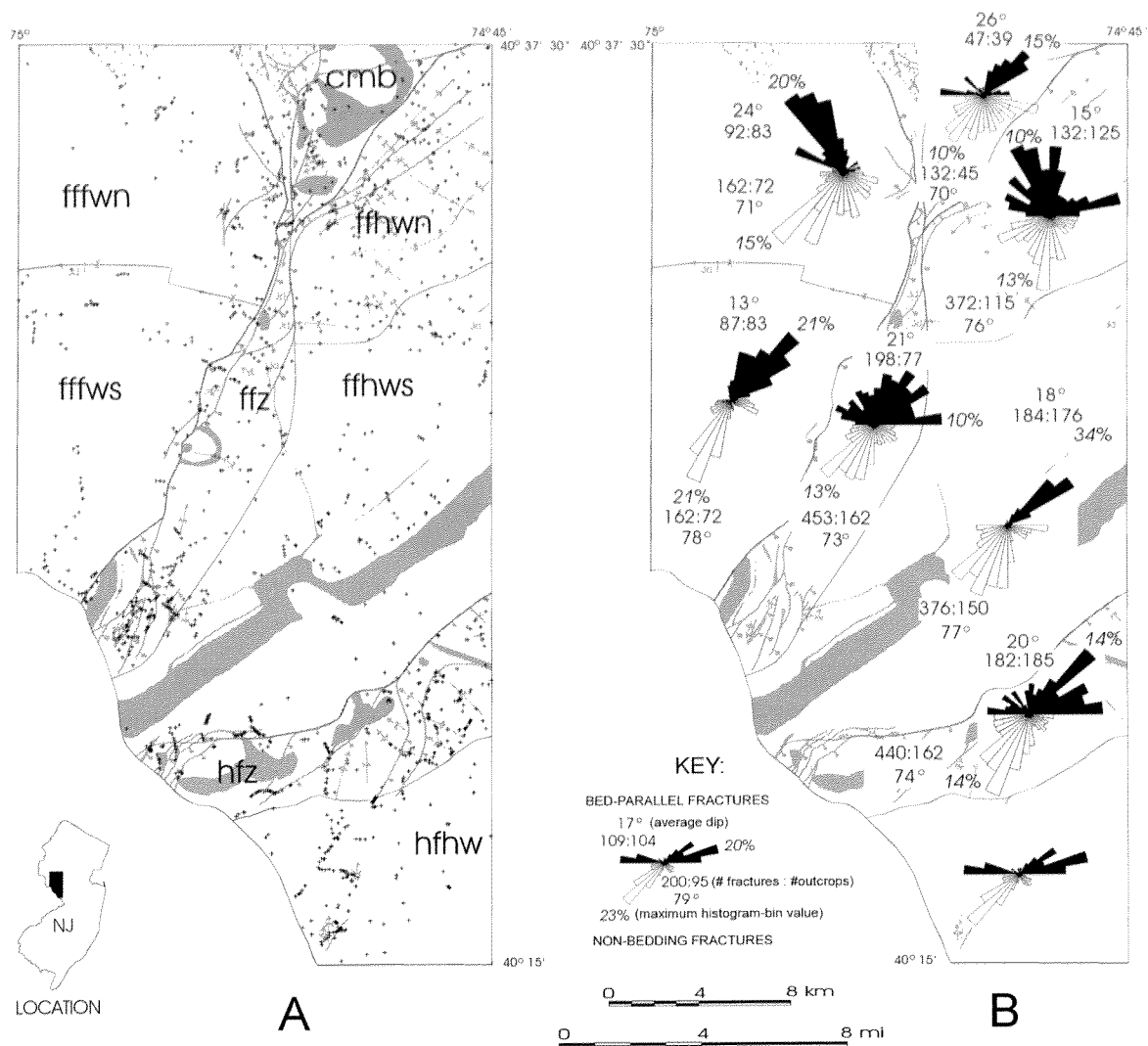


Figure 3.3. Map on left shows the distribution of outcrops in the study area where structural data were measured and the set of structural domains used for examining structural trends. The structural domains include: fffwn (Flemington fault, footwall, north), fffws (Flemington fault, footwall, south), cmb (Cushetunk Mountain block), ffz (Flemington fault zone), ffhwn (Flemington fault, hanging wall, north), ffhws (Flemington fault, hanging wall, south), hfz (Hopewell fault zone), and hfhw (Hopewell fault, hanging wall). Map on right summarizes the structural orientations for bedding and other fracture sets for each domain. Bed-parallel fractures are summarized in the upper half of each histogram (shaded histogram petals) and non-bedding fractures are summarized in the lower half (unshaded histogram petals).



EXPLANATION

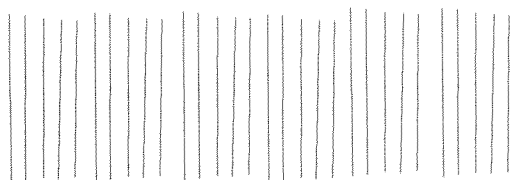
- Ja Jurassic diabase dike
- Jurassic igneous rocks
- pre-Mesozoic bedrock

- geologic contact
- anticline showing direction of plunge
- syncline showing direction of plunge
- minor fold showing direction of plunge

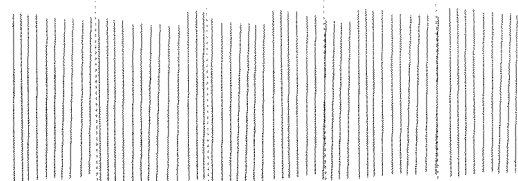
- reverse fault with teeth on hanging wall
- normal fault with ball and stick on hanging wall
- strike-slip fault showing direction of slip

Figure 3.4. Diagram illustrating the method used for grouping subparallel fractures into classes of fractures based on inter-fracture spacing. The occurrence of spaced fracture sets complicates the fracture classification system which is based on the number of subparallel fractures within a distance of 1 meter measured normal to the fracture plane (or fracture trace if using a pavement outcrop). A comparison of the diagrams on the left and right shows that the classification system is scale dependant and the fracture spacing should be measured over lengths greater than 1 meter wherever possible to account for having both equally-spaced fractures and spaced fracture sets in the study area.

EQUALLY-SPACED FRACTURES
CLASS C4 (>25 and < 51 / m)



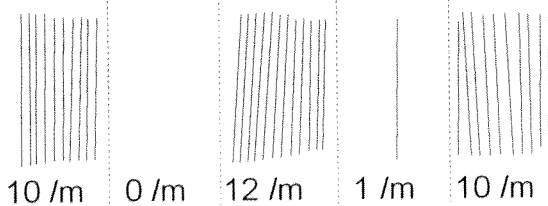
EQUALLY-SPACED FRACTURES
CLASS C3 (>5 and < 25 / m)



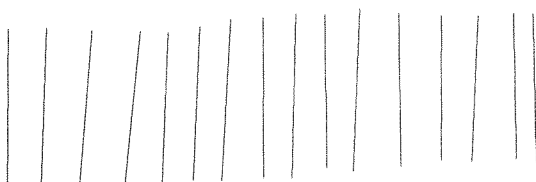
SPACED FRACTURE SETS
CLASS C3 (>5 and < 26 / m)



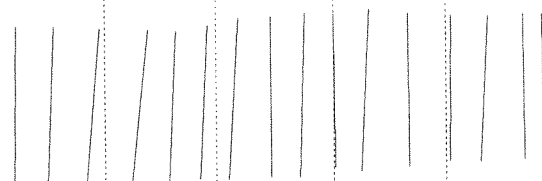
SPACED FRACTURE SETS
CLASS C2 (average >1 and < 6 / m)



EQUALLY-SPACED FRACTURES
CLASS C3 (>5 and < 26 / m)



EQUALLY-SPACED FRACTURES
CLASS C2 (>1 and < 6 / m)



1 m.

5 m.

Figure 3.5 Maps showing the distribution of bedding-plane fracture sets based on the ARC/INFO GIS coverages.

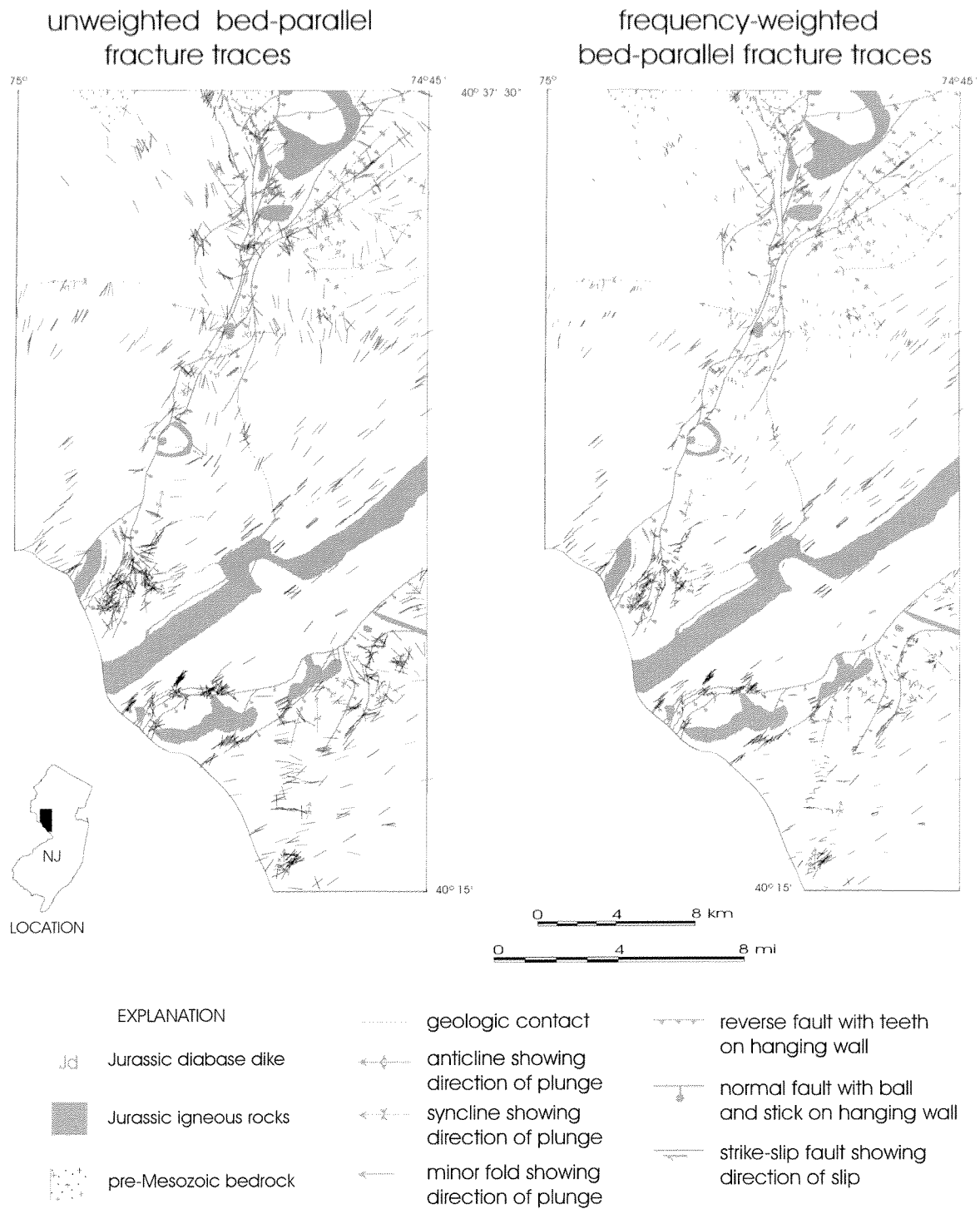
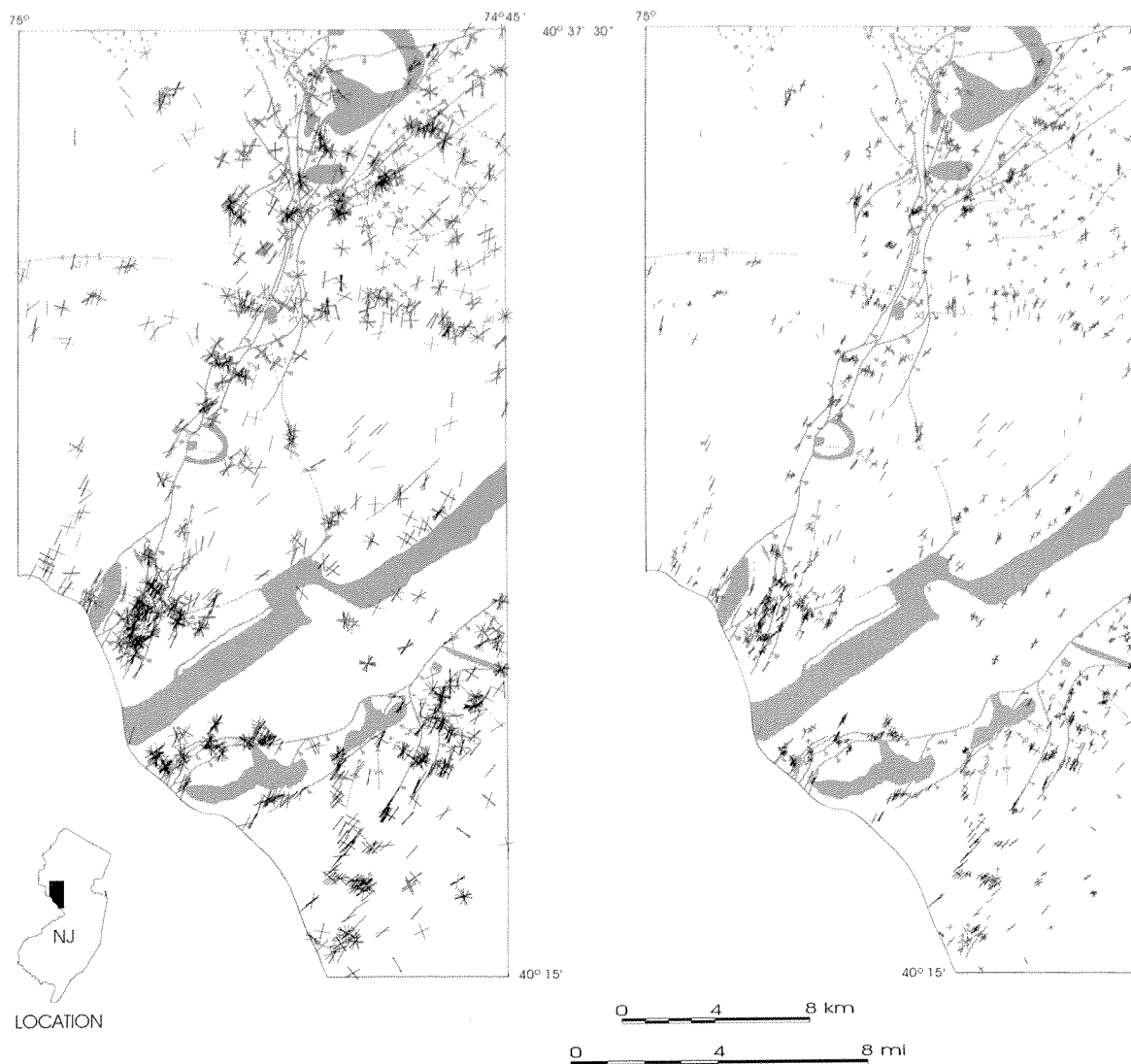


Figure 3.6. Maps showing the distribution of unmineralized non-bedding fracture sets based on the ARC/INFO GIS coverage.

unweighted fracture
traces (non-bedding)

frequency-weighted fracture
traces (non-bedding)



EXPLANATION

Jd Jurassic diabase dike

Jurassic igneous rocks

pre-Mesozoic bedrock

geologic contact

anticline showing
direction of plunge

syncline showing
direction of plunge

minor fold showing
direction of plunge

reverse fault with teeth
on hanging wall

normal fault with ball
and stick on hanging wall

strike-slip fault showing
direction of slip

Figure 3.7. Relative frequency histogram plots showing the comparison of structural bearing for fault traces, unmineralized fractures, and fold traces in the study area.

APPENDIX A. GEOLOGIC-UNIT VARIABLES USED BY THE NJGS FOR DEVELOPING GIS GEOLOGIC THEMES

geonum geoabb geoname (5,6,I)= 5 input characters, 6 output characters, integer (I) or
(C) alphabetic character

(5,6,I) (8,9,C) (80,81,C)

25	af	artificial fill	220	Qta	Talus
50	ebo	extensive bedrock outcrop	221	Qtl	Lower Terrace Deposits
75	sbo	scattered bedrock outcrop	223	Qtu	Upper Terrace Deposits
100	Cz	Cenozoic Era	225	Qrt	Raritan Terrace Deposits
110	Q	Quaternary System	230	Qe	Eolian Deposits
112	ct	continuous till	240	Qbs	Beach Sand
114	dt	discontinuous till	300	Qt	Till
116	m	morainic deposits	305	Qtt	Discontinuous till
118	im	morainic deposits (Illinoian age)	310	Qtw	Late Wisconsinian Till
119	d	deltaic sediment	312	Qtwr	Rahway Till
120	l	lake-bottom sediment	314	Qtwm	Netcong Till
122	f	fluvial sediment	316	Qtwk	Kittatinny Mountain Till
124	fl	fluvial over lacustrine sediment	318	Qtwqc	Till derived from quartzite and conglomerate
126	if	fluvial sediment (Illinoian age)	320	Qtwc	till derived from carbonate rock
128	ic	ice-contact sediment	322	Qtwg	till derived from gneiss
130	it	till of Illinoian age	324	Qtwss	till derived from gray slate
132	jt	till of Jerseyan age	326	Qtwrs	till derived from red shale
134	js	sand and gravel of Jerseyan age	328	Qtwb	till derived from basalt and diabase
136	x	non-glacial material	350	Qti	Illinoian Till
160	Qs	Swamp and Marsh Deposits	352	Qtif	Flanders Till
170	Qal	Alluvium	354	Qtib	Bergen Till
172	Qalb	Alluvium and Boulder Lag	370	Qtj	Pre-Illinoian (Jerseyan) Till
174	Qalfp	Floodplain Deposits	380	Qtl	Tillstone Lag
176	Qalc	Channel Deposits	400	Qsd	Stratified Drift
180	Qcal	Colluvium and Alluvium	410	Qsdw	Late Wisconsinian Stratified Drift
190	Qmm	Estuarine Deposits	420	Qsdwd	Glaciolacustrine Sand and Gravel
200	Qaf	Alluvial Fan Deposits	422	Qsdwde	Deltaic Deposits
210	Qst	Stream Terrace Deposits	424	Qsdwlf	Lacustrine Fan Deposits

430	Qsdwlb	Glaciolacustrine Lake Bottom Deposits
440	Qsdwf	Glaciofluvial Sand and Gravel
442	Qsdwfv	Valley Outwash Deposits
444	Qsdwft	Meltwater Terrace Deposits
450	Qsdi	Illinoian Stratified Drift
460	Qsdid	Glaciolacustrine Sand and Gravel
462	Qsdi	Deltaic Deposits
464	Qsdilf	Lacustrine Fan Deposits
470	Qsdilb	Glaciolacustrine Lake Bottom Deposits
480	Qsdif	Glaciofluvial Sand and Gravel
482	Qsdifv	Valley Outwash Deposits
484	Qsdift	Meltwater Terrace deposits
500	Qsdj	Pre-Illinoian (Jerseyan) Stratified Drift
520	Qsdjd	Glaciolacustrine Sand and Gravel
522	Qsdjde	Deltaic Deposits
524	Qsdjlf	Lacustrine Fan Deposits
530	Qsdjlb	Glaciolacustrine Lake Bottom
542	Qsdjfv	Valley Outwash Deposits
540	Qsdj	Glaciofluvial Sand Deposits and Gravel
544	Qsdjft	Meltwater Terrace Deposits
600	Qic	Ice Contact Deposits
700	Qm	Morainic Deposits
710	Qmw	Late Wisconsinan Moraines
720	Qmi	Illinoian Moraines
800	Qc	Colluvium
810	Qcg	Gneiss Colluvium
820	Qcb	Basalt Colluvium
830	Qcd	Diabase Colluvium
840	Qcs	Slate
850	Qcc	Conglomerate Colluvium
860	Qcq	Quartzite Colluvium
870	Qcsg	Sand and Gravel Colluvium
880	Qcsl	Sand and Silt Colluvium
885	Qccb	Carbonate Colluvium
890	Qct	Till Colluvium
900	Qw	Weathered Bedrock
910	Qwg	Weathered Gneiss
920	Qwb	Weathered Basalt
930	Qwd	Weathered Diabase
940	Qws	Weathered Slate
950	Qwc	Weathered Conglomerate
960	Qwcb	Weathered Carbonate
962	Qwcp	Weathered coastal-plain formations
970	Qwq	Weathered Quartzite
980	Qwsc	Weathered Schist
990	Qcm	Cape May Formation
1000	T	Tertiary System
1100	Tp	Pensauken Formation
1200	Tb	Bridgeton Formation
1205	TQb	Bridgeton Formation (arkosic phase)
1210	TQbg	Bridgeton Formation (glaucinitic phase)
1250	Tg	Upland Gravel
1300	Tbh	Beacon Hill Formation
1390	Tcm	Unnamed Formation at Cape May
1400	Tch	Cohansey Formation
1450	Tck	Cohansey & Kirkwood Formations
1460	Tbp	Belleplain Formation

1470 Tw	Wildwood Formation	3100 J	Jurassic System
1480 Tsm	Shiloh Marl Formation	3110 Jb	Boonton Formation
1500 Tkw	Kirkwood Formation	3120 Jbcb	Basalt-clast Conglomerate
1600 Tsr	Shark River Formation	3130 Jbcg	Gneiss-clast Conglomerate
1700 Tmq	Manasquan Formation	3140 Jbcq	Quartzite-clast Conglomerate
1800 Tvt	Vincentown Formation	3200 Jbs	Jurassic Basalt
1900 Tht	Hornerstown Formation	3300 Jh	HookMt. Basalt
2000 M	Mesozoic Era	3400 Jt	Towaco Formation
2100 K	Cretaceous System	3450 Jtc	Towaco Formation Conglomerate facies
2150 Krb	Redbank Formation	3500 Jp	Preakness Basalt
2200 Kt	Tinton Formation	3550 Jps	Preakness Basalt Second flow
2250 Kns	Navesink Formation	3600 Jf	Felville Formation
2300 Kml	Mt. Laurel Formation	3650 Jfc	Felville Formation Conglomerate facies
2350 Kmw	Mt. Laurel & Wenonah Formations	3700 Jo	Orange Mountain Basalt
2400 Kwe	Wenonah Formation	3800 Jd	Jurassic Diabase
2450 Kmt	Marshalltown Formation	3850 Jg	Jurassic Granophyre
2500 Ket	Englishtown Formation	3900 JTrc	Jurassic-Triassic Conglomerate
2550 Kwb	Woodbury Formation	3950 JTrcq	Jurassic-Triassic Quartzite-clast Conglomerate
2600 Kmv	Merchantville Formation	3960 JTrcsh	Jurassic-Triassic Shale Clast Conglomerate
2610 Kcq	Cheesequake Formation	3970 JTrcl	Jurassic-Triassic Limestone Clast Conglomerate
2650 Kmrp	Magothy	4000 JTrp	Passaic Formation
2700 Km	Magothy Formation	4100 JTrpg	Passaic Formation Gray bed
2710 Kmas	Amboy Stoneware Clay Member	4150 JTrpgh	Passaic Formation Gray-bed Hornfels
2720 Kmob	Old Bridge Sand Member	4200 JTrph	Passaic Formation Red-bed Hornfels
2730 Kmsa	South Amboy Fire Clay Member	4250 JTrpcq	Passaic Formation Quartzite-clast Conglomerate facie
2740 Kmss	Sayerville Sand Member		
2800 Kr	Raritan Formation		
2803 Krs	Red Bank Shrewsbury Member		
2805 Krsh	Red Bank Sandy Hook Member		
2810 Krwc	Woodbridge Clay Member		
2820 Krfs	Farrington Sand Member		
2830 Krfc	Raritan Fire Clay Member		
2900 Kp	Potomac Formation		
3000 JTr	Jurassic & Triassic Systems		

4300 JTrpcl	Passaic Formation Limestone-clast Conglomerate facies	5450 Trssc	Stockton Formation Cobble Conglomerate and Sandstone facies
4350 JTrpcsh	Passaic Formation Shale-clast Conglomerate facies	5500 Trscq	Stockton Formation Quartz-Cobble Conglomerate facies
4400 JTrpcs	Passaic Formation Conglomerate and Sandstone facies	6000 Pal	Paleozoic Era
4450 JTrpss	Passaic Formation Conglomerate and Pebbly Sandstone facies	6100 D	Devonian System
4500 JTrps	Passaic Formation Sandstone and Siltstone facies	6150 Dsk	Skunnemunk Conglomerate
4505 JTrpst	Passaic Formation Siltstone and Mustone facies	6200 Dbv	Bellvale Sandstone
4510 JTrpm	Passaic Formation Mudstone facies	6250 Dcw	Cornwall Shale
5000 Tr	Triassic System	6300 Dm	Marcellus Shale
5100 Trl	Lockatong Formation	6350 Db	Buttermilk Falls Limestone
5150 Trlr	Lockatong Formation Red bed	6400 Dkec	Kanouse Formation, Esopus Formation, and Connelly Conglomerate
5200 Trlh	Lockatong Formation Hornfel	6450 Dkn	Kanouse Sandstone
5250 Trla	Lockatong Formation Arkosic Sandstone facies	6500 Ds	Schoharie Formation
5300 Trls	Lockatong Formation Sandstone facies	6550 De	Esopus Formation
5310 Trlcq	Lockatong Formation Quartz-Cobble Conglomerate facies	6600 Dcc	Connelly Conglomerate
5350 Trlsc	Lockatong Formation Sandstone and glomerate facies	6650 Do	Oriskany Group
5400 Trs	Stockton Formation	6720 Drs	Ridgely Sandstone
		6740 Dsc	Shriver Chert
		6760 Dg	Glenarie Formation
		6800 Dh	Helderberg Group
		6820 Dp	Port EwenShale
		6840 Dmn	Minisink Limestone & New Scotland Formation
		6860 Dmi	Minisink Limestone
		6880 Dn	New Scotland Formation
		6900 Dc	Coeymans Formation Undivided
		6920 Dkl	Kalkberg Limestone
		6940 Dcl	Coeymans Limestone
		6960 Dml	Manlius Limestone
		7000 DS	Devonian & Silurian Systems

7100 S	Silurian System	8340 Ojta	Jutland Klippe Sequence Unit A
7150 DSr	Rondout Formation	8500 OCu	Ordovician & Cambrian Systems
7200 DSrd	Rondout & Decker Formations	8550 OCjk	Jacksonburg Limestone and Kittatinny Supergroup
7250 Sd	Decker Formation	8400 Oj	Jacksonburg Limestone
7300 Sbv	Bossardville Limestone	8420 Ojr	Jacksonburg Limestone Cement-Rock Facies
7400 Sbv	Berkshire Valley Formation	8440 Ojl	Jacksonburg Limestone Cement Limestone Facies
7500 Sp	Poxono Island Formation	8460 Ow	Sequence at Wantage
7550 Spbv	Berkshire Valley & Poxono Island Formations	8490 Oj+	All Paleozoic units above Beekmantown Group
7600 Sb	Bloomsburg Red Beds	8575 OCjwb	Jacksonburg Limestone, Wantage Sequence, and Beekmantown Group undivided
7700 Sl	Longwood Shale	8600 OCK	Kittatinny Supergroup
7800 Sgp	Green Pond Conglomerate	8610 Ob	Beekmantown Group
7900 Ss	Shawangunk Formation	8620 Obu	Beekmantown Group Upper Part
8000 O	Ordovician System	8630 Obl	Beekmantown Group Lower Part
8100 Obsu	Beemerville Intrusive Suite	8640 Oo	Ontelaunee Formation
8120 Ons	Nepheline Syenite	8642 Ooh	Ontelaunee Formation Harmonyvale Member
8140 Ol	Lamprophyre and Related Rocks	8644 Oobr	Ontelaunee Formation Beaver Run Member
8160 Oub	Ouachitite Breccia - Volcanic Breccia	8650 Oe	Epler Formation
8200 Om	Martinsburg Formation	8652 Oel	Epler Formation Lafayette Member
8210 Omhp	Martinsburg Formation High Point Member	8654 Oebs	Epler Formation Big Springs Member
8220 Omhph	Martinsburg Formation High Point Member Hornfel	8656 Oebr	Epler Formation Branchville Member
8230 Omr	Martinsburg Formation Ramseyburg Member	8660 Or	Rickenbach Dolomite
8240 Omrh	Martinsburg Formation Ramseyburg Member Hornfel		
8250 Omb	Martinsburg Formation Bushkill Member		
8260 Ombh	Martinsburg Formation Bushkill Member Hornfel		
8300 Ojt	Jutland Klippe Sequence		
8320 Ojtb	Jutland Klippe Sequence Unit B		

8662	Orh	Rickenbach Dolomite Hope Member Limestone Facies
8664	Orl	Rickenbach Dolomite Lower Member
8670	Os	Stonehenge Formation
8700	C	Cambrian System
8750	OCa	Allentown Dolomite
8752	OCau	Allentown Dolomite Upper Member
8754	OCal	Allentown Dolomite Limeport Member
8800	Cl	Leithsville Formation
8820	Clw	Leithsville Formation Walkill Member
8840	Clha	Leithsville Formation Hamburg Member
8860	Clc	Leithsville Formation Califon Member
8900	Clh	Leithsville Formation & Hardyston Quartzite
8920	Ch	Hardyston Quartzite
9000	Pc	Precambrian
9100	Pz	Proterozoic Era
9200	Zu	Late Proterozoic Era
9220	CZm	Manhattan Schist
9240	CZs	Serpentine
9260	Zch	Chestnut Hill Formation
9270	db	diabase dike
9280	Zd	Late Proterozoic Diabase
9300	Yu	Middle Proterozoic Era
9350	Ygm	Mt. Eve Granite
9400	Ybi	Byram Intrusive Suite
9420	Ybh	Hornblende Granite
9440	Ybs	Hornblende Syenite
9460	Ybb	Biotite Granite
9480	Yba	Microperthite Alaskite
9500	Ylh	Lake Hopatcong Intrusive Suite
9520	Ypg	Pyroxene Granite
9540	Yps	Pyroxene Syenite
9560	Ypa	Pyroxene Alaskite
9600	Ys	Syenite Gneiss
9700	Yms	Metasedimentary Rocks
9710	Yk	Potassic Feldspar Gneiss
9720	Ym	Microcline Gneiss
9730	Yb	Biotite-Quartz-Feldspar Gneiss
9740	Ymh	Hornblende-Quartz- Feldspar Gneiss
9750	Ymp	Clinopyroxene-Quartz- Feldspar Gneiss
9760	Yp	Pyroxene Gneiss
9762	Ypb	Pyroxene Gneiss with abundant biotite
9764	Yph	Pyroxene Gneiss with abundant hornblende
9766	Ypbh	Pyroxene Gneiss with abundant biotite and hornblende
9770	Ype	Pyroxene-Epidote Gneiss
9780	Ymr	Marble
9785	Yfl	Franklin Limestone
9790	Yq	Quartzite
9795	Ye	Epidote Gneiss
9800	Yl	Losee Metamorphic Suite
9820	Ylo	Quartz-Oligoclase Gneiss
9840	Yla	Albite-Oligoclase Granite
9860	Ylb	Biotite-Quartz-Oligoclase Gneiss
9870	Ylh	Hornblende-Quartz- Oligoclase Gneiss
9880	Yh	Hypersthene-Quartz- Plagioclase Gneiss
9900	Yd	Diorite
9910	Ya	Amphibolite

9920	Yam	Migmatite
9930	Ymg	Monazite Gneiss
9940	Yhp	Hornblende-Plagioclase Gneiss
9950	Ybp	Biotite-Plagioclase Gneiss
9960	Yma	Microantiperthite Alaskite

APPENDIX B. NJGS METADATA-FILE FORMAT

1. IDENTIFICATION INFORMATION

1.1. Citation (list information on how this set of data are to be referenced by the user)

1.1.1. Originator (N.J. Geological Survey, Trenton, NJ 08625)

1.1.2. Publication date (the date when the first version of the data are completed)

1.1.3. Title (formal title for the data set)

1.2. Description

1.2.1. Abstract describing data set, currentness, availability, intended use of data

1.2.2. List of names of component coverages, themes, or directories

1.2.2.3. List of names of files

1.2.2.4. List of keywords related to or describing coverage or file

1.3. Geographic extent - describe the area that the data set covers with respect to state, counties, quadrangles, physiographic provinces, project area, etc.

1.4. Contacts information

1.4.1. Name(s)

1.4.2. Agency

1.4.3. Address

1.4.4. Phone, fax, and email

2. DATA QUALITY INFORMATION

2.1. Name of digital data

2.1.1. Type of data (ARC/INFO coverage, dBase file, ASCII text file, etc.)

2.1.2. Data source (brief narrative, data stems from paper or mylar maps, GPS, etc.)

2.1.3. Data organizer(s)

2.1.4. Chronological record of data completion and maintenance

2.1.5. Data accuracy, scale, and other data limitations

3. SPATIAL DATA ORGANIZATION INFORMATION

3.1. Name of digital data

3.1.1. Automation methods (digitized, scanned and vectorized, GPS, generate file, etc.)

3.1.2. Automation date(s) (A complete chronologic record of origination and maintenance)

3.1.3. Notes

4. SPATIAL REFERENCE INFORMATION

4.1. Name of digital data

4.1.1. Type of data (raster, vector, point, or relational data file)

4.1.2. Object type (pixel if raster, line or polygon if vector, cartesian coordinate, etc.)

4.1.3. Data parameters (when applicable)

4.1.3.1. Scale.

4.1.3.2 Datum

4.1.3.3 Coordinate system

4.1.3.4 Projection

4.1.3.5 Global quadrant

4.1.3.6 Zone

5. ENTITY AND ATTRIBUTE INFORMATION

5.1. Name of digital data

5.1.1. Item or field name

5.1.1.1 Item or field type and attributes (ex. character, 9 input, 10 output)

5.1.1.2 Item or field description

5.2. List and description of related text files, data files, and look-up tables that are not part of the current workspace that directly relate to the item or field attribute values.

6. DISTRIBUTION INFORMATION

6.1. Distributor name, address, telephone, etc.

6.2. Available data format options

6.3. Details on how to obtain the information

6.4. Fees

7. METADATA REFERENCE INFORMATION

7.1. Original publication date and data originators, names, organizations, etc.

7.2. Revision dates and data revisionists, names, organizations, etc.

8. PUBLISHED REFERENCES (Published citations that relate to digital data)

9. AUTHORS NOTES

REFERENCES

- Apotria, T. G., Snedden, W. T., Spang, J. H., and Wiltchko, D. V., 1994, Kinematic models of deformation at an oblique ramp, in McClay, K. R., ed., *Thrust Tectonics*: Unwin-Hyman Press, Arnhem, The Netherlands, p. 141-154.
- Barnett, S. G., 1976, Geology of the Paleozoic Rocks of the Green Pond outlier: N. J. Geological Survey Geological Report Series no. 11, 9 p., 1 map, scale 1:24,000.
- Bayley, W. S., Salisbury, R. D., and Kummel, H. B., 1914, Description of the Raritan Quadrangle, New Jersey: U. S. Geological Survey Geology Atlas folio 191, 29 p., 6 pl.
- Beardsley, R. W., and Cable, M. S., 1983, Overview of the evolution of the Appalachian Basin: *Northeastern Geology*, v. 5, no. 3-4, p. 137-145.
- Bell, T. H., 1981, Foliation development -- the contribution, geometry, and significance of progressive, bulk inhomogenous shortening: *Tectonophysics*, v. 75, p. 278-296.
- Berg, T. M., and 8 others, compilers, 1980, Geologic map of Pennsylvania: Commonwealth of Pennsylvania Topographic and Geological Survey Map 1, 2 pl., scale 1:250,000.
- Beutner, E. C., 1978, Slaty cleavage and related strain in Martinsburg Slate, Delaware Water Gap, New Jersey: *American Journal of Science*, v. 278, p. 1-23.
- Beutner, E. C., and Diegel, F. A., 1985, Determination of fold kinematics from syntectonic fibers in pressure shadows, Martinsburg Slate, New Jersey: *American Journal of Science*, v. 285, p. 16-50.
- Beutner, E. C., Jancin, M. D., and Simon, R. W., 1977, Dewatering origin of cleavage in light of deformed calcite veins and clastic dikes in Martinsburg Slate, Delaware Water Gap, New Jersey: *Geology*, v. 5, p. 118-122.
- Bosworth, William, and Vollmer, F. W., 1981, Structures of the medial Ordovician flysch of eastern New York: Deformation of synorogenic deposits in an overthrust environment: *Journal of Geology*, v. 89, no. 9. p. 551-568.
- Boyer, S. E., and Elliott, David, 1982, Thrust systems: *American Association of Petroleum Geologists Bulletin*, v. 86., p. 1196-1230.

Boyer, S. E., and Mitra, G., 1988, Relations between deformation of crystalline basement and sedimentary cover at the basement/cover transition zone of the Appalachian Blue Ridge Province: Geological Society of America Special Paper 222, p. 119-136.

Bradley, D. C. and Kidd, W. S. F., 1991, Flexural extension of the upper continental crust in collisional foredeeps: Geological Society of America Bulletin, v. 103, p. 1416-1438.

Broughton, J. G., 1946, An example of the development of cleavages: The Journal of Geology, v. 54, no. 1, p. 1-18.

Burton, J.C., 1994, Expedited Site Characterization for Remedial Investigations at Federal Facilities: Federal Environmental Restoration and Waste Management Conference, p.1407- 1415

Christensen, N. I., and Szymanski, D. L., 1991, Seismic properties and the origin of reflectivity from a classic Paleozoic sedimentary sequence, Valley and Ridge Province, southern Appalachians: Geological Society of America Bulletin, v. 103, p. 277-289.

Cloos, E., and Broedel, C. H., 1943, Reverse faulting north of Harrisburg, Pa.: Geological Society of America Bulletin, v. 54, p. 1375-1398.

Costain, J. R., and Coruh, Cahit, 1989, Tectonic setting of Triassic half-grabens in the Appalachians: Seismic data acquisition, processing, and results, *in* Tankard, A. J., and Blakewill, H. R., eds., Extensional tectonics and stratigraphy of the Atlantic margins: American Association of Petroleum Geologists Memoir 46, Tulsa, Oklahoma, p. 155-174.

Dahlstrohm, C. D., 1969, Balanced cross sections: Canadian Journal of Earth Science, v. 6, p. 743-757.

Davis, D., Suppe, J., and Dahlen, F. A., 1983, Mechanics of fold and thrust belts and accretionary wedges: Journal of Geophysical Research, v. 88, B2, p.1153-1172.

Davis, R. E., Drake, A. A. Jr., and Epstein, J. B., 1967, Geologic map of the Bangor Quadrangle, Pennsylvania - New Jersey: U. S. Geological Survey Geologic Quadrangle Map GQ 665, scale 1:24,000.

de Boer, J. Z., and Clifford, A. E., 1988, Mesozoic tectogenesis: Development and deformation of 'Newark' rift zones in the Appalachian (with special emphasis on the

Hartford basin, Connecticut), *in* Manspeizer, W., ed., Triassic-Jurassic Rifting, Continental Breakup, and the Origin of the Atlantic Ocean and Passive Margin, Elsevier, New York, ed. p. 275-306.

de Paor, D. G., 1988, Balanced section in thrust belts Part 1: Construction: American Association of Petroleum Geologists Bulletin, v. 7, no. 1, p. 73-90.

Drake, A. A., Jr., 1967a, Geologic map of the Easton quadrangle, New Jersey - Pennsylvania: U.S. Geological Survey Geologic Quadrangle Map GQ594, scale 1:24,000.

_____ 1967b, Geologic map of the Bloomsbury quadrangle, New Jersey: U. S. Geological Survey Geologic Quadrangle Map GQ595, scale 1:24,000.

_____ 1969, Precambrian and lower Paleozoic geology of the Delaware Valley, New Jersey-Pennsylvania, *in* Subitsky, S., ed., Geology of selected areas in New Jersey and eastern Pennsylvania and guidebook of excursions: New Brunswick, N. J., Rutgers University Press, p. 51-115.

_____ 1984, The Reading Prong of New Jersey and eastern Pennsylvania: An appraisal of rock relations and chemistry of a major Proterozoic terrane in the Appalachians: Geological Society of America Special Paper 194, p. 75-109.

Drake, A. A., Jr., Epstein, J. B., and Aaron, J. M., 1969, Geological map and sections of parts of the Portland and Belvidere quadrangles New Jersey-Pennsylvania: U. S. Geological Survey Miscellaneous Geologic Investigation Map I-552, scale 1:24,000.

Drake, A. A., Jr., Kastelic, R. L., Jr., and Lyttle, P. T., 1985, Geologic map of the eastern parts of the Belvidere and Portland quadrangles, Warren County, New Jersey: U. S. Geological Survey Geologic Quadrangle Map I-1530, scale 1:24,000.

Drake, A. A., Jr., and Lyttle, P. T., 1985, Geologic map of the Blairstown quadrangle, Warren County, New Jersey: U. S. Geological Survey Geological Quadrangle Map GQ-1585, scale 1:24,000.

Drake, A. A., Jr., and Lyttle, P. T., 1980, Alleghanian thrust faults in the Kittatinny Valley, New Jersey, *in* Manspeizer, Warren, ed., Guidebook for field trips: New York Geological Association Annual Meeting, 52nd, p. 92-114.

Drake, A. A., Jr., and Monteverde, D. H., 1992, Bedrock geologic map of the Branchville

quadrangle, Sussex County, New Jersey: U. S. Geological Survey Geologic Quadrangle Map GQ-1699, scale 1:24,000.

Drake, A. A., Jr., Volkert, R. A., Monteverde, D. H., Herman, G. C., Houghton, H. H., and Parker, R. A., 1994, Geologic map of New Jersey; Northern bedrock sheet: U. S. Geological Survey Open-File Report OFR 94-178, 1:100,000 scale, 2 sheets.

Elliott, D., 1976, The energy balance and deformation mechanisms of thrust sheets: Royal Society of London Philosophical Transactions, v. A283, p. 289-312.

Engelder, Terry, Fischer, M. P., and Gross, M. R., 1993, Geological aspects of Fracture Mechanics: Geological Society of America Short Course Notes, 281 p.

Epstein, J. B., 1973, Geologic map of the Stroudsburg Quadrangle, Pennsylvania - New Jersey: U. S. Geological Survey Geologic Quadrangle Map GQ1047, scale 1:24,000.

Epstein, J. B., and Epstein, A. G., 1969, Geology of the Valley and Ridge Province between Delaware Water Gap and Lehigh Gap, Pennsylvania, *in* Subitsky, S., ed., Geology of selected areas in New Jersey and eastern Pennsylvania and guidebook of excursions: New Brunswick, N. J., Rutgers University Press, p. 132-205.

Epstein, J. B., and Lyttle, P. T., 1987, Structure and stratigraphy above, below, and within the Taconic unconformity, southeastern New York: *in* Waines, R. H., ed., Guidebook for field trips: New York Geological Association Annual Meeting, 59th, p. C1-C78.

Finks, R. M., 1968, Trip E: Taconian Islands and the shores of Appalachia: *in* Finks, R. M., ed., Guidebook for field trips: New York Geological Association Annual Meeting, 40th, p. 117-153.

Fisher, D.W., Isachsen, Y. W., and Rickard, L. V., 1970, Geologic map of New York, New York State Museum and Science Service, Geologic Survey Map and Chart Series, no. 5, scale 1:250,000.

Gates, A. E., 1993, Chemical changes in mylonites and cataclasites of the Reservoir Fault zone, New Jersey: *in* Puffer, J. H., (ed.), Field Guide and Proceedings, Annual Meeting of the Geological Association of New Jersey, 10th, p. 148-167.

Geiser, P. A., 1988, The role of kinematics in the construction and analysis of geological cross section in deformed terranes: Geological Society of America Special Paper 222, p.

47-76.

Geiser, P. A., and Engelder, Terry, 1983, The distribution of layer-parallel shortening fabrics in the Appalachian foreland of New York and Pennsylvania: Evidence for two non-coaxial phases of the Alleghanian orogeny: Geological Society of America Memoir 158, p. 161 - 175.

Ghatge, S. L., Jagel, D. L., and Herman, G. C., 1992, Gravity investigations to delineate subsurface geology in the Beemerville Intrusive Complex area, Sussex County, N. J. : New Jersey Geological Survey Geologic Map Series Map 92-2, scale 1:100,000.

Gibbs, A. D., 1984, Structural evolution of extensional basin margins: Journal Geological Society of London, v. 141, p. 609-620.

Gillespie, T. D., 1987, The structure and geochemistry of a breccia dike at McAfee, N.J.: [M.S. Thesis] Rutgers University, New Brunswick, N. J., 90 p.

Gray, N. H., and Lewis, C. L., 1985, PC Voronoi: Sterographic plotting and contouring personal-computer software. University of Connecticut Geology Department, Storrs, CT.

Groshong, R. H., Jr., 1976, Strain and pressure solution in the Martinsburg slate, Delaware Water Gap, New Jersey; American Journal of Science, v. 276, p. 1131-1146.

Gross, M. R., 1993, The origin and spacing of cross joints: examples from the Monterey Formation, Santa Barbara Coastline, California: Journal of Structural Geology, v. 15, p. 737- 751

Hague, J. M., Baum, J. L., Hermann, L. A., and Pickering, R. J., 1956, Geology and structure of the Franklin-Sterling area, New Jersey: Geological Society of America Bulletin, v. 67, p. 435-474.

Hamblin, W. K., 1965, Origin of 'reverse drag' on the down-thrown side of normal faults: Geological Society of America Bulletin, v. 76, p. 1145-1164.

Harris, J. F., Taylor, G. L., and Walper, J. L., 1960, Relation of deformational fractures in sedimentary rocks to regional and local structures: American Association of Petroleum Geologists, V. 44, p. 1853-1873

Hatcher, R. D., Jr., Osberg, P. H., Drake, A. A. Jr., Robinson, P., and Thomas, W. A.,

1990, Tectonic map of the U.S. Appalachians, *in* Hatcher, R. D., and others, eds., The Appalachina-Ouchita orogen in the United States: Boulder, Colorado, Geological Society of America, Geology of North America, v. F-2, Pl. 1.

Herman, G. C., 1987, Structure of the Green Pond outlier from Dover to Greenwood Lake, New Jersey: Geological Society of America Abstracts with Programs, v. 19, p. 18.

Herman, G. C., 1992, Deep crustal structure and seismic expression of the central Appalachian orogenic belt: *Geology*, v. 20, p. 275-278.

Herman, G. C., French, M. A., and Monteverde, D. H., 1993, Automated mesostructural analysis using GIS, beta test: Paleozoic structures from the New Jersey Great Valley region: Geological Society America Abstracts with Programs, v. 25, no. 2, p. 23

Herman, G. C., French, M.A., and Monteverde, D.H., 1996, Field data Management System (ver. 2.1) and User's Guide: N.J. Geological Survey Digital Geodata Series DGS 96-4. Digital Data file available from the Internet World-Wide-Web at URL: <http://www.nj.us.state/dep/njgs/geodata.htm>.

Herman, G. C., Houghton, H. F., Monteverde, D. H., and Volkert, R. A., 1992, Bedrock geologic map of the Pittstown and Flemington quadrangle, Hunterdon and Somerset Counties, New Jersey: N. J. Geological Survey Open-File Map no. 10, scale 1:24,000

Herman, G. C., and Mitchell, J. P., 1991, Bedrock geologic map of the Green Pond Mountain Region from Dover to Greenwood Lake, New Jersey: New Jersey Geological Survey Geologic Map 91-2, 3 pl., scale 1:24,000.

Herman, G. C., and Monteverde, D. H., 1988, The Jenny Jump-Crooked Swamp structural front in northern New Jersey: Alleghanian overthrusting of a Taconic foreland: Geological Society of America Abstracts with Programs, v. 20, p. 26.

_____, 1989, Tectonic framework of Paleozoic rocks of northwestern New Jersey; Bedrock structure and balanced cross sections of the Valley and Ridge province and southwest Highlands, *in* Grossman, I. G., ed., Paleozoic geology of the Kittatinny Valley and southwest Highlands area, N. J.; Field Guide and Proceedings, Geological Association of New Jersey Annual Meeting, 6th, p. 1-57, 3 pl.

Herman, G. C., Monteverde, D. H., Volkert, R. A., Drake, A. A., Jr., and Dalton, R. F., 1994, Environmental map of Warren County, N.J.; Bedrock fracture map: New Jersey

Geological Survey Open-File Map 15B, scale 1:48,000, 2 sheets.

Herman, G. C., Monteverde, D. H., Volkert, R. A., Drake, A. A., Jr., and Dalton, R. F., 1994, Environmental Geology of Warren County, New Jersey; Bedrock fracture map: N. J. Geological Survey Open-File Map 15b, scale 1:48,000, 2 pl.

Hobson, J. P., 1963, Stratigraphy of the Beekmantown Group in southeastern Pennsylvania: Pennsylvania Geological Survey, Fourth Series, General Geology Report 37, 331 p.

Houghton, H. F., Herman, G. C., and Volkert, R. A., 1992, Igneous rocks of the Flemington fault zone, central Newark basin, New Jersey; Geochemistry, structure, and stratigraphy: Geological Society of America Special Paper 268, p. 219-232

Huang, Q., and Angelier, J., 1989, Fracture spacing and its relation to bed thickness: Geological Magazine, v. 126, p. 355-362

Hull, J., Koto, R., and Bizub, R., 1986, Deformation zones in the Highlands of New Jersey: *in* Husch, J. M., and Goldstein, F. R., eds., Geology of the New Jersey Highlands and Radon in New Jersey; Field Guide and Proceedings, Geological Association of New Jersey Annual Meeting, 2nd, p. 19-67.

Jacobi, R. D., 1981, Peripheral bulge -- a causal mechanism for the lower/middle Ordovician unconformity along the western margin of the Northern Appalachians: Earth and Planetary Science Letters, v. 56, p. 245-251.

Jagel, D. L., 1990, A gravity and magnetic model of the Beemerville Intrusive Complex, Beemerville, New Jersey: [M. S. thesis] Rutgers University, New Brunswick, N. J., 104 p.

Kaeding, M., and Herman, G. C., 1988, Field data management system (FMS); A computer software program for organization and analysis of geologic data: New Jersey Geological Survey Technical Memorandum 88-4, 48 p., 1 floppy disk.

Kummel, H. B., and Weller, S., 1902, The rocks of the Green Pond Mountain Region: in New Jersey Geological Survey Annual Report to the State Geologist for 1901, p. 3-51.

Lewis, J. V., and Kummel, H. B., 1940, The geology of New Jersey: New Jersey Geological Survey Bulletin 50, 201 p.

LKB Resources, Inc., 1980, Magnetic contour maps: *in*, NURE aerial gamma-ray and magnetic detail survey - Reading Prong area, Volume II-A: prepared for the Department of Energy, Grand Junction, CO, 21 sheets, scale 1:62,250.

Lucas, M., Hull, Joseph, and Manspeizer, Warren, 1988, A foreland-type fold and related structures of the Newark rift basin, *in* Manspeizer, Warren, ed., Triassic-Jurassic Rifting, Continental Breakup, and the Origin of the Atlantic Ocean and Passive Margin, Elsevier, New York, ed. p. 307-332

Mabee, S. B., Hardcastle, K. C., and Wise, D. U., 1994, A method of collecting and analyzing lineaments for regional-scale fractured-bedrock aquifer studies: *Ground Water*, v. 32, no. 6, p. 884-894

Markewicz, F. J., and Dalton, R. F., 1977, Stratigraphy and applied geology of the lower Paleozoic carbonates in northwestern New Jersey; Guidebook to the 42nd annual field conference of Pennsylvania geologists: Bureau of Topography & Geological Survey, Department of Environmental Resources, Harrisburg, Pennsylvania, 117 p.

Malizzi, L. D., and Gates, A. E., 1989, Late Paleozoic deformation in the Reservoir Fault zone and Green Pond Outlier: *in* Weiss, D., ed., Field trip Guidebook, New York State Geological Association Annual Meeting, 61st, p. 75-93.

Marshak, Stephen, and Tabor, J. R., 1989, Structure of the Kingston orocline in the Appalachian fold-thrust belt, New York: *Geological Society of America Bulletin*, v. 101, p. 683-701.

Maxey, L. R., 1976, Petrology and geochemistry of the Beemerville carbonatite-alkalic rock complex, New Jersey: *Geological Society of America Bulletin*, v. 87, p. 1551-1559.

Maxwell, J. C., 1962, Origin of slaty and fracture cleavage in the Delaware Water Gap Area, New Jersey and Pennsylvania: *in* Engel, A. E. J., James, H. L., and Leonard, B. F., eds., Petrologic Studies; Buddington volume, Boulder, Colorado, Geological Society of America, p. 281-311

Merchant, J. S., and Teet, J. E., 1954, Kittatinny limestone, Sussex County, New Jersey: The New Jersey Zinc Company, Ogdensburg, N. J., Progress report on file at the New Jersey Geological Survey, Trenton, NJ., 24 p.

Mitchell, J. P., and Forsythe, R. D., 1988, Late Paleozoic noncoaxial deformation in the Green Pond outlier, New Jersey Highlands: *Geological Society of America Bulletin*, v. 100, p. 45-59.

Mitra, G., 1979, Ductile deformation zones in the Blue Ridge basement and estimation of finite strains: *Geological Society of America Bulletin*, v. 90, p. 935-951.

Monteverde, D. H., 1992, Bedrock geology of the Sussex County, New Jersey portions of the Culvers Gap and Lake Maskenhoza quadrangles: *New Jersey Geological Survey Geologic Map Series Map GMS 92-1*, scale 1:24,000.

Monteverde, D. H. and Herman, G. C., 1989, Lower Paleozoic environments of deposition and the discontinuous sedimentary deposits atop the Middle Ordovician unconformity in New Jersey, *in* Grossman, I. G., ed., *Paleozoic geology of the Kittatinny Valley and southwest Highlands area, N.J.*: Geological Association of New Jersey, 6th annual meeting, p. 95-120.

Monteverde, D. H., Herman, G. C., and Dalton, R. F., 1989, Guide to field stops and road log for the Cambrian and Ordovician rocks of the Phillipsburg-Easton area, *in* Grossman, I. G., ed., *Paleozoic geology of the Kittatinny Valley and southwest Highlands area, N.J.*: Geological Association of New Jersey, 6th annual meeting, p. 121-147.

Monteverde, D. H., Volkert, R. A., Herman, G. C., Drake, A. A., Jr., and Dalton, R. F., 1994, Environmental Geology of Warren County, New Jersey; Bedrock geologic Map: N. J., Geological Survey Open-File Map 15a, scale 1:48,000, 2 pl.

Morley, C. K., 1989, Out-of-sequence thrusts: *Tectonics*, v. 7, no. 3, p. 539-561.

Narr, W., and Suppe, J., 1991, Joint spacing in sedimentary rocks: *Journal of Structural Geology*, v. 13, p. 1037-1048

Offield, T. W., 1967, Bedrock geology of the Goshen-Greenwood Lake area, New York: New York State Museum and Science Service, Map and Chart Series no. 9, 77 p. Includes 1:62,500 scale map.

Olsen, P. E., Kent, D. V., Cornet, Bruce, Witte, W. K., and Schlische, R. W., 1996, High-resolution stratigraphy of the Newark rift basin (early Mesozoic, eastern North America): *Geological Society of America Bulletin*, v. 108, no. 1, p. 40-77.

- Phinney, R. A., 1986, A seismic cross section of the New England Appalachians, the orogen exposed, *in* Barazangi, M., and Brown, L., eds., *Reflection seismology: The continental crust*: American Geophysical Union Geodynamic Series, v. 14, p. 157-172.
- Pollard, D. P., and Aydin, A., 1988, Progress in understanding jointing over the past century: *Geological Society of America Bulletin*, v. 100, p. 1181-1024.
- Price, R. A., 1986, The southeastern Canadian Cordillera: thrust faulting, tectonic wedging, and delamination of the lithosphere: *Journal of Structural Geology*, v. 8, nos. 3 and 4, p. 239-254..
- Pristas, R. S., and Herman, G. C., 1995, The New Jersey Geological Survey Digital-Map Production Effort; An integrated Approach for Publishing Geological Maps and Developing Spatial Coverages: *Geological Society America Abstracts with Programs*, v. 27, no. 1, p. 75.
- Ragan, D. M., 1985, *Structural geology. An introduction to geometrical techniques* (3rd edition): New York, John Wiley, 393 p.
- Rankin and 9 others, 1989, Pre-orogenic terranes, *in* Hatcher, R. D., Jr., Thomas, W. A., and Viele, G. W., eds., *The Appalachian-Ouchita Orogen in the United States*: Boulder, Colorado, Geological Society of America, *The Geology of North America*, v. F-2, p. 7 -100.
- Ramsay, J. G., and Huber, M. I., 1987, *The techniques of modern structural geology*, v. 2: *Folds and fractures*: London, Academic press, 700 p.
- Ratcliffe, N. M., 1980, Brittle faults (Ramapo Fault) and phyllonitic shear zones in the basement rocks of the Ramapo seismic zones, New York and New Jersey, and their relationship to current seismicity: *in* Manspeizer, Warren, ed., *Field studies of New Jersey Geology*, Annual Meeting of the New York State Geological Association, 52nd , p. 278-311.
- _____ 1981, Cortland-Beemerville magmatic belt: A probable late Taconian alkalic cross trend in the central Appalachians: *Geology*, v. 9, p. 329-335.
- Ratcliffe, N. M., and Costain, J. K., 1985, Northeastern seismicity and tectonics, *in* Jacobson, M. L., and Rodriguez, T. R., compilers, *National Earthquake Hazards*

Reduction Program; Summaries of Technical Reports, v. 20: U. S. Geological Survey Open-File Report 85-464, p. 54-58.

Reynolds, M. W., Queen, J. E., and Taylor, R. B., 1995, Cartographic and digital standards for geologic map information: U. S. Geological Survey Open-File Report OFR 95-525.

Rich, J. L., 1934, Mechanics of low-angle overthrust faulting as illustrated by Cumberland thrust block, Virginia, Kentucky and Tennessee: American Association Petroleum Geologists Bulletin, v. 18, p. 1584-1596.

Rodgers, J., 1970, The tectonics of the Appalachians: New York, Wiley-Interscience, 270 p.

Salkind, Moris, 1979, Silurian tectonic activity in southeastern New York: Northeastern Geology, v. 1, no. 1, p. 48-59.

Sanders, J. E., 1983, Reinterpretation of the subsurface structure of the Middletown gas well 1 (Crom-Wells, Inc. 1 Fee) in light of concept of large-scale bedding thrusts: Northeastern Geology, v. 5, no. 3-4, p. 172-182.

Schlische, R. W., 1992, Structural and stratigraphic development of the Newark extensional basin, eastern North America: Evidence for the growth of the basin and its bounding structures: Geological Society of America Bulletin, v. 104, p. 1246-1263.

Sevon, W. D., Berg, T. M., Schultz, L. D., and Crowl, G. H., 1989, Geology and mineral resources of Pike County, Pennsylvania: Pennsylvania Geological Survey County Report 52, 141 p.

Shanmugam, G., and Lash, G. G., 1982, Analagous tectonic evolution of the Ordovician foredeeps, southern and central Appalachians: Geology, v. 10, p. 562-566.

Sheridan, R. E., Olsson, R. K., and Miller, J. J., 1991, Seismic reflection and gravity study of proposed Taconic suture under the New Jersey Coastal Plain, Implications for continental growth: Geological Society of America Bulletin, v. 103, p. 402-414.

Sherwin, Jo-Ann, and Chapple, W. M., 1968, Wavelengths of single-layer folds: A comparison between theory and observation: American Journal of Science, v. 266, p. 167-179.

Sherwood, W. C., 1964, Structure of the Jacksonburg Formation in Northampton and Lehigh Counties, Pennsylvania: Pennsylvania Geological Survey General Geology Report G 45 64 p., 1 map, scale 1:62,500.

Sibson, R. E., 1977, Fault rocks and fault mechanisms: Geological Society of London, v. 133, p. 101-213.

Snyder, S. L., Aeromagnetic map of New Jersey and parts of adjacent States; North sheet: New Jersey Geological Survey Map, scale 1:100,000, in press.

Soller, D. R., and Berg, T. M., 1995, Developing the national geologic map database: *Geotimes*, v. 40, p. 16-18.

Spink, W. J., 1967, Stratigraphy and structure of the Paleozoic rocks of northwestern New Jersey [Ph.D. thesis]: New Brunswick, N. J., Rutgers University., 311 p.

Suppe, J., 1983, Geometry and kinematics of fault bend folding: *American Journal of Science*, v. 283, p. 684-721.

Telford, W. M., Geldart, L. P., Sheriff, R. E., and Keys, D. A., 1976, *Applied Geophysics*: Cambridge, Cambridge University Press, 860 p.

Walker, J. D., Black, R. A., Linn, J. K., Thomas, A. J., Wiseman, R., and D'Atilio, 1996, Development of geographic information systems - Oriented databases for integrating geological and geophysical applications: *GSA Today*, V. 6, no. 3, p. 1-7.

Williams, H. (compiler), 1978, Tectonic lithofacies map of the Appalachian orogen: Memorial University of Newfoundland Map no. 1, scale 1:1,000,000.

Wilson, T. H., and Shumacher, R. C., 1988, Three-dimensional structural interrelations within Cambrian-Ordovician lithotectonic unit of central Appalachians: *American Association Petroleum Geologists Bulletin*, v. 72, p. 600-614.

_____, 1994, Crustal structures and the eastern extent of lower Paleozoic shelf strata within the central Appalachians: A seismic reflection interpretation: Alternate interpretation and reply: *Geological Society of America Bulletin*, v. 106, p. 1502-1511.

Wintsch, R. P., and Kunk, M. J., 1992, $^{40}\text{Ar}/^{39}\text{Ar}$ evidence for an Alleghanian age of the

slaty cleavage in the Martinsburg Formation, Lehigh Gap, Eastern Pennsylvania: Geological Society of America Abstracts with Programs, v. 24, no. 3, p. 85.

Withjack, M.O., Olsen, P.E., and Schlische, R.W., 1995, Tectonic evolution of the Fundy rift basin, Canada: Evidence of extension and shortening during passive margin development: Tectonics, v. 14, p. 390-405.

Wood, G. H., Jr., and Bergin, M. J., 1970, Structural control of the anthracite region, Pennsylvania, *in* Fisher, G. W., Pettijohn, F. J., Reed, J. C., and Weaver, K. N., eds., Studies in Appalachian geology, central and southern: New York, Wiley-Interscience, p. 147-160.

Woodward, N. B., Boyer, S. E., and Suppe, J., 1985, An outline of balanced cross sections: Studies in geology, 2nd edition., Department Geological Sciences, University of Tennessee, Knoxville, 170 p.

Wright, T. O., and Platt, L. B., 1982, Pressure dissolution and cleavage in the Martinsburg Shale: American Journal of Science, v. 282, p. 122-135.

Zartman, R. E., Brock, M. R., Heyl, A. V., and Thomas, H. H., 1967, K-AR and Rb-Sr ages of some alkali intrusive rocks from central and eastern United States: American Journal of Science, v. 265, p. 848-870.

Vita

Gregory C. Herman

- | | |
|-----------|--|
| 1974 - 79 | Attended Ohio State University, Business Administration
Columbus, Ohio |
| 1980 - 82 | B.S. in Geological Sciences, Ohio University
Athens, Ohio |
| 1982 - 83 | Petroleum Geologist, Amoco Production Company
Houston, Texas |
| 1982 - 84 | Research and Teaching Assistant, Department of
Geology and Geophysics, University of Connecticut
Storrs, Connecticut |
| 1982 - 84 | M.S. in Geological Sciences, University of Connecticut
Storrs, Connecticut |
| 1984 - 85 | Geologist, Department of Environmental Protection
Division of Water Resources
Bureau Ground Water Discharge Permits
Trenton, New Jersey |
| 1986- 96 | Geologist, Department of Environmental Protection
Division of Science and Research
New Jersey Geological Survey
Trenton, New Jersey |
| 1987 - 90 | Instructor, Hydrogeology Short Course, Cook College,
New Brunswick, New Jersey |
| 1992 - 97 | Ph.D. in Geological Sciences, Rutgers Univesity |